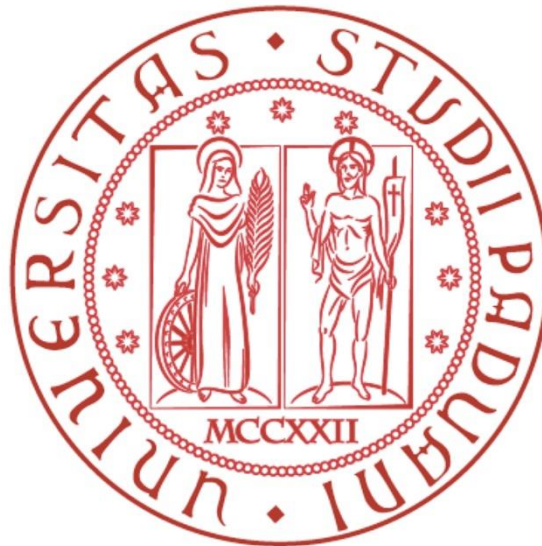University of Padua

Faculty of Engineering Department of Industrial Engineering

Master thesis in Mechanical Engineering

A.Y. 2013/2014

Analysis of the structural behaviour of modern ski boots

Supervisors: Eng. Nicola Petrone

Dott. Giuseppe Marcolin

Student: Gori Stefano

Matr.: 1041098

Alla mia famiglia

Sommario

Introduction

I was four years old when I started skiing, and that is when I feel in love with skiing. The challenge of balancing myself while going down the slope was a fascination that grew with me as I got older.

I started to practice day after day to achieve my goal as to become a professional skier. The feeling of getting better after every day of skiing let me to continuously be passionate about the sport and the curiosity about skiing dynamics.

University of Padua collaborates with various companies to improve skiing and snowboard equipment in order to enhance security and performance while skiing.

The part of the equipment that has the most significant effects on skiing quality is the boot. This is because when the boot is in the binding it is part of the ski.

There are numerous types of ski boots in the market with different shapes, number of buckles, and number of "nominal flex".

The nominal Flex Index is the most common value communicated, which allows the customer to recognize the stiffness of a boot: in fact the stiffer boot, is the one with the higher index.

The boot is the lever that the skier controls with both his feet and legs to apply loads to the skies.

A person turns the ski by pushing against the front part of the boot called "Cuff".

The boot is directly in contact with the skin of the skier and he can have some sensations about the comfort and the thermal comfort.

This induced some some questions below:

Is the Flex Index written on the boot an engineering parameter?

Which are the forces acting on the buckles during skiing?

How do the force vary with the tightening of the boot?

Can the tightening of the boot influence the flex index?

There have been numerous tests done at the University of Padua to try to answer to these questions. This was done by conducting tests reproducing the effect of a simulated ski but also in-field tests where data were collected using a real skiing session.

At the University of Padua, Department of Industrial Engineering, Lab of Spors Engineering, it is also possible to test boots by using a machine that is able to work in torque and rotation control to evaluate the stiffness of the boots.

This kind of machine is able to reproduce the methods used in Nordica to obtain the same information about their production of boots.

Chapter 1: Flex index

1.1 Definition

Considering that the technical specification of ski boots are the most of the companies report on their product there is a number that is also called the Flex Index which is useful to characterize the market segment of the product.

Flex Index can vary between 60 and 150 and it is connected to the stiffness of the boot in the forward flexion; usually boots with lower flex index are indicated for beginner skiers and the stiffer boots are for racers.
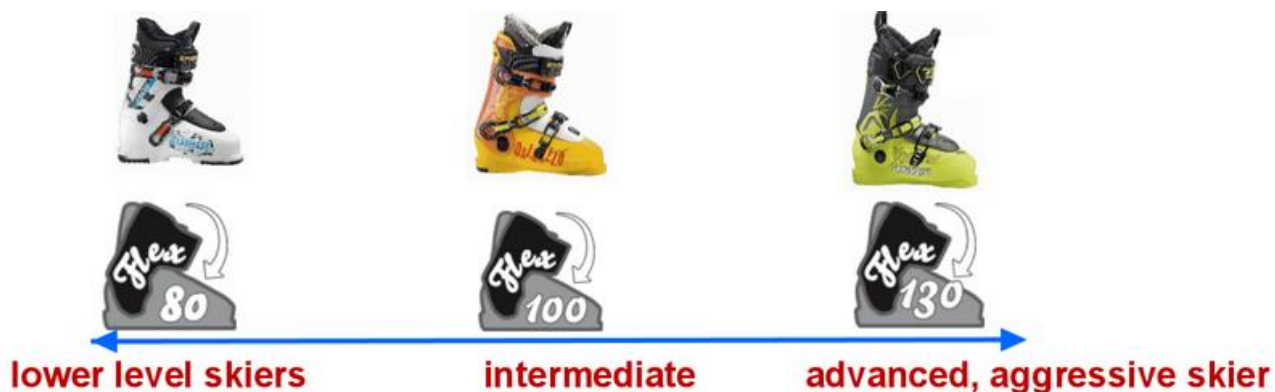

Figure1. 1 Market Flex Index segmentation

It is possible to say that this index is more of a marketing expression because it has not been standardized. Therefore an engineering test method to asses it has not yet been established.

As reported on the article [2], different manufacturers have their own test methods to find the value of the index. From the technical point of view, usually the boot is applied on an adjustable binding and a prostatic leg simuling the human shank-foot is insert into the boot. Also, a loading arm is rigidly connected to the dummy leg to flex the boot cyclically.

A servo controlled (rotational) motor can control the loading arm with the axes parallel to the boot ankle hinge.

The test method may also vary on the fact that the test cycle is defined by the extreme values of the moment acting on the boot hinge (moment control); or by the extreme of the force values acting on the prostatic leg (force control). Lastly, the extreme values of the flexion angles (angle control).

It is also important to understand the behaviour of the materials used in ski boots. In fact, the polymeric materials used in ski boots are visco-elastic, with a strong influence of strain levels, loading path, and strain rate.

Therefore, the Flex index is a value that depends on a big number of variables, such as the test method, the environment of the laboratory, depending on temperature and humidity in which the test are performed, the difference of test machines, the closure of the buckles, and the shape of the prostatic leg.

According to these variables, it is clear how the nominal Flex Index (nFI) is only useful to segment of the market.

From the engineering perspective, it is essential to consider the effective Flex Index (eFI). The Flex Index is defined as the value of the bending moment (expressed in Nm) applied to boot hinge and a specific prosthetic leg to obtain a forward leaning angle of 10° from the neutral position (i.e., the natural leg posture with closed buckles and no bending moment applied).

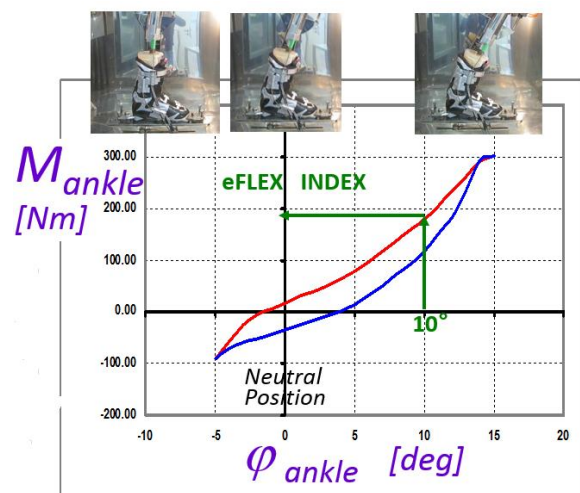This definition of Flex Index corresponds to its original introduction in the ski boot industry. It implies the use

Figure1. 2 Flex Index definition

of a test machine is able to flex the ski boot with a loading arm that is hinged to the ski boot ankle and is actuated under angle control in a climatic chamber.

The Moment–Angle curves show highly nonlinear behaviour both in forward and in backward bending, together with large hysteresis loops, so that the forward bending loading branch of the loop is different from the unloading backward bending branch.

From an engineering point of view, the use of a single number as the Flex Index (even when consistently measured at 10° in a standard defined test cycle) is not sufficient to completely describe the stiffness behaviour of the boot. In fact, the same value of the bending moment at 10° can be reached with a linear slope or with a nonlinear stiffening portion of the curve: from the user point of view, the stiffening of the curve is forward and associated with the ''progression'' of the boot, that is appreciated particularly in free-ride and free-style boots.

On the other hand, the boot behaviour should be quantified also in backward bending, with a ''backward Flex Index'' that is at present never mentioned but that can be correlated with the risk of ''boot induced drawer.'' In the past it is justified that the comparison of some boots are with a ''Backward release'' system.

The conventional test procedure currently used at the boot manufacturer laboratories involved in this study consists in the cyclic application of flexion angles of +15° (forward) and -15° (backward) from the neutral position of the boot.

While recording the bending moment and the flexion angle; the same boot manufacturer was interested in understanding how this established procedure (that will be indicated Current Test in what follows) was representative of the real usage of the ski boots.

Chapter 2: Force on the buckles

2.1 Boot terminology and boot buckles

The figure below explains the used terminology to describe the boot:

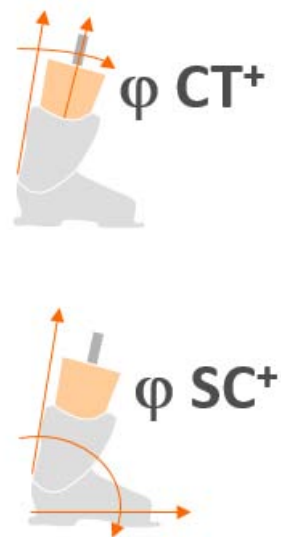*Figure 2. 1 Name of the parts of the boot*

Figure 2. 2 Angles definition

Most of all the ski boots that are in the market use the same type of closure system that is based on a lever mechanism with a hook at the extremity. This engages with the teeth of a rack fixed on the boot.

The number of teeth of the rack can vary from 3 to 6 and allows the user of the boot to reach his perfect feeling for tightening the boot to perform his skiing technique along the slope.

Figure2. 3 Examples of boot closing system

The systems are designed for multiplying the closing force and to obtaining a chuck mechanism.

Since the layout of the closing system is similar for many products on the market the thing that could be a variable is the number of the buckles that can vary from 2 to 4.

Most of the modern boots have also a Velcro Strap at the top of the boot that allows a more comfortable closure and gives a sensation of "elasticity" to the skier.

The Velcro strap can have different dimensions but all of them have usually the same closing system.

All Velcro system of the ski boots at the University of Padua have been measured with a calibre.

– The biggest one has a ring with a thickness of 5mm and a Velcro Strap with a width of 55mm.

Figure2. 4Velcro Strap closure

– The smallest one has a ring with a thickness of 2mm and a Velcro Strap with a width of 20mm.
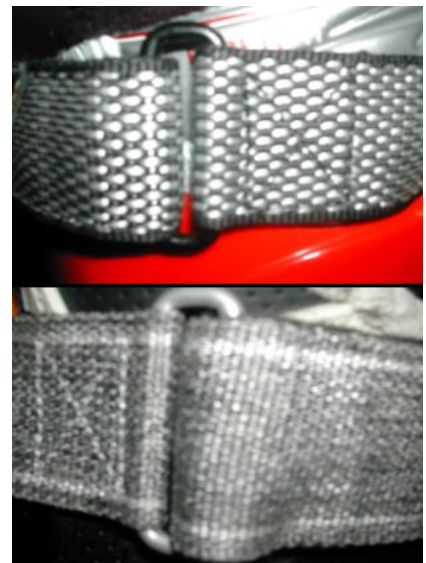
2.2 How to measure the buckle closing force?

It is certain that in the actual conditions of a pair of ski boots most of the skiers set their own tightening closure. The sensation that they want to reach is a comfortable compromise between the best skiing feeling to avoid pain in the foot and the leg.

It recognisable that if the idea of a boot that is too big or tight, that this is only subjective but not objective to engineers.

As mentioned, there are other variables that could influence the behaviour of the boot and the flex index. For example, the boot closure. It is interesting to understand the force acting on the hooks during a simulated skiing test and also during field tests.

This could also give knowledge of the ski boot behaviour and the structure of the boot while performing a test both in the laboratory and on the field.

To reach this goal there were two different systems used.

1. Applying a set of strain gauges on the buckle
2. Develop some load cells clips for buckles

2.3 Strain Gauges

A strain gauge is a device used to measure the strain of an object invented by Edward E. Simmons and Arthur C. Ruge in 1938.

The most common type of strain gauge consists in an insulating flexible backing, which supports a metallic foil pattern. The gauge is attached to the measuring object by a suitable adhesive such as cyanoacrylate.

When the object is deformed, also the metallic foil deforms and this deformation causes the change of its electrical resistance.

This resistance change is usually measured using the Wheatstone bridge and is connected to the strain by the gauge factor.

The gauge factor is defined as:

$$= \frac{(\quad / \quad)}{\underline{\qquad\qquad}}$$

Where:

- ‹ ΔR is the change of resistance caused by strain
- ‹ is the resistance of the undeformed object
- ‹ is the strain

A strain gauge takes advantage from the propriety of the physical propriety of electrical conductance and its dependence on the geometry of the conductor.

When an electrical conductor is stretched within the limit of its elasticity such that it does not break or permanently deform, it becomes narrower and longer, which changes that increase its electrical resistance.

Conversely, when a conductor is compressed so that it does not buckle, it will broaden and shorten, changes that decrease its electrical resistance end-to-end.

Figure2. 5 Strain Gauges working on a beam in bending

From the measured electrical resistance of the strain gauge, the amount of applied stress may be inferred. Strain gauges measure only local deformations and can be manufactured little enough to allow a "finite element" like the analysis of the stresses to which the specimen is subject.

This can be positively used in fatigue studies of materials. An excitation voltage is applied to input leads of the gauge network, and a voltage reading is taken from the output leads. Typical input voltages are 5 V or 12 V and typical output readings are in millivolts.

Foil strain gauges are used in many situations. Different applications place different requirements on the gauge. In most cases the orientation of the strain gauge is significant.

Gauges attached to a load cell would normally be expected to remain stable over a period of years, if not decades; while those used to measure response in a dynamic experiment may only need to remain attached to the object for a few days, be energized for less than an hour, and operate for less than a second.
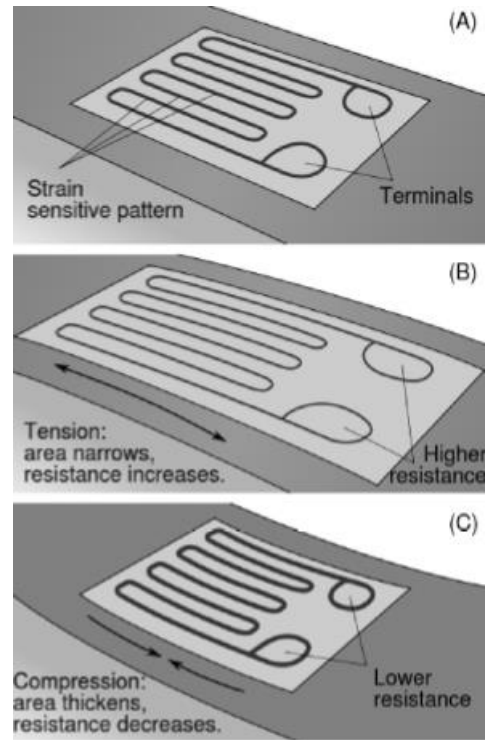
Strain gauges are attached to the substrate with a special glue. The type of glue depends on the required lifetime of the measurement system. For short term measurements (up to some weeks) cyanoacrylic glue is appropriate, for long lasting installation epoxy glue is required. Usually epoxy glue requires high temperature curing (at about 80-100°C). The preparation of the surface where the strain gauge is to be glued is of the utmost importance.

2.3.1 Operating instructions for proper bonding

1. To smooth the surface with very fine sand paper to promote adhesion of the glue.

2. To run a trace with the greatest care, avoiding to seriously affect the surface.

3. To position the gauge on a transparent tape.

4. To degrease the surface with alcohol and cotton without touching the surface with hands.

5. To apply a drop of glue to the surface to be coupled.

6. To fix the gauge with a piece of Teflon to avoid adherence to the fingers and with the utmost care.

7. To verify a correct alignment. The alignment accuracy determines the accuracy of the measurement.

8. To solder the ends of the threads, following the scheme of the bridge.

9. To check the correct functionality of the bridge with a tester.

10. To clean the connections with alcohol and to cover them with silicone.

11. To connect the wires to plugs and sockets.

If these steps are not followed, the strain gauge binding to the surface may be unreliable and unpredictable measurement errors may be generated.

2.3.2 Wheatstone bridge configurations

The main important configuration to realize a Wheatstone bridge is the full bridge one. To design a full bridge configuration it's necessary to connect in series 4 strain gauges with known resistances R1, R2, R3, R4 of the same value and connect the alimentation V in the connection 1, 4 and 2,3. So reading the output value U between the connection 1,2 and 3,4 like in the following figure, are valid the following formulas:

Figure2. 1 Wheatstone Bridge

$$\frac{U_0}{} = \left(\frac{R_1}{R_1} - \frac{R_2}{R_2} + \frac{R_3}{R_3} - \frac{R_4}{R_4}\right)/4$$

It is known for the strain gauges: $\quad = (\quad / \quad)$

$$\frac{U_0}{} = (\varepsilon_1 - \varepsilon_2 + \varepsilon_3 - \varepsilon_4)/4$$

$$\frac{U_0}{} = \quad /4$$

Using only two adjacent active gauges and two dummy resistors it's realized a half-bridge. The output U from the bridge so configured is: $\quad U_0 = \quad (\varepsilon_1 - \varepsilon_2)/4$

Using only a single active gauge and three dummy resistors, a quarter-bridge is realized. The output U from the bridge so configured is: $\quad U_0 = \quad /4$.

2.4 Strain Gauges on the buckle

The first idea developed in order to measure the force acting on the buckle of the boot was to attach a strain gauge in a full bridge configuration directly on the lever to the mechanism of the closing system.

The final part of the buckle is acting as a curved beam and it can be the value of bending.

It is important to say that from now in this paper, it has been used a convection in order to appoint the buckles on the boot.

Figure2. 6 Strain Gauges applied on the buckle of the boot

The buckles are classified from the tip of the shell to the upper part of the shank in ascending order from 1 to 4.

The boot used for the test is the Tecnica Phnx 70 and the full bridge of strain gauges was placed on the third buckle.

2.4.1 Calibration of the buckle

In order to determine the clamping forces on the buckle during the flexion and extension it is necessary to calibrate the system of acquisition. A possible way for doing this is to set the boot on two tables while having the same height from the ground in order to have the buckle with the strain gauges free.

This position has been used as the zero starting point.

Figure2. 2 Calibration "Zero" position

Figure2. 8 Masses application for the buckle calibration

The calibration is done by applying some known masses until a maximum value and then removing them with the logic "last in first out."

[Kg]	[N]	Cumulative [N]
0	0	0
0,075	0,73575	0,73575
0,5	4,905	5,64075
1	9,81	15,45075
2	19,62	35,07075
2	19,62	54,69075
2	19,62	74,31075
5	49,05	123,36075

Figure2. 9 Load application sequence

The further step is to calculate the coefficient of calibration. The coefficient of calibration C is calculated as the reciprocal of the slope of the trend line and is defined as the value in which it allows to calculate the force value acting on the load cell by multiplying it to the value read by the load cell in mV.

$$C = 1/S \quad [N/mV]$$

Where S is the slope of the trend line of the calibration data.

The force value is given by:

$$F = C \cdot V_0$$

Where V_0 is the output signal from the bridge.

Applying the weight to the system makes unbalance to the bridge measured in mV and this can be seen by the graph below of loading ramp.
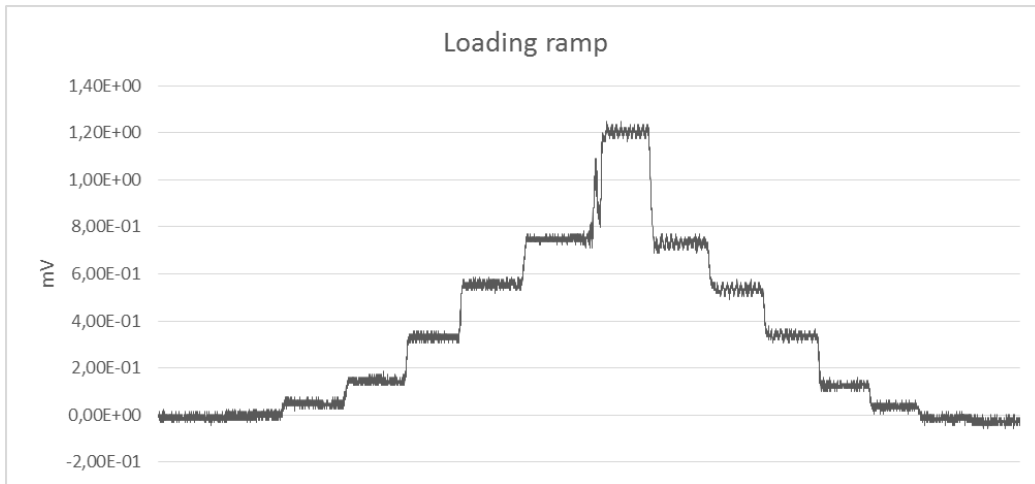
Figure2. 10 Loading Ramp

For each step of the ramp the mean value is taken of the mV unbalance.

[kg]	[N]	Cumulative [N]	[mV]
0	0	0	-0,008376
0,075	0,73575	0,73575	-0,002194
0,5	4,905	5,64075	0,49701
1	9,81	15,45075	0,14571
2	19,62	35,07075	0,33272
2	19,62	54,69075	0,55512
2	19,62	74,31075	0,75009
5	49,05	123,36075	1,2026
-5	-49,05	74,31075	0,73076
-2	-19,62	54,69075	0,53569
-2	-19,62	35,07075	0,33616
-2	-19,62	15,45075	0,12624
-1	-9,81	5,64075	0,036703
-0,5	-4,905	0,73575	-0,01375
-0,075	-0,73575	0,00	-0,02649

Figure2. 11 Calibration resume table

16
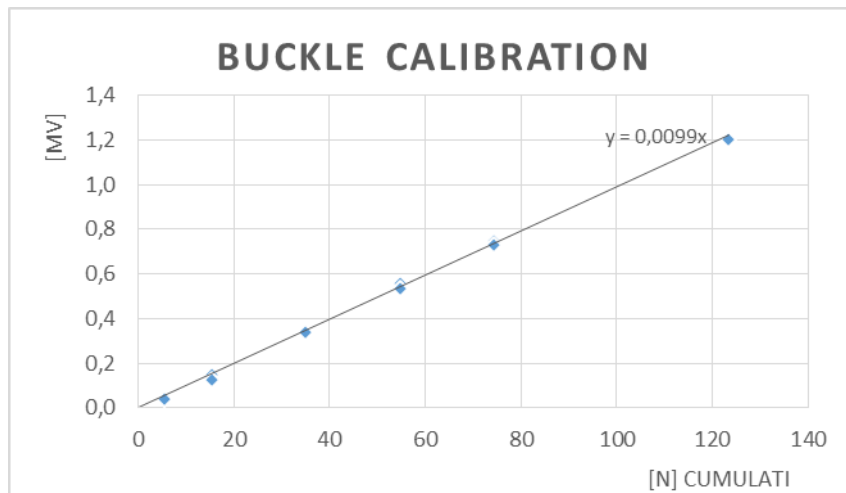
Figure2. 12 Calibration trend line

From this graph one can see that the trend line slope is:

$$= 0,0 0 9 9 \left[\frac{-}{-} \right]$$

The calibration constant C is given by:

$$= \frac{1}{0,0 0 9 9} = 1 0,0 1 \left[\frac{-}{-} \right]$$

2.5 Dynamic in vivo test

The first test that was done in laboratory in order to understand how the system works was to see how it feels in an in vivo flex test in laboratory.

Figure2. 13 Setting of the test

2.5.1 Protocol and instrumentation used

The strain gauge full bridge is connected to an recording data logger system SOMAT built by HBM

A series of events are scheduled in order to give repeatability to the test as follows:

1. Wearing boot completely open (zero position)
2. Light closure of the buckle
3. Max closure of the buckle
4. Approaching the ski
5. Unweight boot
6. Hook tip
7. Hook heel
8. Max forward flexion (FW)
9. Max backward extension (BW)
10. 5 cycles of forward/backward flexion/extension movements

11. Unhook heel

12. Unhook tip

13. Unweight the boot

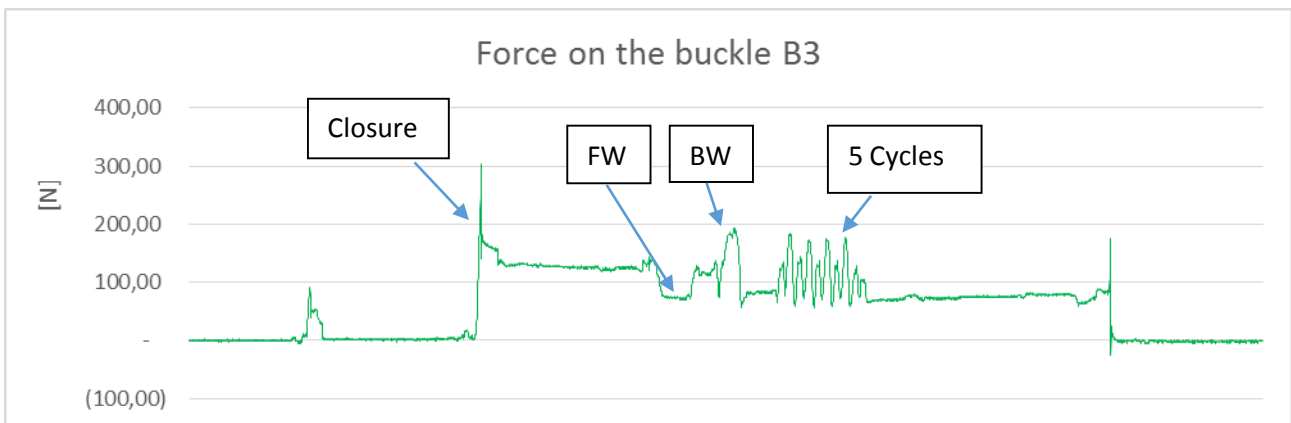14. Enclosure the boot's buckle

The acquired signal:

Figure2. 34 Acquired signal for the buckle

From the graph it is possible to clearly recognize some of the operations described above such as the closing moment of the buckle were the force has its maximum value of more of less 300 N.

It is possible to comprehend also the maximum forward flection and the maximum backward flexion with the adjustment of the boot.

Lastly, it is simple to find on the graph the moment when it was performed from the 5 cycles of forward/backward movements. It is possible to see that in both cases the buckle goes in tension with the highest values in the backward extension.

2.6 Dynamometric Load Cells Clips

The problem of directly applying the strain gauges set on the buckles is that this procedure is rather long. It is valid for only one model and one size of a certain range of the boot.

Therefore, the challenge is to study a wide range of boots of different companies and different sizes. It is necessary to invent a solution to have an external system that can give information on the value of the clamping forces in any model.

The University of Padua [1] designed a load cell able to check load information that will interpose itself as an intermediate element between hook and rack. Since the system will participate in the closing, the load cell has to mimic the original closure mode and an extremity to connect to a hook of the opposite one to the rack.

A load cell has been designed in order to amplify the effect of the clamping force.

A cell of this type is able to obtain an unbalance of the marked bridge since the measured deformation due to bending is greater than that in which it would be with the analysis of the deformation due to the normal stress.

The cell is designed in a sensitive way in order to force F in an indirect way; in fact, it is sensitive to the moment of the force F. Once calibrated the cell may still immediately have the value of the clamping force using the calibration curves.

2.6.1 Bridge design

Buckle clips are designed; clips A,B,C,D. They will be sensorized with a full bridge.

The strain gauges were placed on their lateral faces that go in flexion during tightening.

The small dimension made difficult to the use of the two strain gauges placed in parallel on both faces. To emphasize the signal of unbalance as much as possible, they were placed perpendicular to the longitudinal and the transversal deformations are sensed.

The two parallel faces of the clips are stressed and schematized as shown in the Figure below:
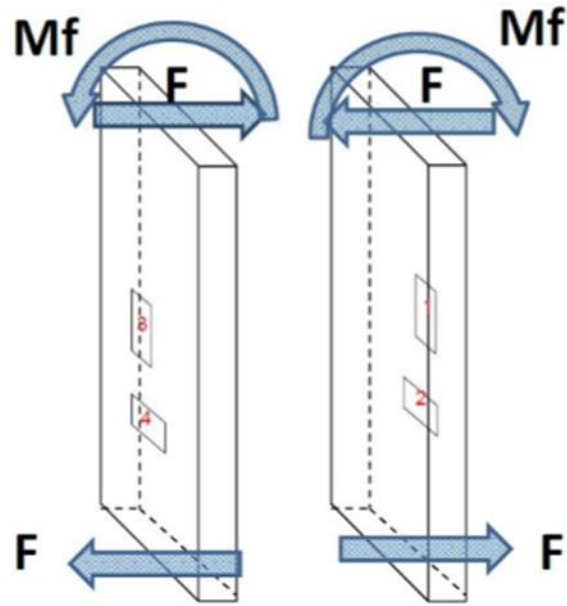
Figure2. 45 Bridge design for the acting forces

Since there is a variable bending moment, section by section, we have: $\epsilon_{1,3} > \epsilon_{2,4}$

This suggests that the lateral contraction detected in proximity of the average line of the strain gauges 2 and 4, is inferior to the one felt in proximity of 1 and 3.

$$\frac{0}{} = (\epsilon_1 - \epsilon_2 + \epsilon_3 - \epsilon_4)/4$$

$$\epsilon_1 = \epsilon_3 = \epsilon_{1,3}$$

$$\epsilon_2 = \epsilon_4 = \epsilon_{2,4}$$

$$\frac{0}{} = (2\epsilon_{1,3} + 2\epsilon_{2,4})/4$$

2.6.2 Dimensioning and Verification

Regarding the dimensioning of the clips, the data obtained from tests performed on the closure hook of a boot have been very useful. During the tests in the company, the maximum clamping force detected has been around for 200N.
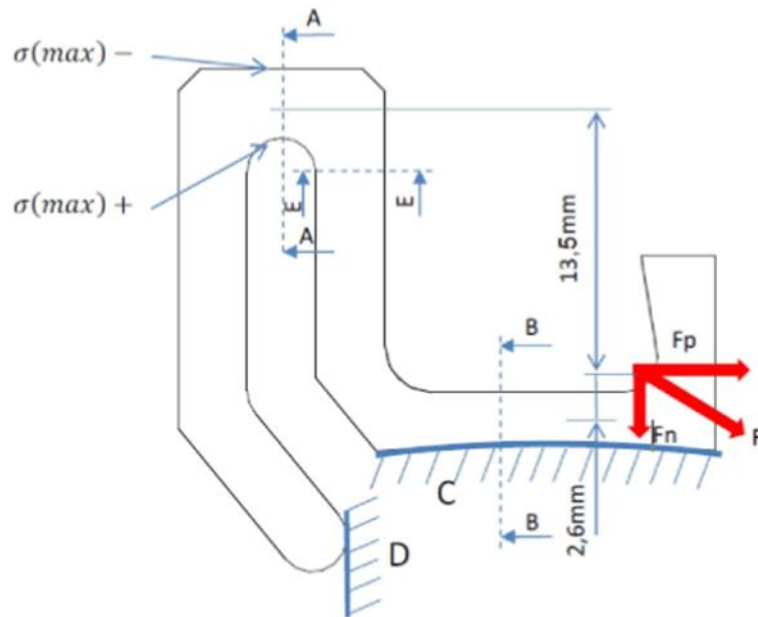
Below is the profile designed:

Figure2. 56 Dimension of the Clip

The section AA and EE have a thickness of 4mm and a width of 8,6 mm

The section BB has a thickness of 2.2 mm and a width of 8,6mm

The interaction between the hook and the clip is expressed according to the direction of F which is a variable depending on the position of engagement in the rack and due to the curvature of the boot.

If the normal force Fn discharges on the support C below, to load the section AA is Fp less the friction effect Fnμ. If we want to be conservative, we substitute the value of Fp with F and omit the friction.

A critique of the model can be done considering that the curved part of the hook is not leaning on a smooth and continuous surface, but on the teeth of the rack and that the support D is actually the bottom of a tooth of the rack so that portion will engage a greater surface.

The buckle clips will be made in ergal. They have been verified in their critical section A-A paying attention to obtain coefficient of security > 4 for security reason.

Initial Datas:

- ‹ = 2 0 0
- ‹ width: = 8,6
- ‹ thickness: = 4
- ‹ arm: = 1 35

22

- ‹   = 4 8 0
- ‹   Young's module: = 7 2 5 0 0
- ‹   Poisson's coefficient: = 0.3 3

Formulas:

- ‹   =
- ‹   = (^{3})/1 2
- ‹   = /(   )
- ‹   = (/   )   (/2)
- ‹   =   +
- ‹   =   −
- ‹   =   /   > 3   =   /
- ‹ $\frac{0}{}$ = $(2_{1,3} + 2_{2,4})/4$

After it is dimensioned and verified the clips were made with a milling machine.

2.7 Velcro Strap Clip

An important part of the closing system of the boot is the Velcro Strap and for a better study, it is not possible to omit it.

It has been decided to design a load cell able to check load information on the strip positioned on the upper side of the boot. It is designed with aluminium because it is cheap, light, easy to find, and it is worked with milling machine.

It would be interposed between two rings: One is the ring around where the strap is fixed. The other one is an additional ring around where the free side of the strip will be inserted, pulled, and closed on itself.

At the University of Padua were designed this load cell as showed in the figure:

A thin plate with aluminium and two folds at the extremity is made that will allow the connection between the load cell and the two rings to function.

2.7.1 Bridge design for Velcro Strap

The clip buckle E is designed and will be sensorized with a full bridge.

The strain gauges will be placed on the external surface that go in flexion during tightening.

The four strain gages can be placed anywhere in the surface as the bending moment acting is the same on the entire outer surface.

The limits of size made can use two of the strain gauges placed in parallel on both faces difficult, t then to emphasize as much as possible the signal of unbalance. It has been thought to place them in a perpendicular way so that it is felt the longitudinal and the transversal deformation are felt.
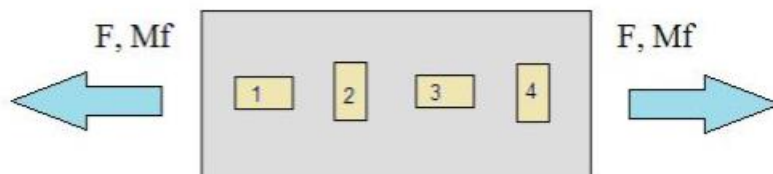
Figure2. 78 Bridge design for Velcro Strap

$$\frac{\quad_0}{\quad} = (\quad_1 - \quad_2 + \quad_3 - \quad_4)/4$$

$$\quad_1 = \quad_3 = \quad_2 = \quad_4 =$$

24

$$\frac{0}{} = \frac{(2 + 2)}{4} = 2{,}6\ 6\ /4$$

2.7.2 Dimensioning and Verification

In the hypothesis of a pulling force of 100N, it has been designed a proper section to have the sensibility U/V of 0,5mV/V paying attention to obtain a coefficient of security > 4 for security reason.

The buckle clip will be made in aluminium.

Initial data:

- ‹ Fx=100N
- ‹ width: w=16mm
- ‹ thickness: t=2,5mm
- ‹ arm: b=4,08mm
- ‹ σadm=250Mpa
- ‹ Young's module: E=70000Mpa
- ‹ Poisson's coefficient: v=0.34
- ‹ gaugefactor : K=2

Formulas:

- ‹ $\quad=$
- ‹ $\quad= (\quad^3)/1\ 2$
- ‹ $\quad= \ /(\quad)$
- ‹ $\quad= (\ /\ )\ (\ /2)$
- ‹ $\quad= \quad+$
- ‹ $\quad= \quad-$
- ‹ $\epsilon e = \sigma e/E$
- ‹ $U/V = K(\epsilon 1 - \epsilon 2 + \epsilon 3 - \epsilon 4)/4 = K(2\epsilon e + 2v\epsilon e)/4$

Once dimensioned and verified, the clips have been made with a milling cutter.

2.8 Clips Calibration

The first step is to design a system that allows it to calibrate well with the load cell.

It has been taken as a ring of the external diameter of 10,8 mm, in steel in order to have the same radius of curvature of the rack. To use the ring in his vertical position and to avoid that it rolls on the table, it is necessary to realize a platform and a system that will allow to fix the ring vertically oriented to the platform. A steel plate has been taken and it has been

Figure 2. 19 Setting of the calibration

welded in an M16 nut in the middle of its upper surface. Than a short beam has been taken with a C section and it has been drilled in the middle in order to have a hole and a diameter of 17 mm.

Finally, a hole of the diameter of 17mm has been made in the external surface of the ring. It is possible to fix the ring vertically oriented, using a M16 screw that unites in order for the ring and the beam (oriented with its axis parallel oriented to the axis of the ring and with the two wings in contact with the external surface of the ring) of the M16 nut welded to the plate. At the end, some holes have been drilled in the upper part of the ring in order to fix a rack to the ring using a M6 screw.

The system designed has been fixed to a table made of steel with a clamp attached.

The calibration is done by applying different known forces, and associating the value read by the strain gauges to the value of these forces. The value zero has been associated to the hook hung on the rack with the pulley-system added like an additional mass, then some known masses have been added up to a maximum value and then removed with logic "LIFO."

Strain gauges proprieties: gauge factor=1,97; Bridge factor=2,66

To understand the method of calibration for the Clip B, the other clips are calibrated with the same method.

For each calibration there were two acquisitions taken.

2.8.1 Calibration 0 degrees

kg	N	Ncumulati	mV1	mV2	mV (media)
0	0	0	-6,62E-03	3,79E-03	-0,001419
3,3	32,373	32,373	6,19E-01	6,13E-01	0,6161226
3,85	37,7685	70,1415	1,35E+00	1,39E+00	1,3706316
3,85	37,7685	107,91	2,18E+00	2,07E+00	2,1237329
-3,85	-37,7685	70,1415	1,51E+00	1,52E+00	1,5148373
-3,85	-37,7685	32,373	7,26E-01	6,87E-01	0,7068492
-3,3	-32,373	0	-2,53E-02	-6,44E-03	-0,015844

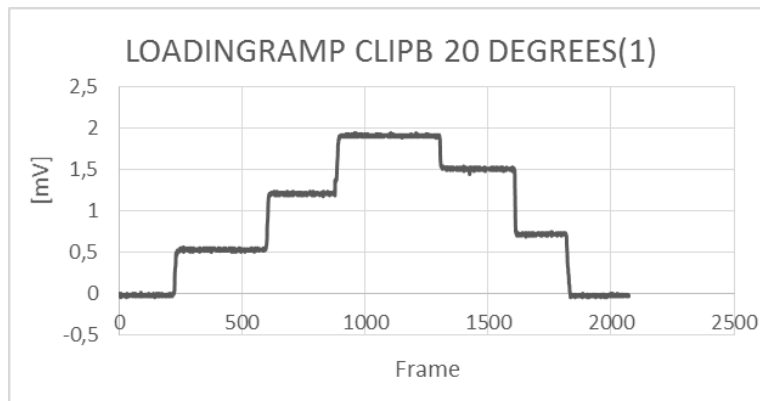*Figure2. 20 Calibration 0 [DEG] data*
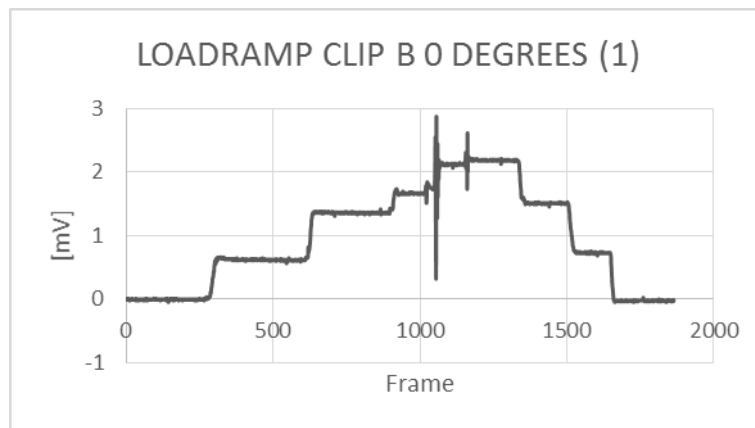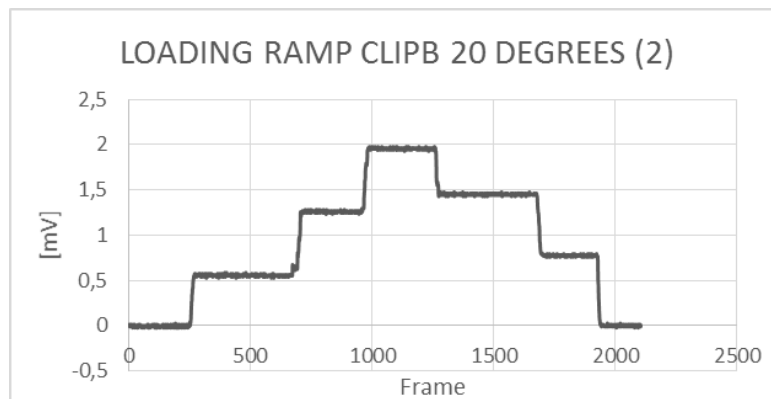

Figure2. 81 Calibration ramp (1)
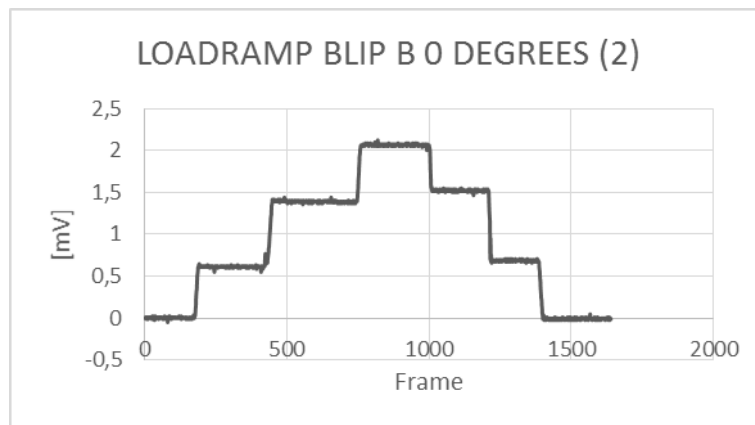
Figure2. 22 Calibration ramp (2)
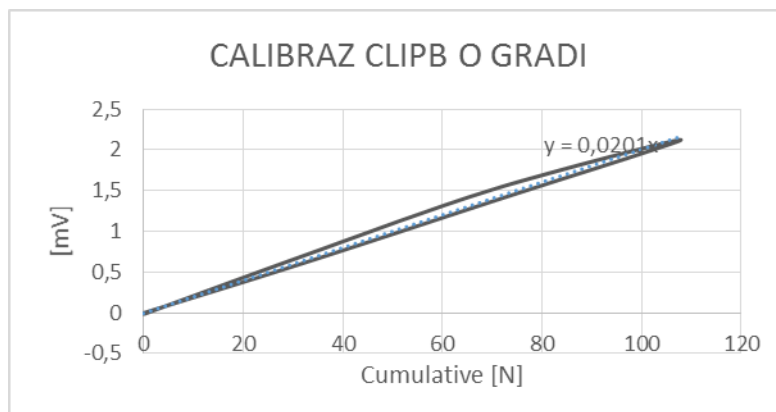
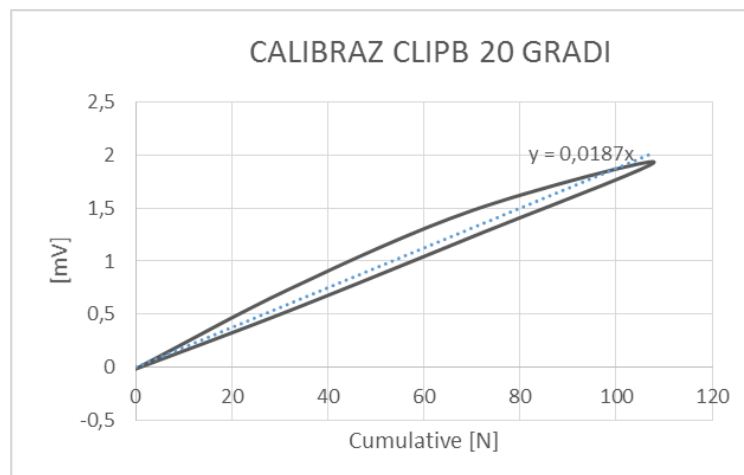*Figure2. 23 Trend line for 0 [DEG] calibration*

From this graph above it is possible to see that the trend line slope is:

$$= 0,0 2 0 \left[\frac{1}{}\right]$$

The calibration constant C is given by:

$$0 = \frac{1}{0,0 2 0 1} = 1 4 9 7 5 1 \left[\frac{2}{4}\right]$$

2.8.2 Calibration 20 degrees

kg	N	Ncumulati	mV1	mV2	mV (media
0	0	0	-2,06E-02	-6,91E-03	-0,01377
3,3	32,373	32,373	5,29E-01	5,54E-01	0,541311
3,85	37,7685	70,1415	1,21E+00	1,26E+00	1,231588
3,85	37,7685	107,91	1,91E+00	1,96E+00	1,932564
-3,85	-37,7685	70,1415	1,51E+00	1,45E+00	1,478882
-3,85	-37,7685	32,373	7,18E-01	7,74E-01	0,746161
-3,3	-32,373	0	-2,65E-02	-9,51E-04	-0,01374

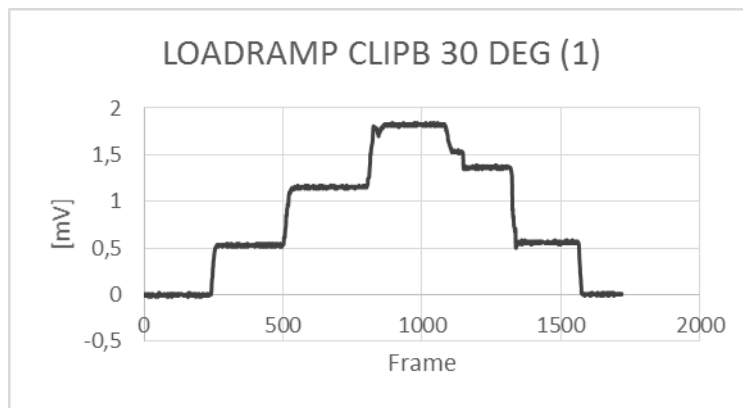*Figure2. 24 Calibration 20 [DEG] data*
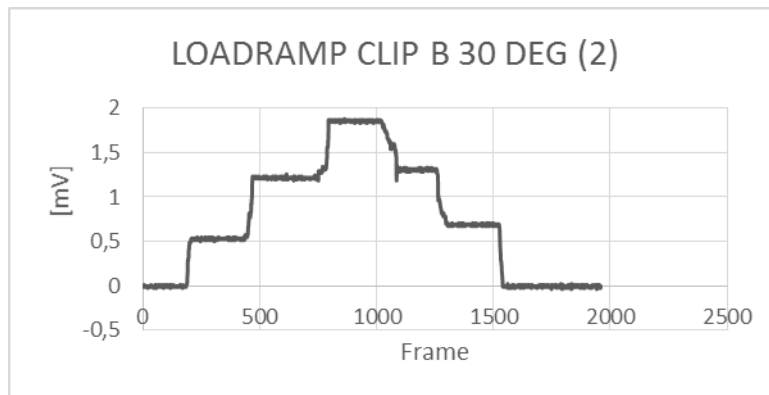

Figure2. 9 Calibration ramp (1)
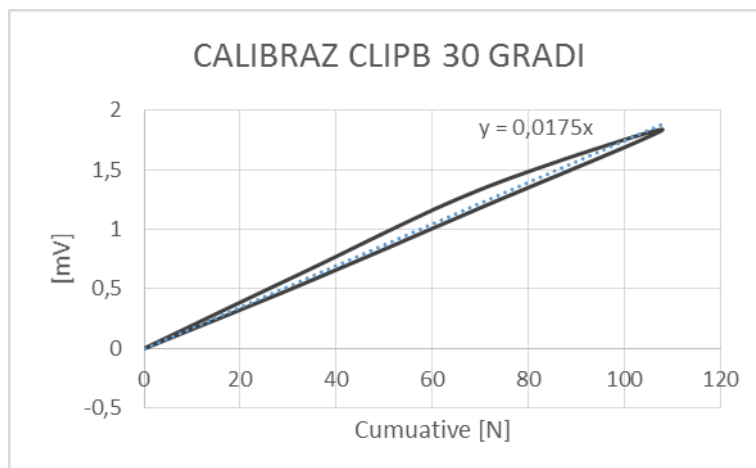

Figure2. 26 Calibration ramp (2)

Figure2. 27 Trend line for 20 [DEG] calibration

From this graph it is possible to see that the trend line slope is:

$$= 0.0\ 1\ 8\ [\ 7\ ]$$

The calibration constant C is given by:

$$2\ 0 = \frac{1}{0.0\ 1\ 8\ 7} = 5\ 3\ 4\ 7\ 5\ [\ 9\ 4\ ]$$

2.8.3 Calibration 30 degrees

kg	N	Ncumulati	mV1	mV2	mV (media
0	0	0	-4,84E-04	-4,23E-03	-0,00236
3,3	32,373	32,373	5,31E-01	5,29E-01	0,530041
3,85	37,7685	70,1415	1,15E+00	1,22E+00	1,18364
3,85	37,7685	107,91	1,82E+00	1,85E+00	1,838038
-3,85	-37,7685	70,1415	1,37E+00	1,31E+00	1,33741
-3,85	-37,7685	32,373	5,60E-01	6,88E-01	0,624444
-3,3	-32,373	0	5,80E-03	-4,20E-03	0,0008

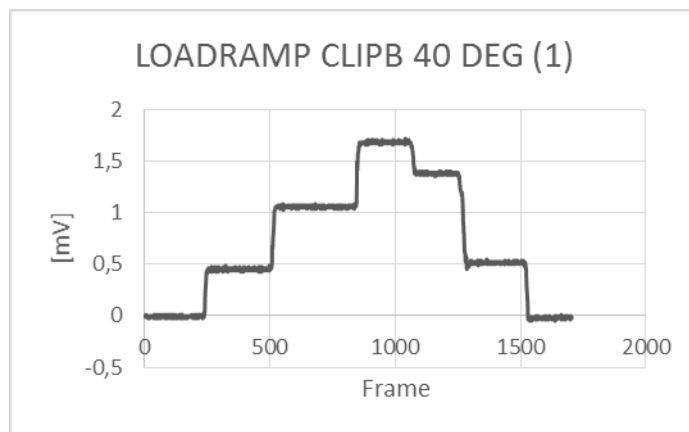*Figure2. 28 Calibration 30 [DEG] data*

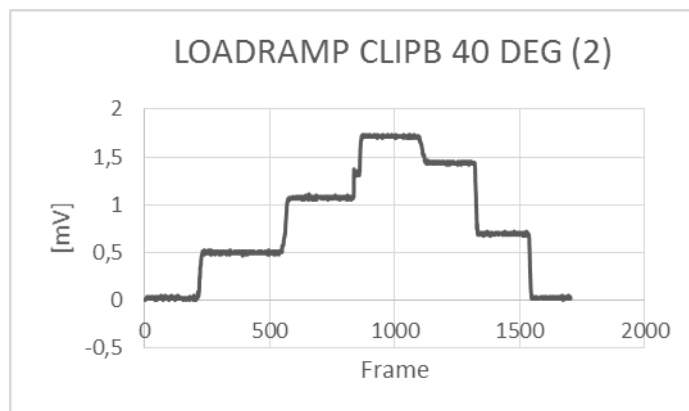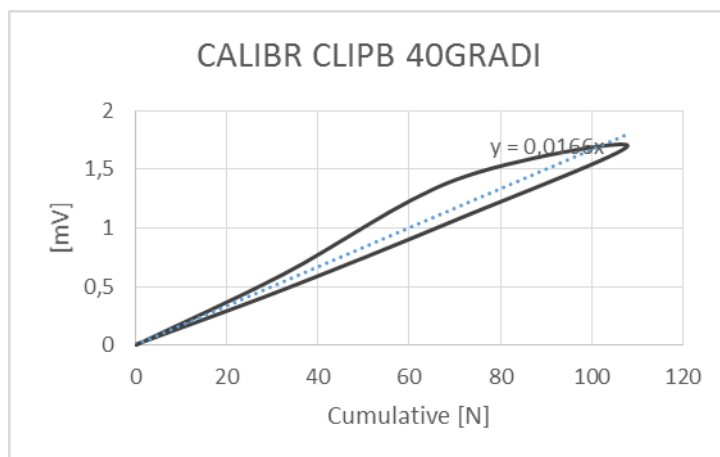*Figure2. 10 Calibration ramp (1)*

Figure2. 30 Calibration ramp (2)

Figure2. 31 Trend line for 30 [DEG] calibration

From this graph it is possible to see that the trend line slope is:

$$= 0{,}0\ 1\ 7[\ \cancel{5}\ ]$$

The calibration constant C is given by:

$$3\ 0 = \frac{1}{0{,}0\ 1\ 7\ 5} = 5\ 7\ 1\ 4\ 2\ [\cancel{3\ 6}]$$

2.8.4 Calibration 40 degrees

kg	N	Ncumulati	mV1	mV2	mV (media
0	0	0	-5,80E-03	2,18E-02	0,007979
3,3	32,373	32,373	4,53E-01	4,97E-01	0,474888
3,85	37,7685	70,1415	1,06E+00	1,07E+00	1,066128
3,85	37,7685	107,91	1,69E+00	1,71E+00	1,700014
-3,85	-37,7685	70,1415	1,38E+00	1,44E+00	1,409302
-3,85	-37,7685	32,373	5,15E-01	6,95E-01	0,605118
-3,3	-32,373	0	-2,06E-02	2,46E-02	0,002015

Figure2. 32 Calibration 40 [DEG] data

Figure2. 33 Calibration ramp (1)

Figure2. 124 Calibration ramp (2)

Figure2. 115 Trend line for 40 [DEG] calibration

From this graph it is possible to see that the trend line slope is:

$$= 0,0 1 6 [6]$$

The calibration constant C is given by:

$$4 0 = \frac{1}{0,0 1 6 6} = 6 0 2 4 0 9 [6]$$

For every boot tested, the force action between the clip and the buckle was between 30 and 40 degrees. It has been laniary interpolated to the constant between these two values.

Below are reported these interpolations for the clip A, clip B and clip C.

Clip A 30°- 40°		CLIP B 30°-40°		CLIP C 30°-40°	
DEGREES	CONSTANT	DEGREES	CONSTANTS	DEGREES	CONSTANT
30	40,4	30	57,14286	30	41,667
31	40,756	31	57,45267	31	41,92507
32	41,112	32	57,76248	32	42,18314
33	41,468	33	58,07229	33	42,44121
34	41,824	34	58,3821	34	42,69928
35	42,18	35	58,69191	35	42,95735
36	42,536	36	59,00172	36	43,21542
37	42,892	37	59,31153	37	43,47349
38	43,248	38	59,62134	38	43,73156
39	43,604	39	59,93115	39	43,98963
40	43,96	40	60,24096	40	44,2477

Figure2. 36 Interpolation of constant values from 30° to 40°

2.9 Dynamic in vivo tests with clips

In order to understand the values of the clamping forces on each buckle a new test has been set using the same events scheduled before for the full bridge buckle.

- ‹ Wearing boot completely open (zero position)
- ‹ Light closure of the buckle
- ‹ Max closure of the buckle
- ‹ Approaching the ski
- ‹ Unweight boot
- ‹ Hook tip
- ‹ Hook boot
- ‹ Put on the clip from buckle 2 to 4
- ‹ Max forward flexion
- ‹ Max backward extension
- ‹ 5 cycles of forward/backward flexion/extension movements
- ‹ Unhook boot
- ‹ Unhook tip
- ‹ Unweight the boot
- ‹ Enclosure the boot's buckle

Figure2. 37 Example of clips positioning on buckle

It is important to note that during the test the clip on the buckle 1 (the one closest to the tip) was not used because of the geometry of the boot.

The buckle 1 cannot be closed using the lever mechanism and the clip all together.

For the first test, the tester was able to close the book how he preferred.

The degrees of the force action to use the proper constant were taken using the software IMageJ.

The test shows these results:
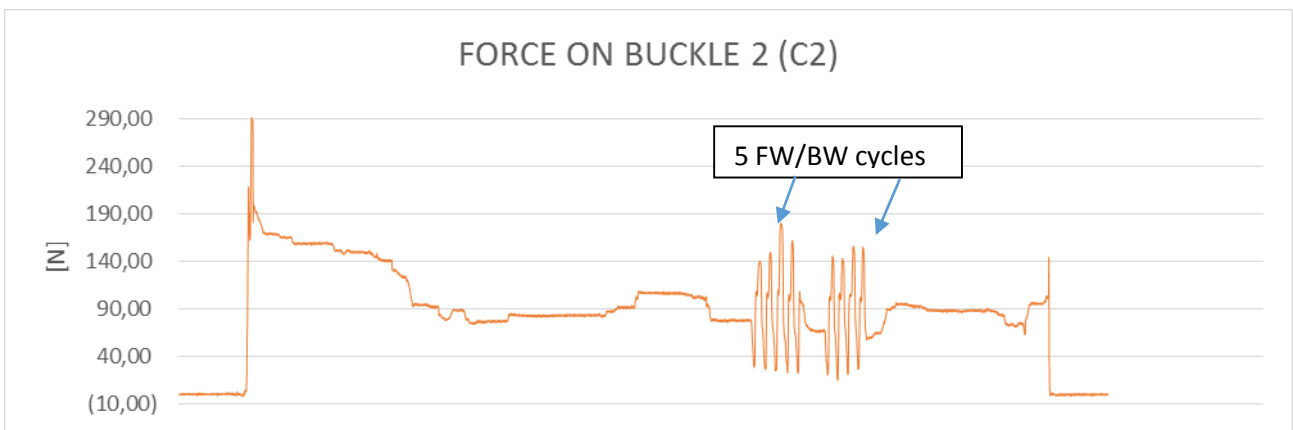
Figure2. 138 Signal for clip on buckle 2 C2

The results on C2 show that during the forward flexion the clip discharges and during the backward extension the clips feels an increasing force.
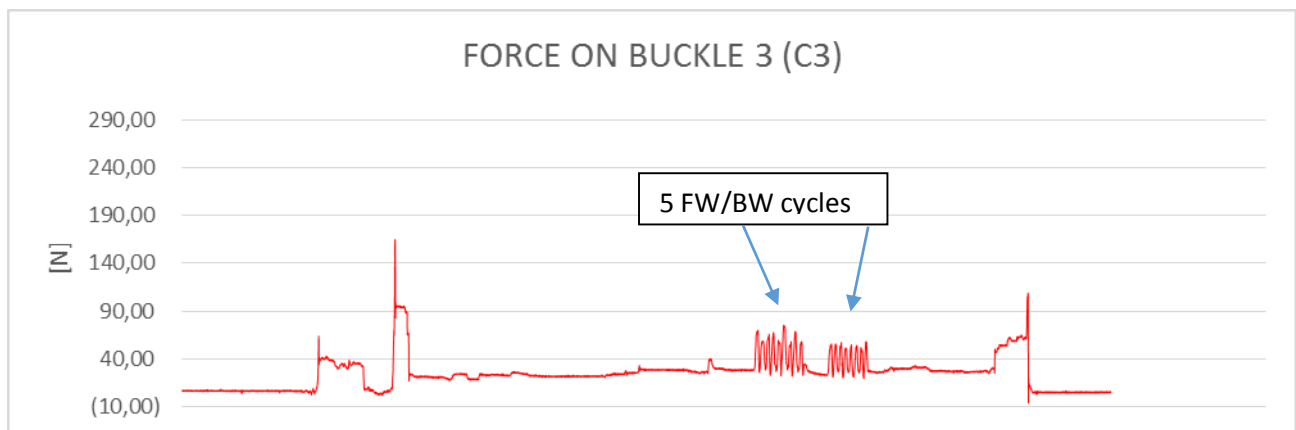
Figure2. 149 Signal for clip on buckle 3 C3

It is possible to see as that during both forward flexion and backward extension the forces increase.
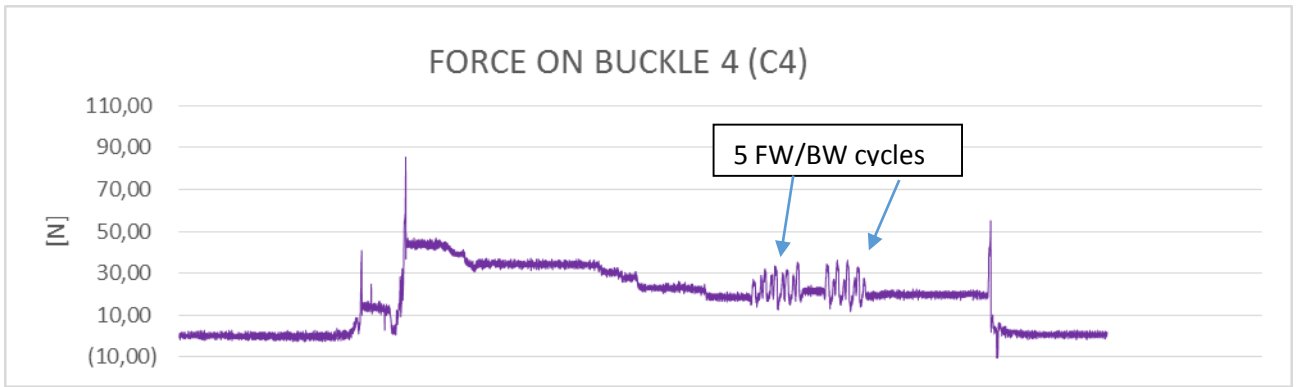
Figure2. 40 Signal for clip on buckle 4 C4

The results of the graph indicate that here the forces increase mostly during forward flexion, however during backward extension it is also possible for the force to enhance.

2.10 comparison between Strain Gauged buckle and Clips

It is interesting to check if while performing multiple tests with the strain-gauged buckle and the load cell clips, the systems are comparable in terms of the force outputs.

In order to understand that the two singles are comparable, one can look at the graph where the difference was calculated between them.

Below is an example for the hard closure but the same conclusions are found for the soft one.
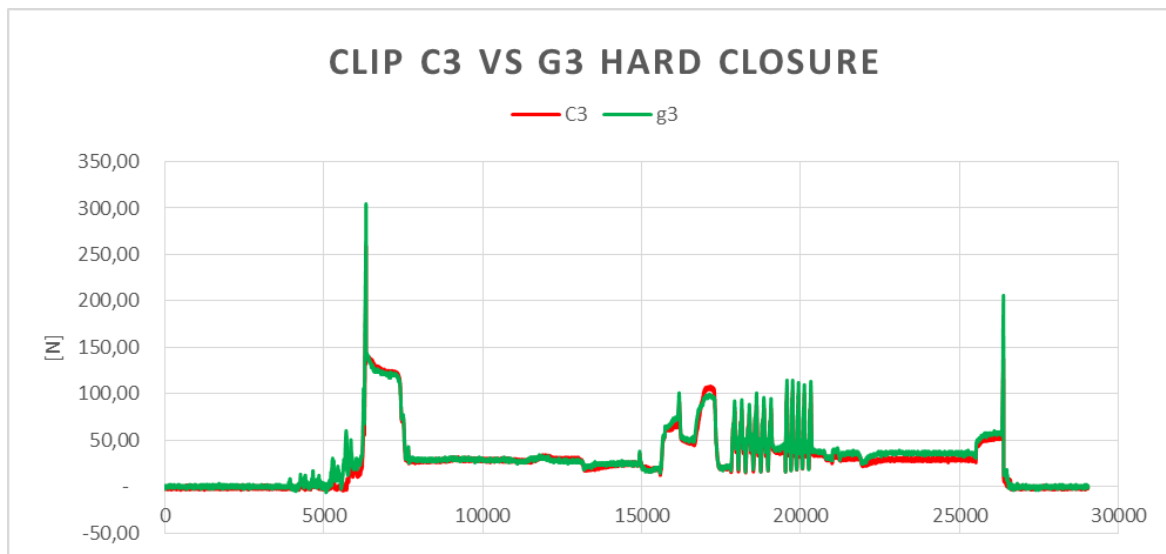
Figure2. 41 Compared signals
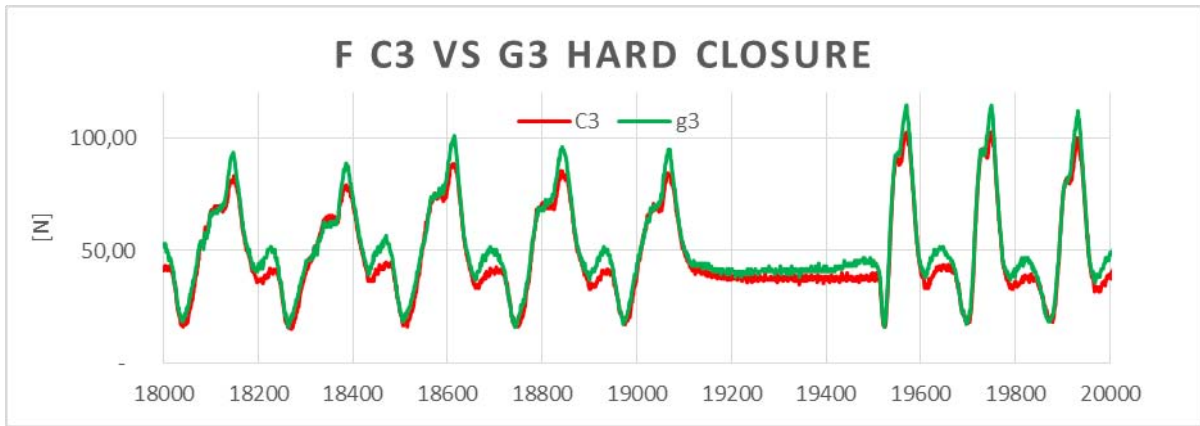
Figure2. 42 Zoom of the signal

Segments of each graph were chosen in order to calculate points independently to identify the difference of Delta and the Delta percentage between the two curves.
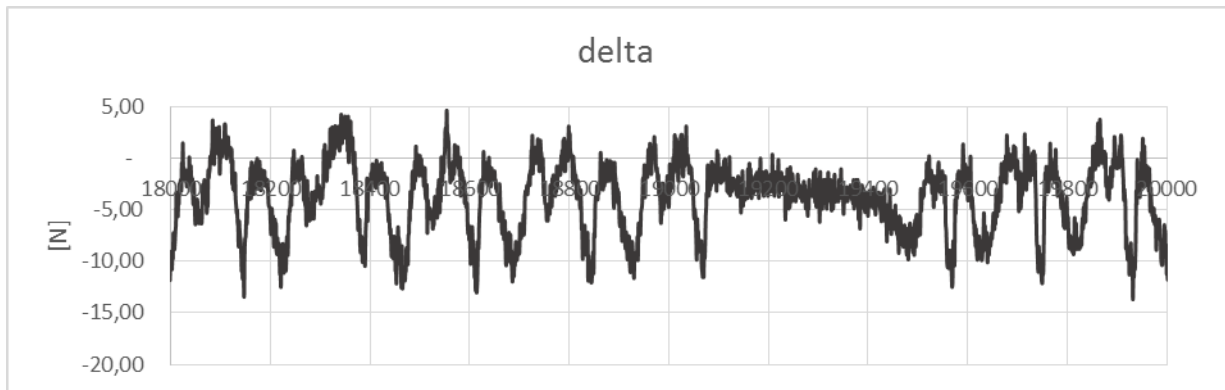
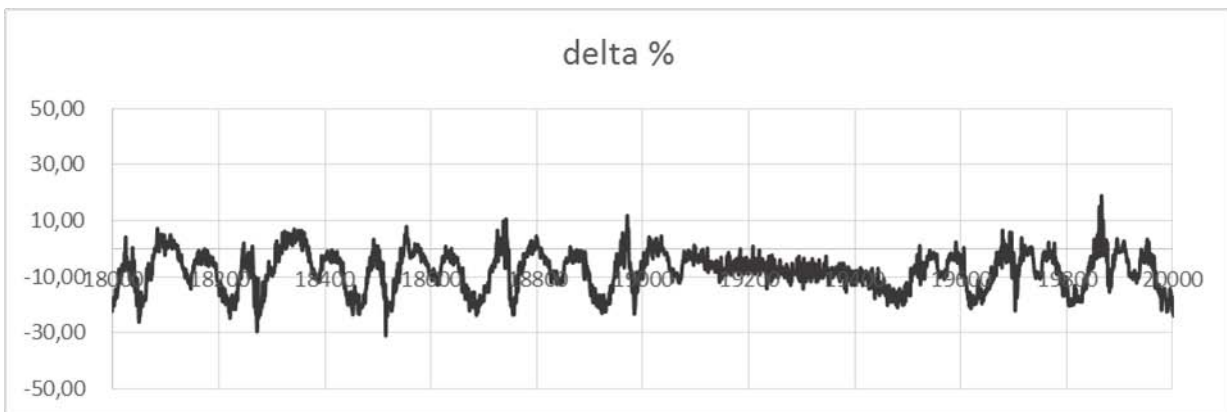

Figure2. 153 Delta [N] of the zoomed part

Figure2. 44 Delta % of the zoomed part

Using the Excel formula, it was calculated that the correlation between the 2 signals outcome was 97%.

In conclusion, it is possible to say that there is a high correlation between the feelings of the two different systems while performing the tests in the laboratory.
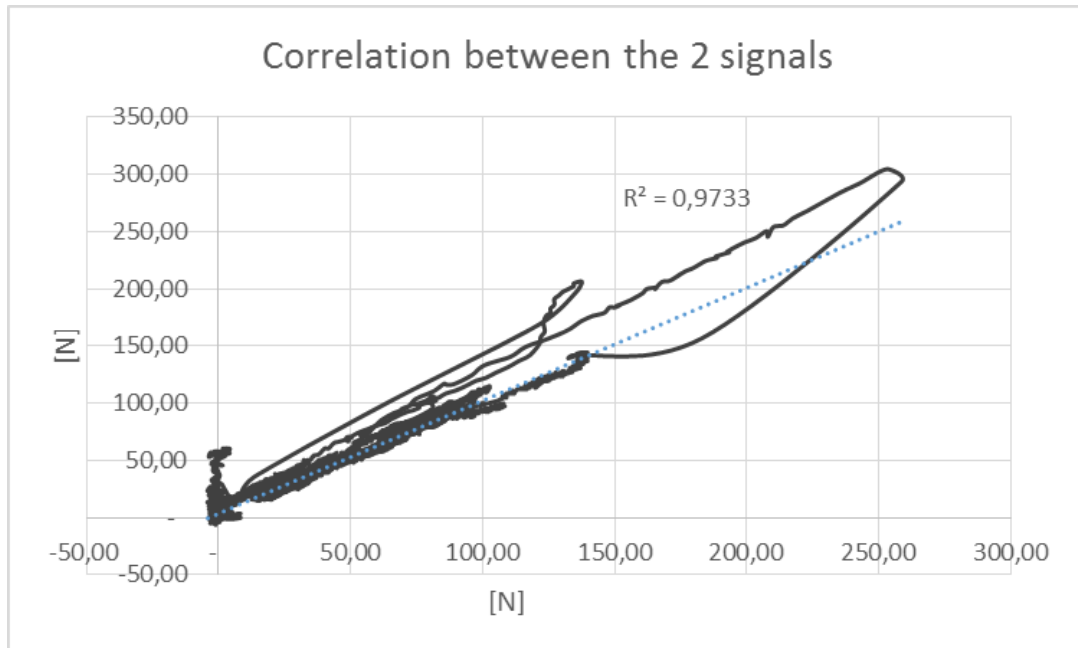
Figure 2. 45 Correlation between the two signals

Chapter 3: San Vito di Cadore Indoor tests

3.1 Aim of the Test

To obtain data for the project it was necessary to plan some tests on the ski slopes where the target was to set all the necessary instruments on a tester and then collect the signals coming out during a real skiing condition.

With these analyses, the work from the group moved a number of times throughout San Vito di Cadore, a small village near Cortina (BL).

During the test days, the weather did not always cooperate to allow skiing. Therefore, the laboratory was used inside the house to perform some of the simulated skiing experiments.

With the collaboration of people coming from The University of Innsbruck, it was planned to test two different pairs of boots on a force platform. This was done by using the load cells clips and electro goniometer to understand how the closure of the boots made changes for clamping forces, and on the angles between shell tibia, reached in a simulated skiing.

3.1.1 Terminology

In order to facilitate the comprehension of this chapter, the terminology will be given.

- ‹ C2 = force on buckle 2 using the load cell clip
- ‹ C3 = force on buckle 3 using the load cell clip
- ‹ B3 = force on buckle 3 using the strain gauges directly applied on the buckle
- ‹ Strap = force on strap using the load cell
- ‹ In vivo test = laboratory test performed using the real tester leg
- ‹ In field test = test performed directly on the slope
- ‹ Soft closure = minimum closure reachable using the load cell clips
- ‹ Hard closure = maximum closure reachable using the load cell clips
- ‹ Mild FWD flexion = mild fwd skiing movement simulation
- ‹ Strong FWD flexion = strong fwd skiing movement simulation

3.1.2 Instrumentation

The two pairs of boots used for the test were the TECNICA DIABLO MAGMA 120 and TECNICA PHX 70.

Figure 3. 2 Tecnica diablo magma 120

Figure 3. 1 Tecnica Phx 70

The other instrumentation used were:

- ‹ Force Clips in order to measure for both the boots the clamping force
- ‹ Acquiring system HBM Somat allows the record of the signals of force clips
- ‹ Strain gauge buckle on the Tecnica Phnx70 in order to compare the signals coming out from the force clip and the buckle
- ‹ Force Platform Bertec used to calculate the ground reaction force and the moment at the hinge of the boot during a simulated skiing session
- ‹ Electro goniometer placed on the boot In order to see the angle variation of shell cuff, cuff tibia and shell tibia during the skiing simulation
- ‹ The Pocket EMG from HP acquired the signals of the electro goniometers.

The same tester tested both the boots with two different types of closure; the lighter closure and hardest closure.

During the setup of the runs it was realized that the one of the load cell clips was not working because of a problem with the strain gauges, and it was not possible to replace it.

For the runs, there were only two left of the load cell clips. It was thought to put them on the buckle number 2 to study its strange behaviour and on the number 3 because it was possible to compare it with the strain gauges applied directly on the buckle of Tecnica PHNX 70.

3.1.3 Test protocol

The sequence of the test was planned in order to give repeatability to the data acquired and to easily compare them.

1. Boot completely open in order to have the Zeros of the system
2. Lift the boot from the ground in order to have the characteristic angle of the boot
3. Hook the boot in the binding of the ski
4. Perform a soft/hard closure of the boot with the clips on the buckle 2 and 3 and on the strap
5. Perform a maximum forward flexion and a backward maximum extension
6. Perform 5 mild flexion movements

7. Perform 5 strong flexion movement

8. Unclose the boot starting from the strap coming down from buckle 4 to 1

9. Unhook the boot from the binding.

3.2 Tecnica Diablo Magma 120

The first tests were performed with the ski boot Tecnica Diablo 120.

This kind of boot, considered as a high performance boot, has a nominal Flex Index of 120, it was designed for an advanced skier.

The constants used for the load cells clips were choose after the calculation of the α angle between the force line of the buckle in respect to the load cell clip using the software ImageJ.

Figure 3. 3 Example of angle measure

Boot	Buckle	Clip	Closure		K [N/mV]
Diablo120	2	B	Soft	32°	57,7625
Diablo120	3	C	Soft	33°	42,4421

Constants for the hard closure are also reported.

Boot	Buckle	Clip	Closure		K [N/mV]
Diablo120	2	B	Hard	30°	57,14286
Diablo120	3	C	Hard	30°	41,66667

3.2.1 Buckle 2 signal (C2)

It is possible to compare the force on buckle 2 in two different conditions of closure:
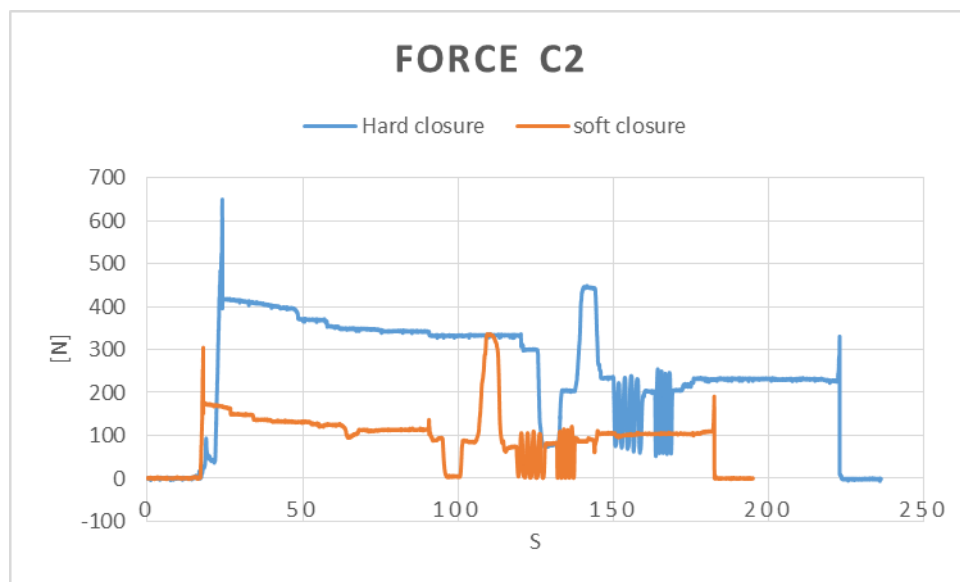
Figure 3. 4 Difference of force on C2

After multiplying the coming out signals for their constants it is possible to see how the force felt on the buckle 2 increases with the closure and its trends to decrease during the forward flection and augment during the backward extension.

It easy to see that with the softer closure with the force in the maximum forward flection, the force goes near to the zero value. This means that the buckle completely unloads; this does not happen with the harder closure.

3.2.2 Buckle 3 signal (C3)
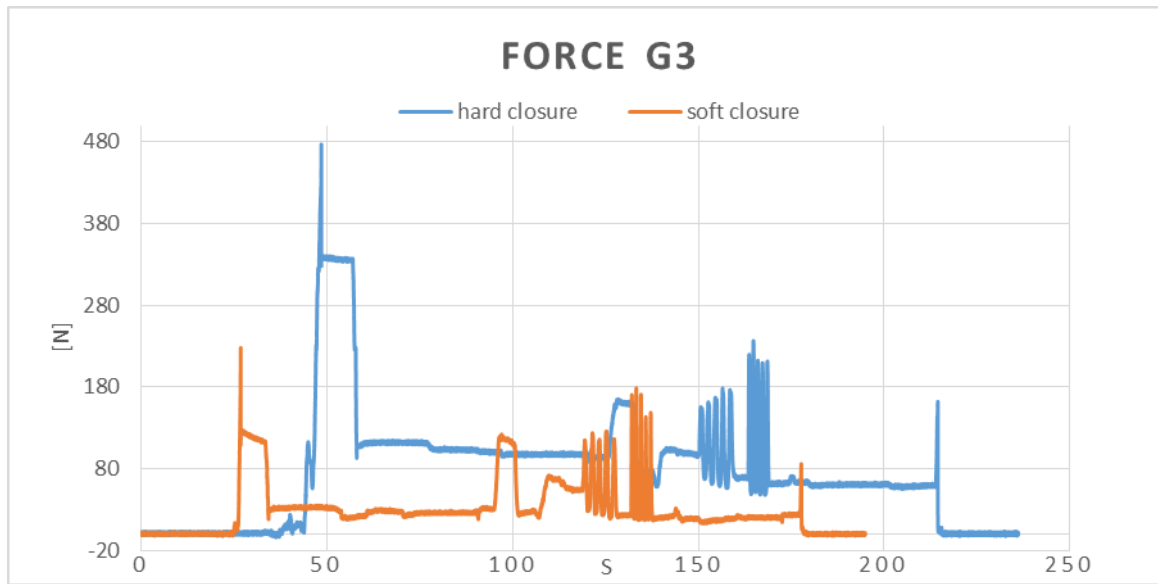
Figure 3. 5 Difference of force C3

It is possible to see the results coming out on the graph that the signal of the force felt on the buckle increases with the closure.

The force on the buckle 3 has different trends than the one of the buckle 2. In fact, it grows during the 5 forward flexion and decrease when the tester performs a backward extension.

From the beginning of the test, it is possible to observe that when the moment of the buckle is closed, the instant pick value of the force is at 50s.

3.2.3 Velcro Strap signal

It is possible to compare the force on strap in the two different conditions of closure:
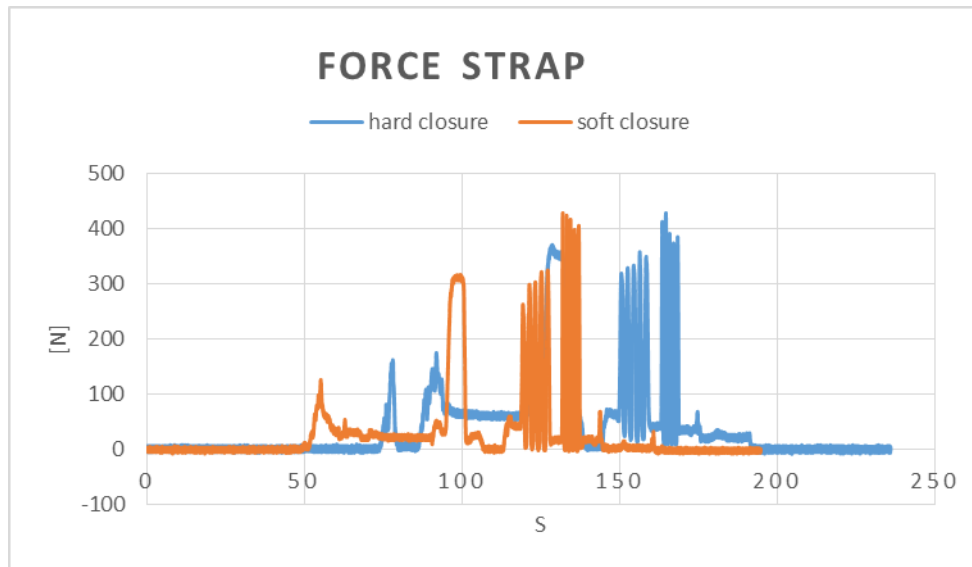
Figure 3. 6 Difference of force on Strap

It is possible to see that the results coming out on the graph have a signal that the force felt on the strap lightly increases with the closure.

The force on the strap has the same trend of the buckle 3; in fact, it grows during the 5 forward flexion and decreases when the tester performs a backward extension.

3.2.4 Measure of the Bending Moment and Shell-Tibia angle

The test was performed on a force platform, which can detect the three force components: force Fx, Fy and the reaction force of Fz perpendicular to the ground.

The ski was clamped on the platform. From this it is possible to calculate the momentum of the hinge after knowing its position. The position has both coordinates of longitudinal axes and in vertical axes. The origins of the axis is the center of the platform.
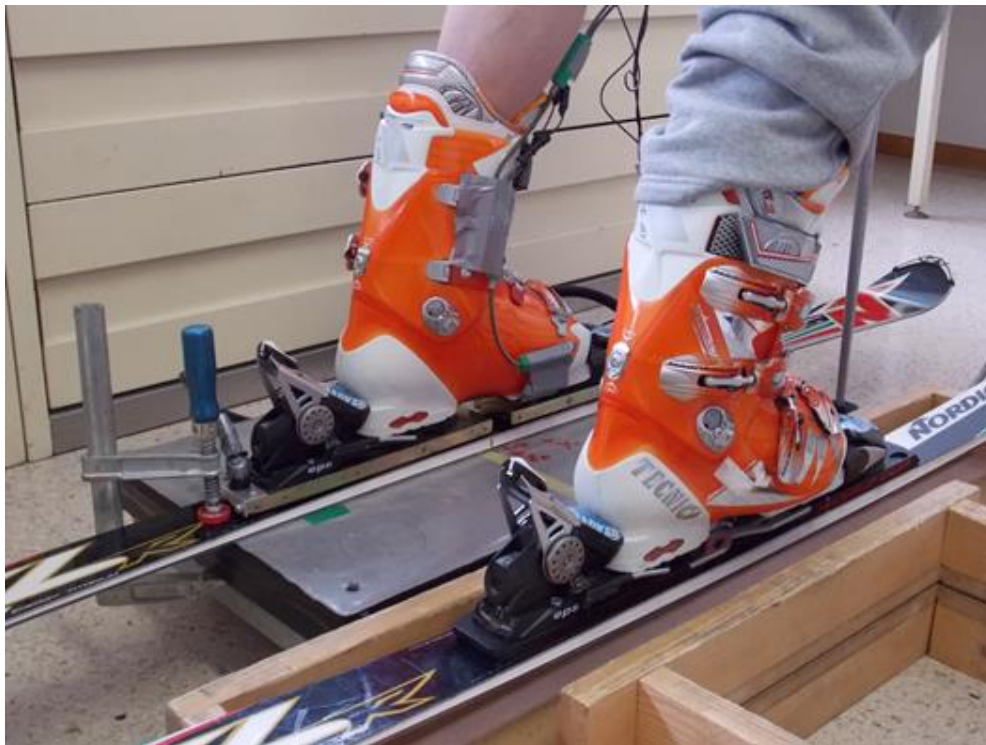
Figure 3. 7 Test setting

The hinge was chosen because it is the nearest measurable point to malleoli of the human leg.

To measure the Shell tibia angle there were two electro goniometer were used and placed in order to give the shell-cuff angle and the cuff-tibia angle; the shell-tiba angle it is the sum of the these two.

In order to have the flatness between the parts of the electro goniometer, attached was the tip of the boot and on the tibia of the tester, two aluminium plates on which it was placed to the electro goniometer.

The aluminium plate nearest to the tip was screwed on the sole of the boot to maintain its stableness and to also make it usable during the in field tests.

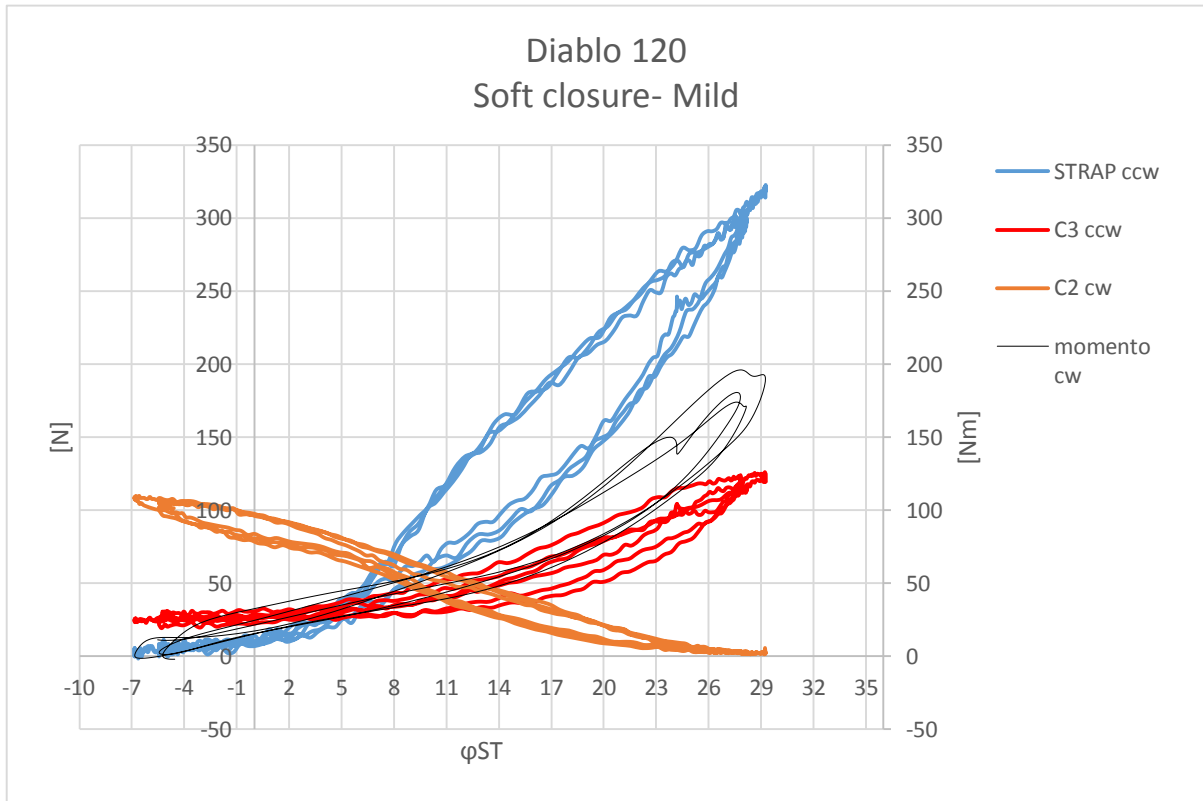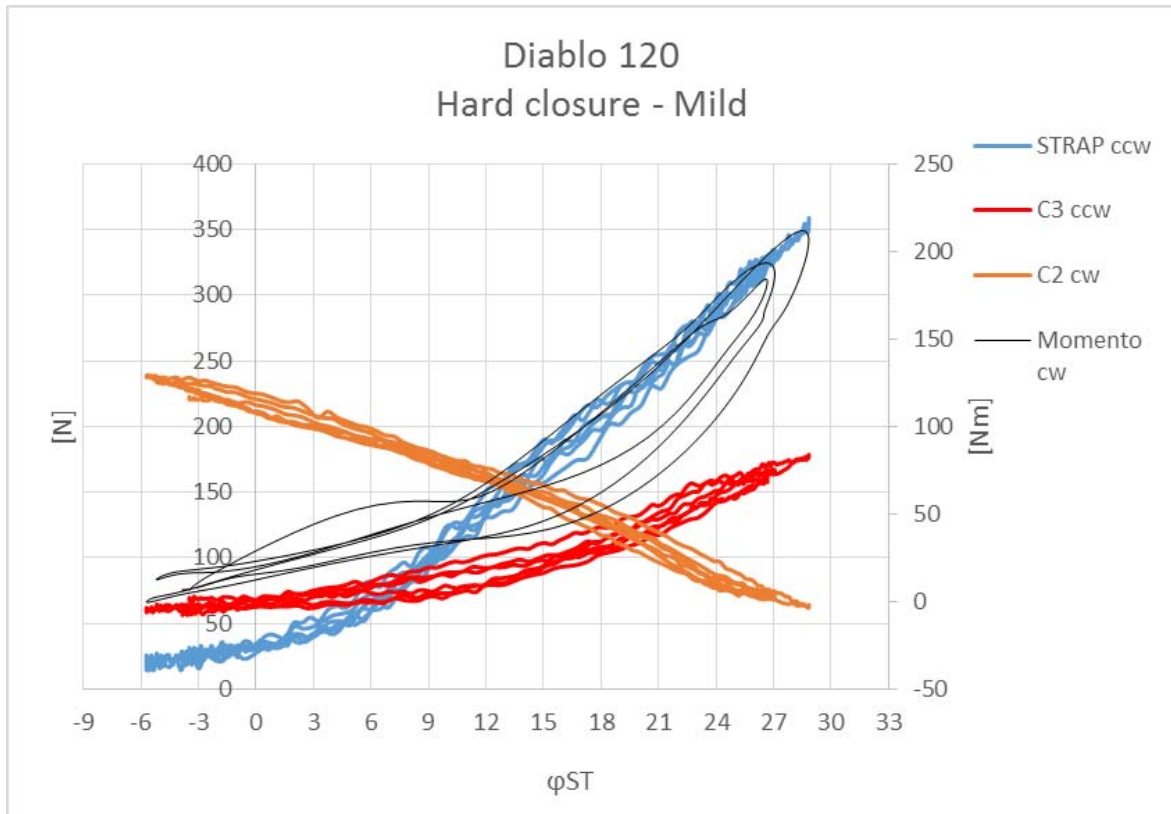*Figure 3. 9 Aluminium thin plate*
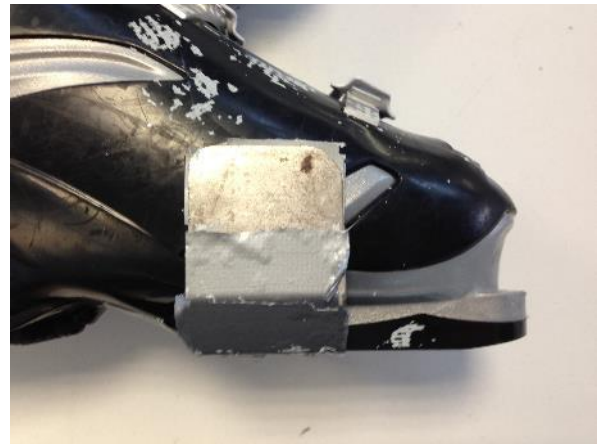
Figure 3. 8 Aluminium thi plate screwed on the boot

Having the values of the force acting on the measured buckles and on the strap and having the momentum acting on the hinge it was thought to graph it in respect to the values of the shell-tibia angles.

After synchronising the angle signal with the force signals, the outcome was three subsequent mild/strong forward flexion's that were taken for both types of closure.

3.2.5 Resulting graphs

Diablo 120
Soft closure- Mild

Diablo 120
Soft closure - Strong

Diablo 120
Hard closure - Mild

Diablo 120
Hard closure - srong
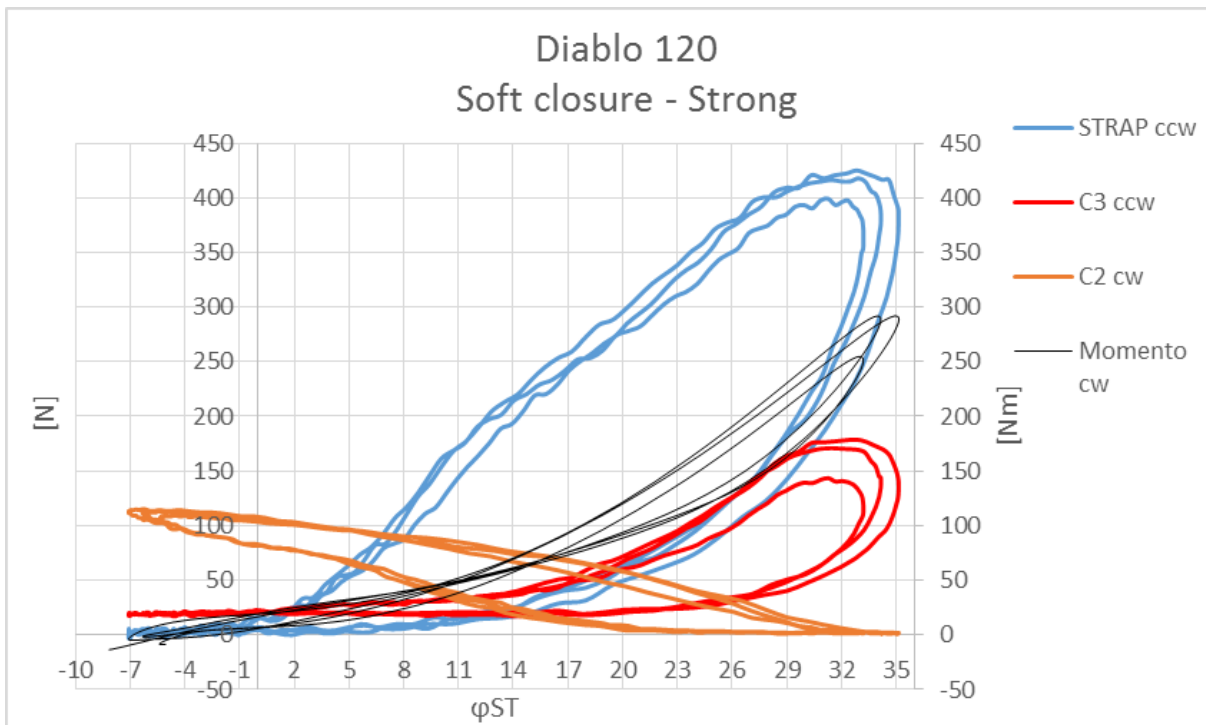
It is possible to see that:

- Between soft closure/hard closure focusing before on the mild flexion and after on the strong flexion that there are not significant changes in the angular range reached in the test.
- Focusing on soft closure it is achievable to see that the cycles in the graph showing the strong flexion have a larger hysteresis area in respect to the one showing the mild flexion.
- Focusing on soft closure it is probable to grasp that the cycles in the graph that are showing the strong flexion have a bigger hysteresis area than as the one showing the mild flexion.

In order to understand the behaviour of the ski boot buckle during this test it would be beneficial for a greater intuitive representation.

3.2.6 Other useful graphs for Tecnica Diablo 120:
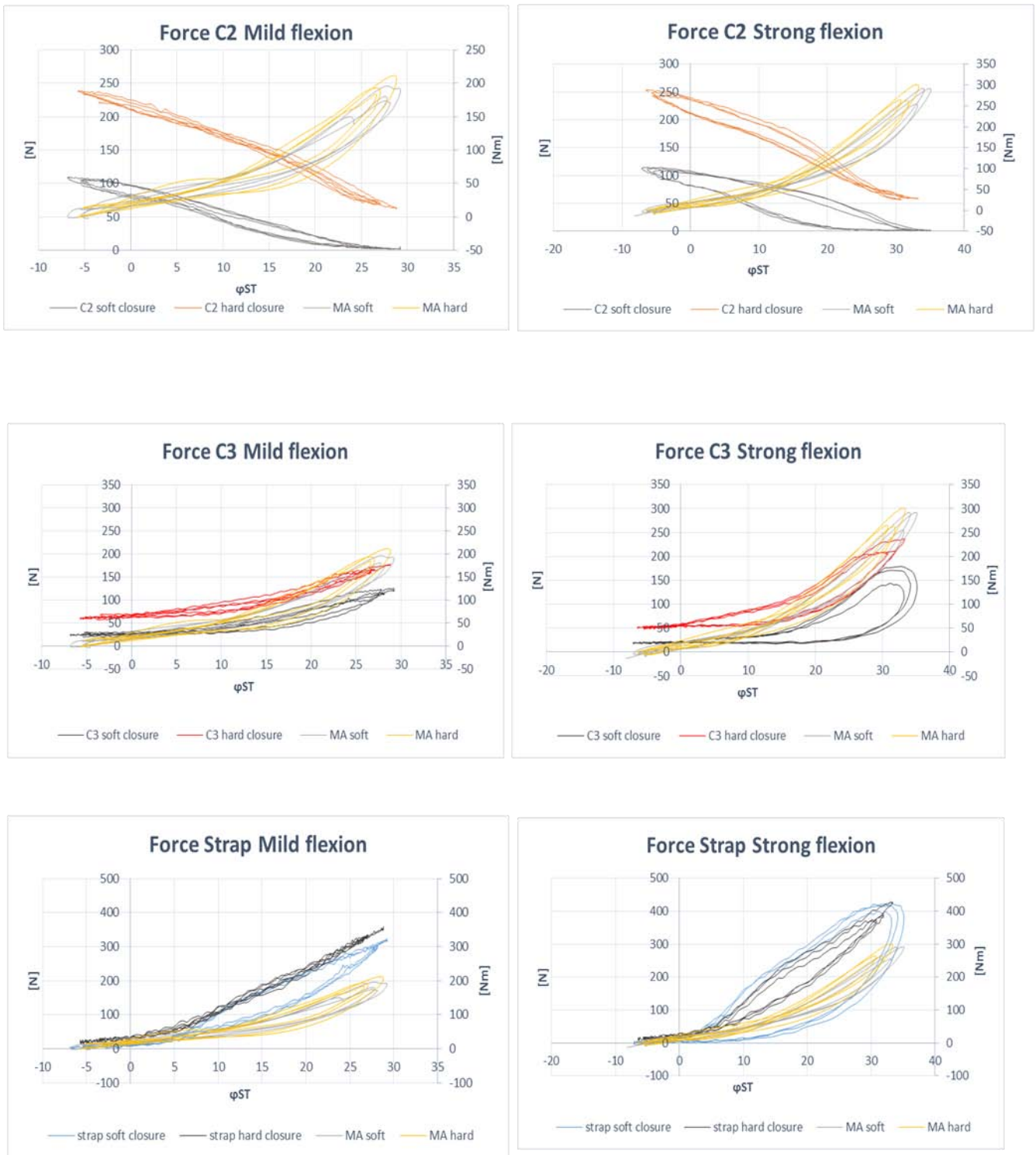
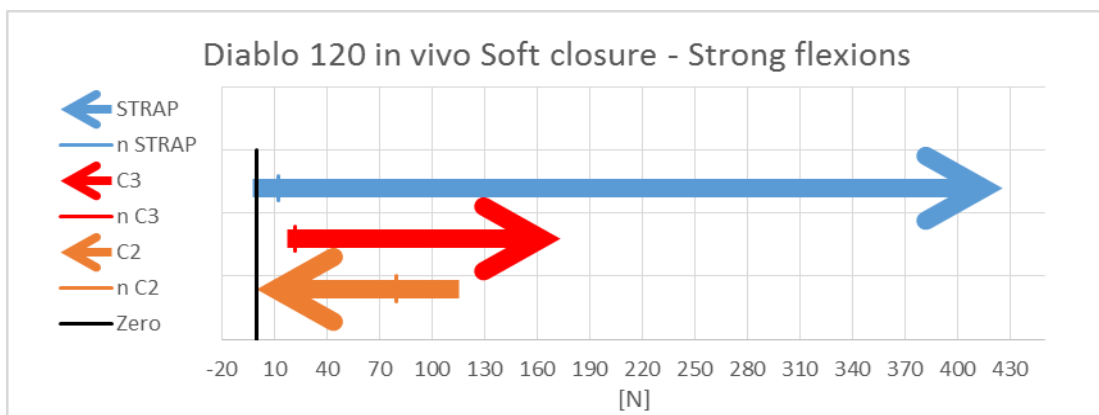

Figure 3. 10 Comparisons with the type of flexion as variable
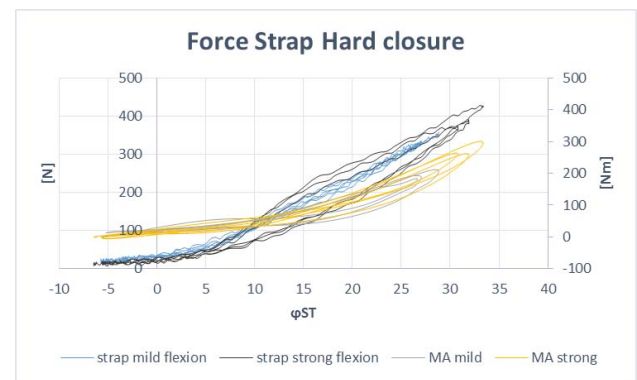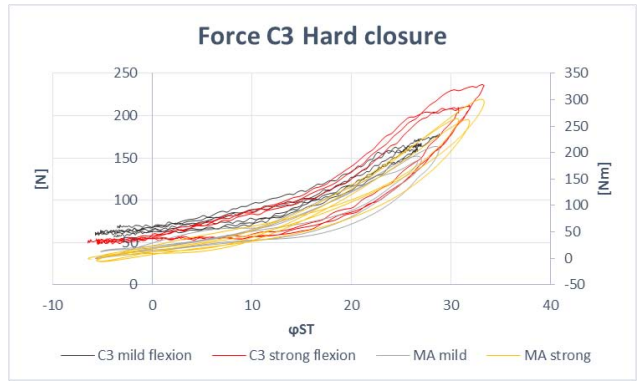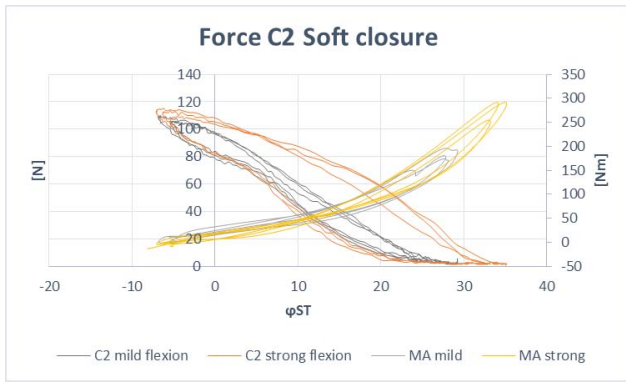
Figure 3. 11 Comparison with the type of closure as variable

3.2.7 Structural review Graphs
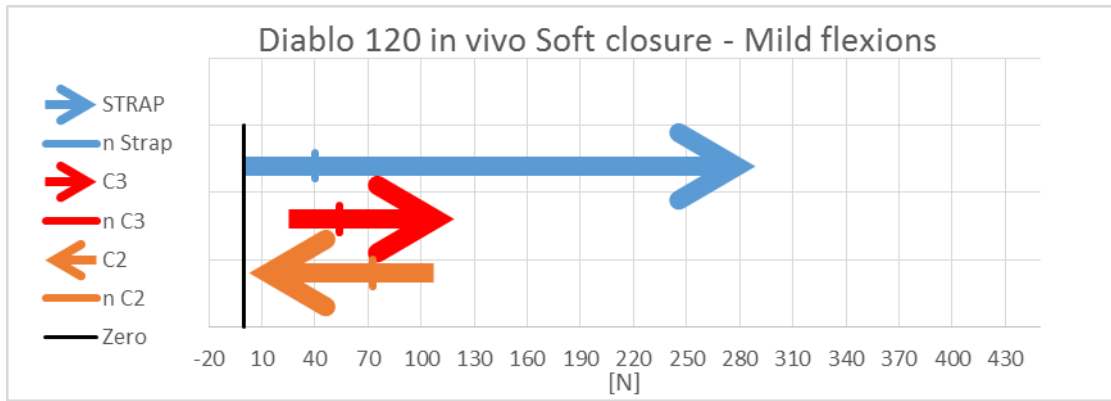
Diablo 120 in vivo Soft closure - Mild flexions

Diablo 120 in vivo Soft closure - Strong flexions

Diablo 120 in vivo Hard closure - Mild flexions

Diablo 120 in vivo Hard closure - Strong flexions

- C2 : force on buckle 2

- C3 : Force on buckle 3

- Strap: force acting on the strap

- n C2: is considered as the buckle 2 closing force when the tester stands in his subjectively zero moment position just before performing the 5 forward flexion

- n C3: is considered as the buckle 3 closing force when the tester stands in his subjectively zero moment position just before performing the 5 forward flexion

- n Strap: is considered as the strap closing force when the tester stands in his subjectively zero moment position just before performing the 5 forward flexion

It is evident to see that in both the runs, with both the soft and hard closure, and in the light and strong flexion the force acting on buckle 2 (C2) is decreasing

Conversely, the forces acting on Buckle 3 (C3) and on the strap (STRAP) augment with the forward movement.

As it was expected that the neutral forces for every buckle increase with the closure but it is possible to see that with the same closure, after the first light movement and before starting the strong flexion, the neutral value reduces its value. This could potentially be because of an adaptation of the plastic material on the boot.

After the forward movement, the tester tried to reach back to the neutral position, but in every condition he passed it.

3.3 Tecnica Phx 70

The second tests were performed with the ski boot Tecnica Phx 70. The same test protocol was used for the previous ski boot.

This boot is considered to be an intermediate performance boot with a nominal Flex Index of 70. Ideally, this boot is meant for an intermediate level skier.

The constants used for the load cells clips were chosen and calculated by the α angle. This is between the force line of the buckle in regard to the load cell clip using the software imagej.

Boot	Buckle	Clip	Closure		K [N/mV]
Phx 70	2	B	Soft	33°	58,07229
Phx 70	3	C	Soft	33°	42,4421

The constants for the hard closure are also reported below:

Boot	Buckle	Clip	Closure		K [N/mV]
Phx 70	2	B	Hard	32°	57,7625
Phx 70	3	C	Hard	34°	42,69928

3.3.1 Buckle 3 (B3) signal

It is feasible to compare the force on buckle 3 in the two different conditions of closure:
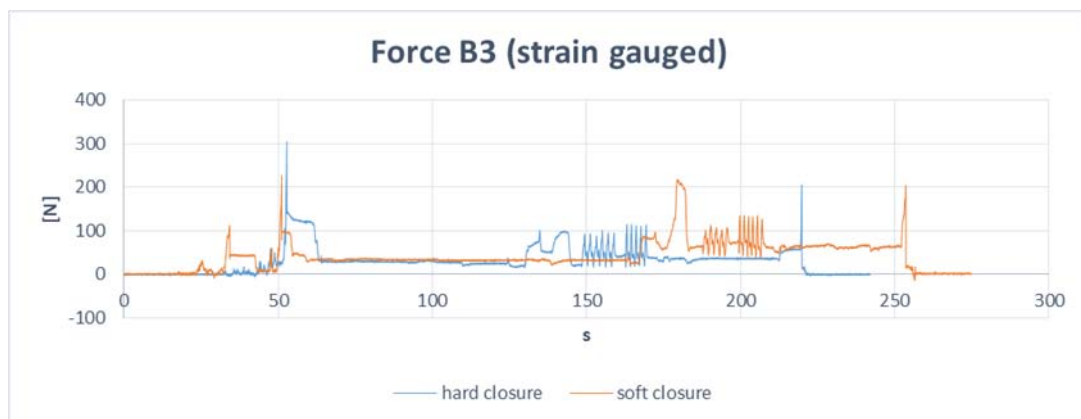
Figure 3. 12 Difference of force signal on B3 with hard and soft closure

The force acting on the buckle 3 (B3) after closing all of the buckles is genuinely the same for the soft and the hard closure.

The force increases on both of the conditions of maximum forward flexion and maximum backward extension.

After the maximum forward flexion and the maximum backward extension, it is possible to observe from the graph that the buckle rests with a greater load through the soft closure.

3.3.2 Buckle 3 (C3) signals

Figure 3. 13 Difference of force signal on B3 with hard and soft closure

This output has the same trend of the one coming out from the Buckle 3 B3 strain gauged and all of the considerations as before are accurate

3.3.3 Velcro Strap signals

It is visible to compare the force on buckle 3 in the two different conditions of closure:

Figure 3. 14 Difference of force on Velcro strap

The results on the graph are detectable as shown on the graph. The signal multiplied for the constant that the force felt on the strap lightly increases with the closure.

The force on strap has the same trend of the buckle 3. In fact, it grows during the 5 forward flection and decrease when the tester performs a backward extension.

Having the values of the force acting on the measured buckles and on the strap while having the momentum acting on the hinge, it was understood to graph it in regards to the values of the shell-tibia angles.

After synchronising the angle signal with the force signals, three subsequent mild/strong forward flexion's were taken for both the type of closure.

The graph below shows the results:

3.3.4 Resulting Graphs

Phx 70
Soft closure - Mild

Phx 70
Soft closure - strong

Phx 70
Hard closure - light

STRAP cw
B3 cw
C3 cw
C2 ccw
MA cw

Phx 70
Hard closure - strong

STRAP cw
B3 cw
C3 cw
C2 ccw
MA cw
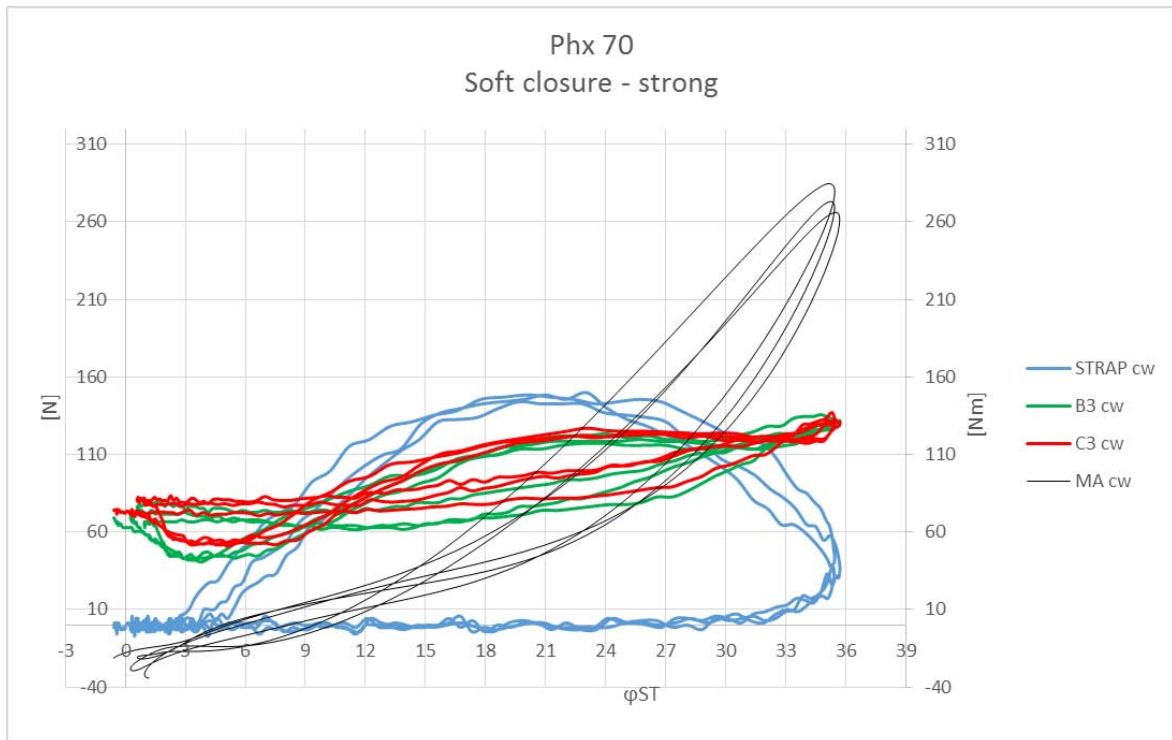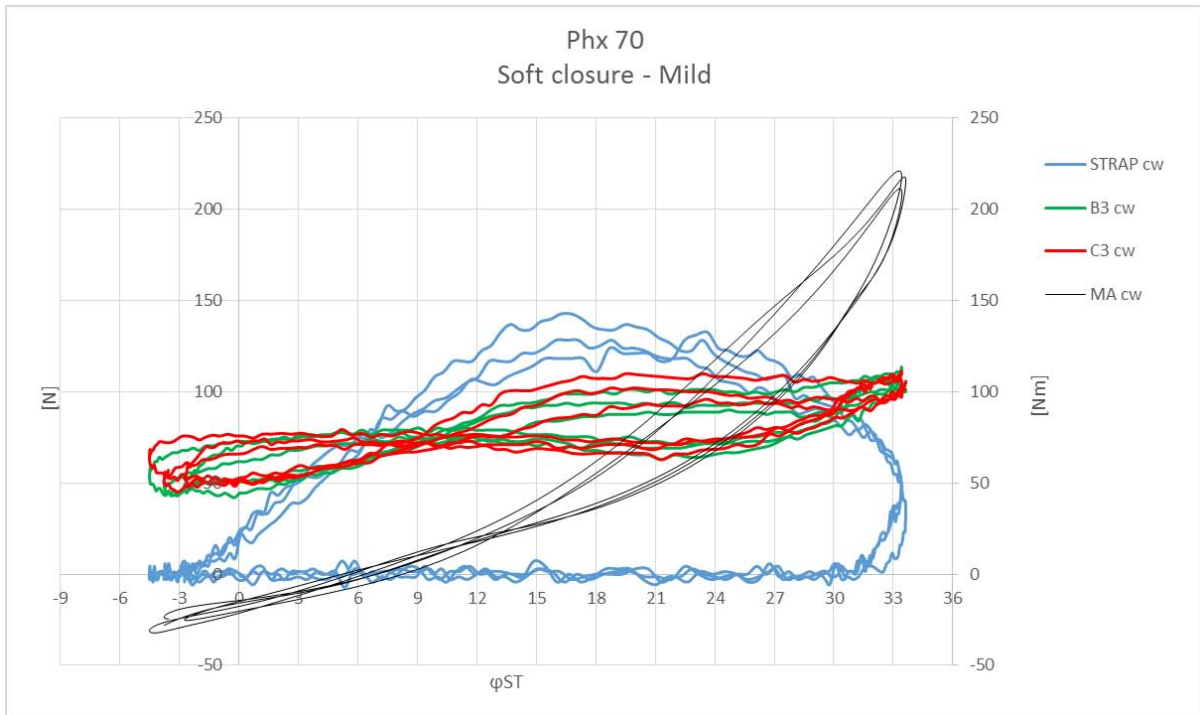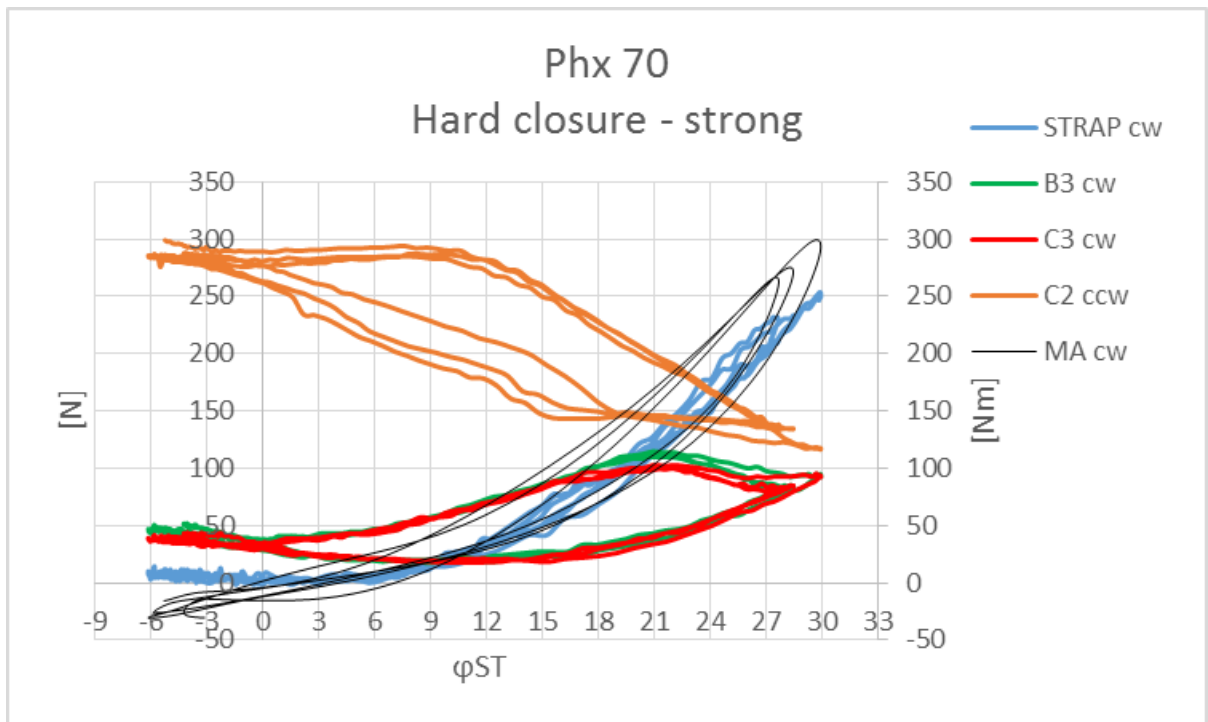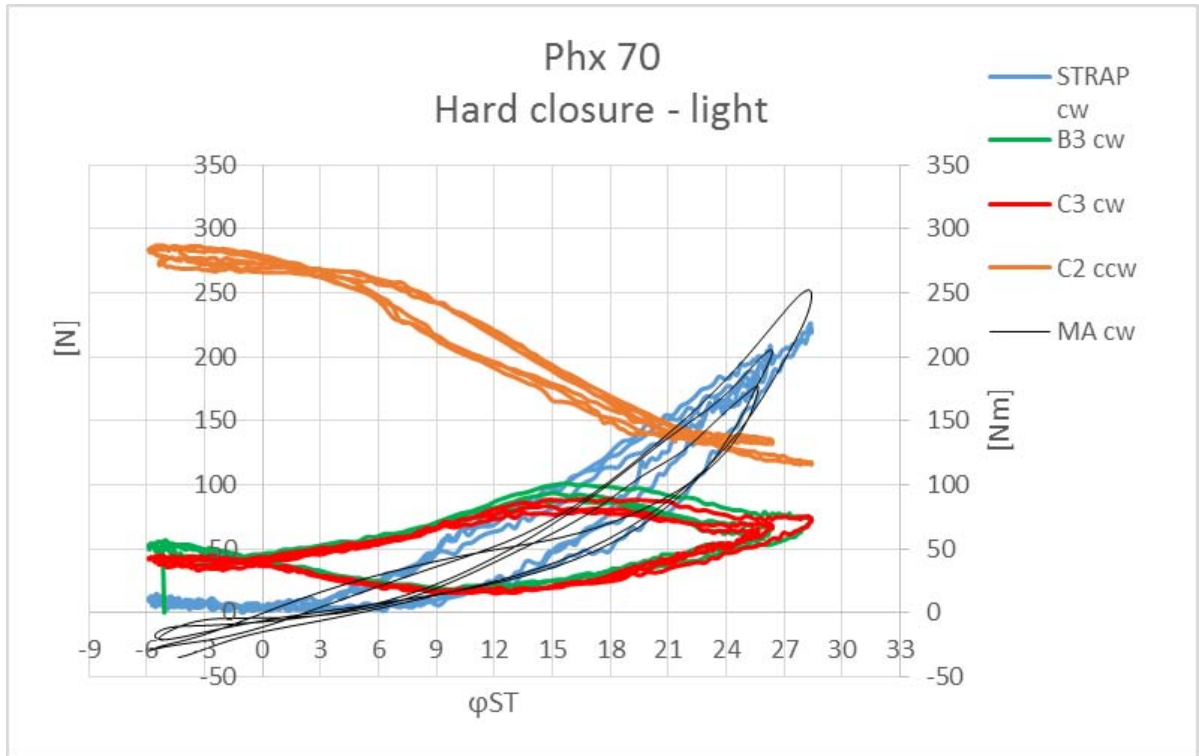
It is possible to see that:

‹ Between soft closure/hard closure when focusing before on the mild flexion and after on the strong flexion there are no significant changes in the angular range reached in the test

‹ Focusing on soft closure it is possible to see that the cycles in the graph show the strong flexion contain a bigger hysteresis area in regards to the one showing the mild flexion.

‹ Focusing on soft closure it is possible to see that the cycles on the graph show that strong flexion has a bigger hysteresis area in regards to the one showing the mild flexion.

‹ At an average angle of 20 degrees of shell-tibia, both C2 and C3 have a slope variation likely due to the fact that the 2 clips measuring the force on the buckle are going to touch.

In order to comprehend the behaviour of the ski boot buckle during this test, it could be helpful for a greater intuitive representation.
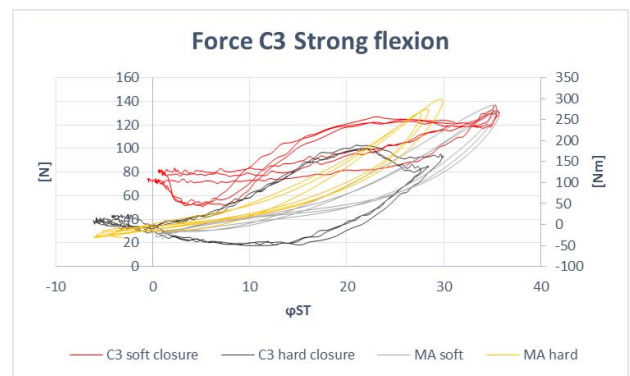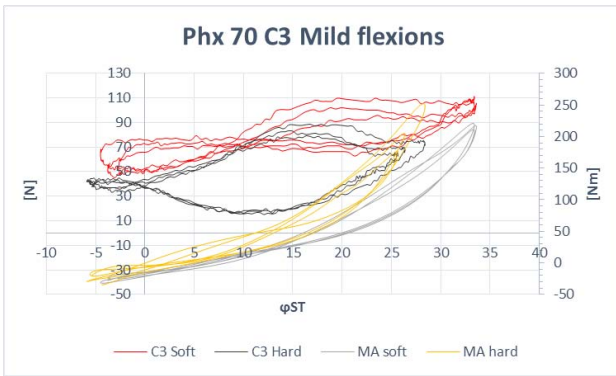
3.3.5 Other useful graphs for Phx 70
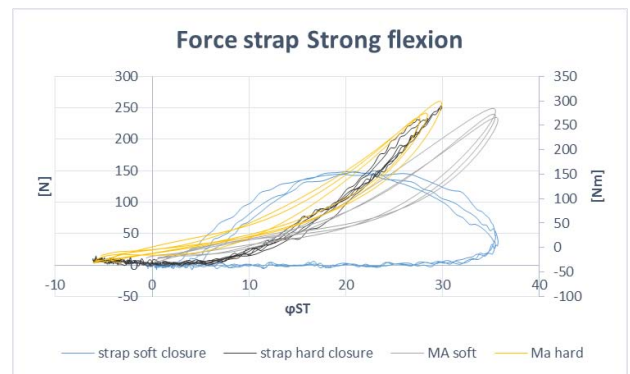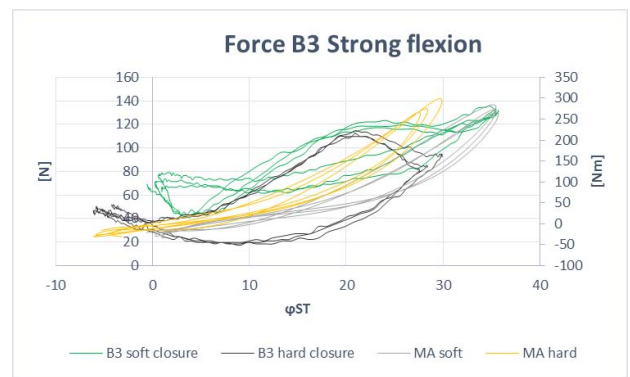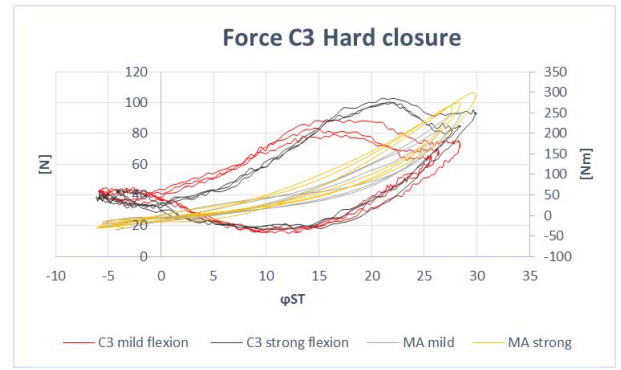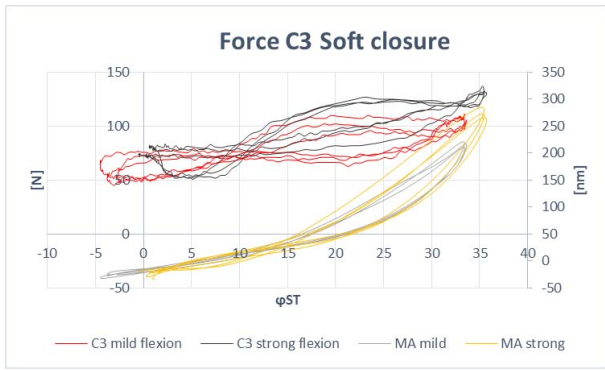

Figure 3. 15 Comparison with type of flexion as variable

Figure 3. 16 Comparison with type of closure as variable

3.3.6 Structural review graphs

Phx 70 in vivo Soft closure - Mild flexions

Phx 70 in vivo Soft closure - Strong flexions

Phx 70 in vivo Hard closure - Mild flexions

Phx 70 in vivo Hard closure - Strong flexions

- ‹ C2 : force on buckle 2

- ‹ C3 : Force on buckle 3

- ‹ Strap: force acting on the strap

- ‹ n C2: is considered as the buckle 2 closes force when the tester stands in his subjective zero moment position just before performing the 5 forward flexion.

- ‹ n C3: is considered as the buckle 3 closes force when the tester stands in his subjective zero moment position just before performing the 5 forward flexion.

- ‹ n Strap: is considered as the strap closes force when the tester stands in his subjective zero moment position just before performing the 5 forward flexion.

It is apparent to see that in both of the runs, with the soft and the hard closure, and in both the light and strong flexion, the force acting on buckle 2 (C2) is decreasing.

Conversely, the forces acting on Buckle 3 (C3) and on the strap (STRAP) augment with the forward movement.

As it was expected, the neutral forces for every buckle increased with the closure. However, it is possible to see that with the same closure, after the first light movement and before starting the strong flexion, the neutral value reduces its value possibly because of an adaptation of the plastic material of the boot.

After the forward movement, the tester tried to reach back to the neutral position but in every condition he passed it.

Chapter 4: San Vito di Cadore in field tests

4.1 Aim of the test

Skiing in person is in actuality very different from the laboratory tests. It is important to understand how the ski book behaves in its natural conditions on the slopes.

Performing tests on the slopes is challenging because the environment can be problematic for all of the acquiring systems.

The tests were performed on the Antelao slope in San Vito di Cadore on a typical day in February.

The slope had a constant average inclination of 16°; due to the sun the slopes altered throughout the day.

Figure 4. 1 Testing slope

Figure 4. 2 Pole slalom on the slope

4.1.1 Instrumentation used and test protocol

The ski boot that was used was the tecnica Phx 70. Each run was composed by a detailed protocol.

- ‹ Boot completely open
- ‹ Hook the load cell clips from the buckle 2 to strap with the Hard closure
- ‹ Mark the start of the pole slalom with three voluntary quick boot flexion's
- ‹ Perform the pole slalom until the final gate
- ‹ Mark the start of the free slalom with three voluntary quick boot flexion's
- ‹ Perform the free slalom at self selected speed and turning radius
- ‹ Perform the free short slalom at self selected speed and turning radius
- ‹ Mark the end of the free slalom with three voluntary quick boot flexion's
- ‹ Make a full stop
- ‹ Disconnect the boot clips from the strap to buckle 2 in order to have the boot completely open again

Instrumentation used:

- ‹ Load cells clips in order to measure the clamping forces on the Buckle 2 (C2) and 3 (C3) during skiing
- ‹ Strain gauges on the Buckle 3 (B3)
- ‹ The acquiring system HBM Somat

The challenge was to make all the systems work while being in a hostile environment. It was even more so complicated while wearing the tester and all of the cables and acquiring systems.

The HBM Somat was placed in a bag that was put on the tester's shoulders. This had all of the cables from the load cell clips that were connected to it.

In order to protect all the strain gauges of the load cells from humidity it was placed in a plastic bag around the ski boot and closed with American tape.

The set up is showed in the following picture below:

Figure 4. 3 Tester set up

Four runs were performed in the morning. The first 2 runs were made with the load cells clips on buckle 2 and buckle 3 and strap.

The last 2 runs that were skied were with the clips placed on the buckle 3 and 4 in order to see how the closing force is distributed along all the cuff of the boot.

4.2 First Results
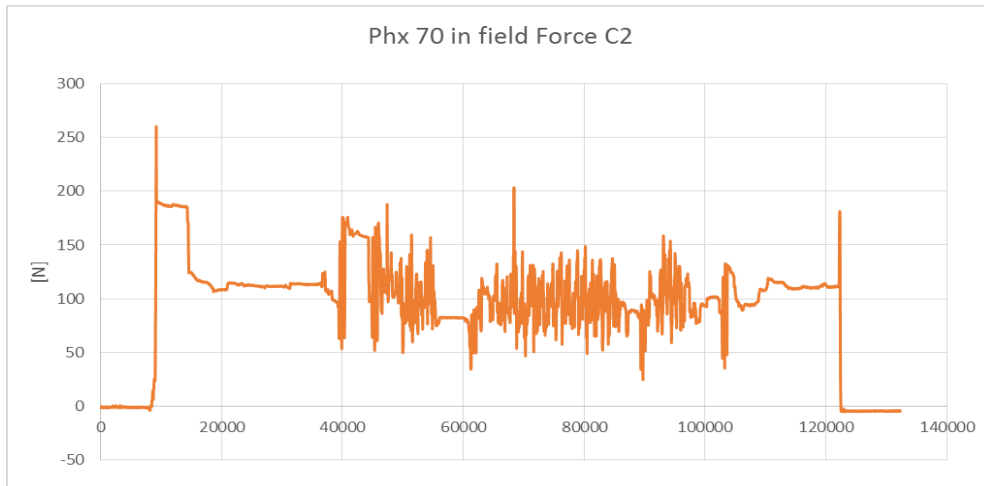
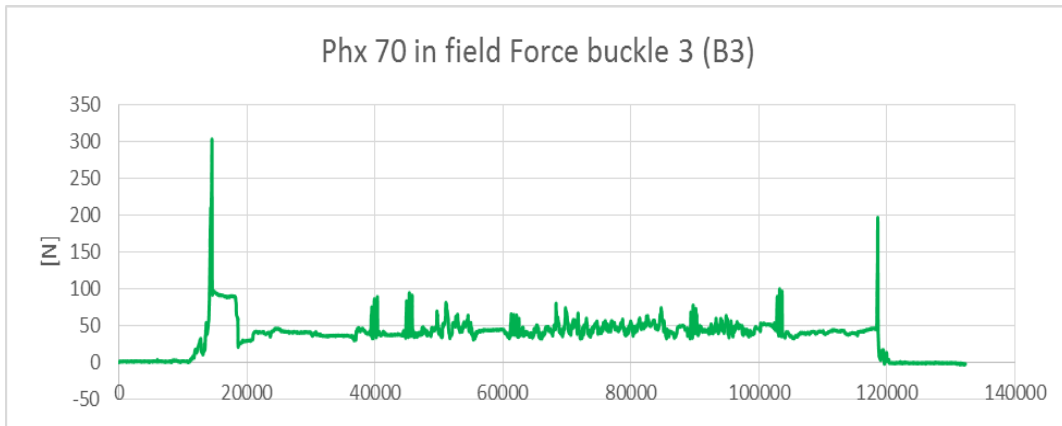### 4.2.1 Signal for buckle 2 (C2)

Figure 4. 4 In field force on buckle clip 2

From the graph of the full slope is simple to find the 3 parts in which were divided by the slope:
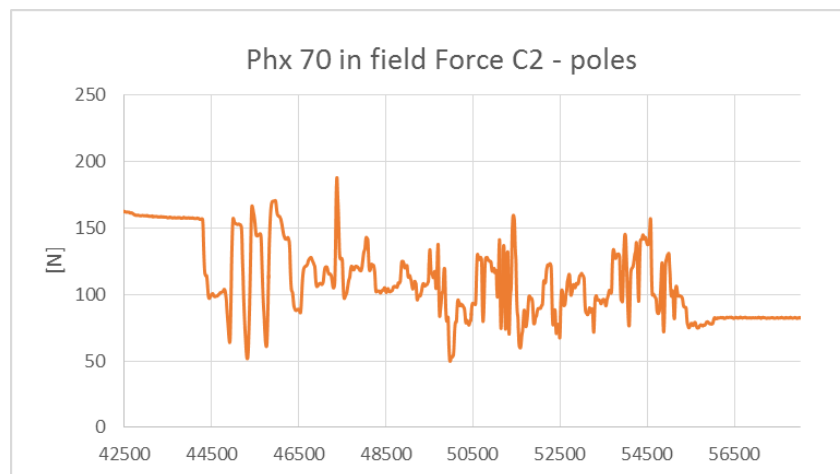
Figure 4. 5 Pole slalom

The average force acting on buckle 2 during the poles giant slalom session is:

$$F_2 = 110,2$$
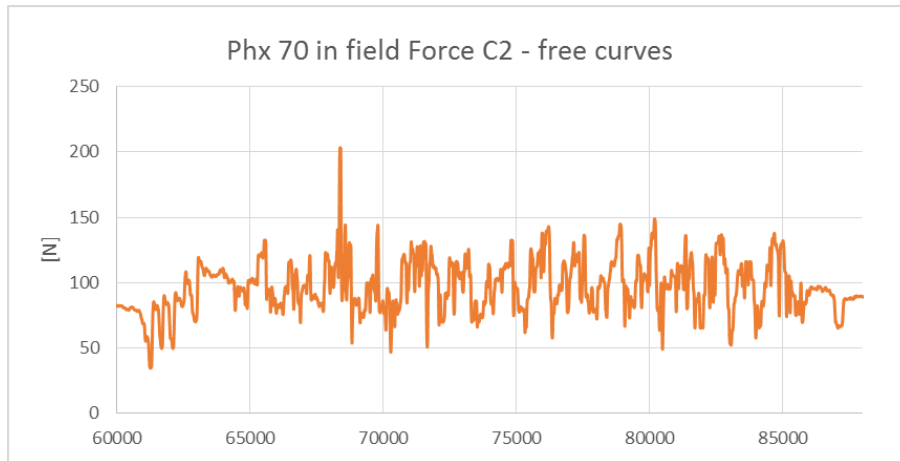
Figure 4. 6 Free carving curves

The average force acting on buckle 2 (C2) during the free curves is:

$$F_{C2} = 99.6$$
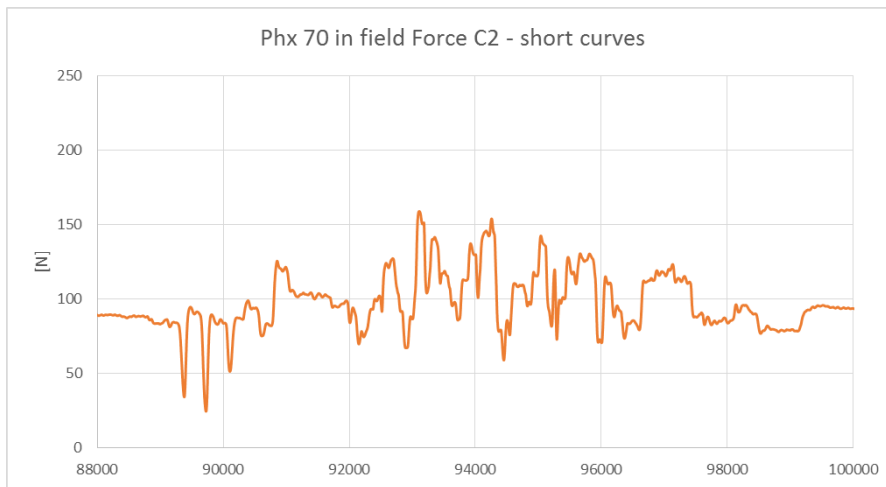
Figure 4. 7 Short skidding curves

The average force acting on buckle 2 (C2) during the short curves is:

$$F_{C2} = 100,42$$

4.2.2 Signal for buckle 3 (B3)

Figure 4. 8 In field force on buckle 3

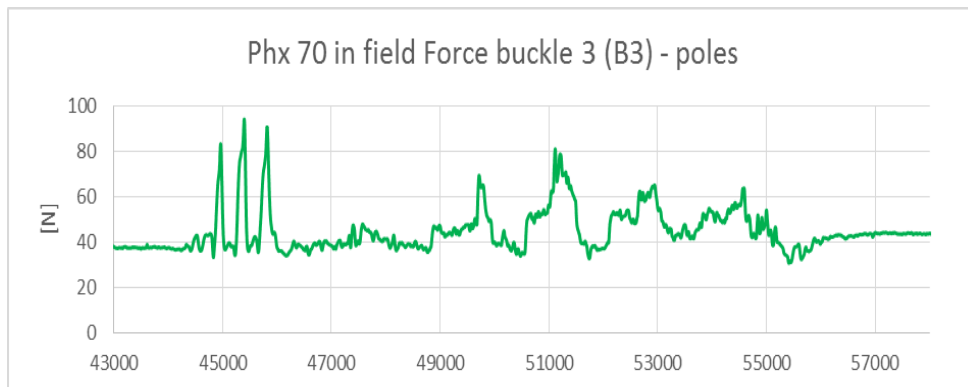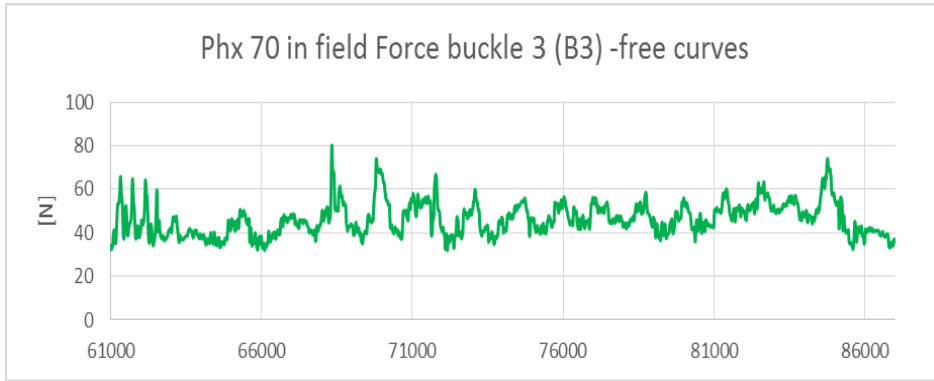From the graph of the full slope it is easy to find the 3 parts in which were divided by the slope:

Figure 4. 9 Poles slalom

The Average force acting on buckle 3 during the Poles Giant Slalom session was:

$$F_{B3} = 45 \ N$$

Figure 4. 10 Free carving curves

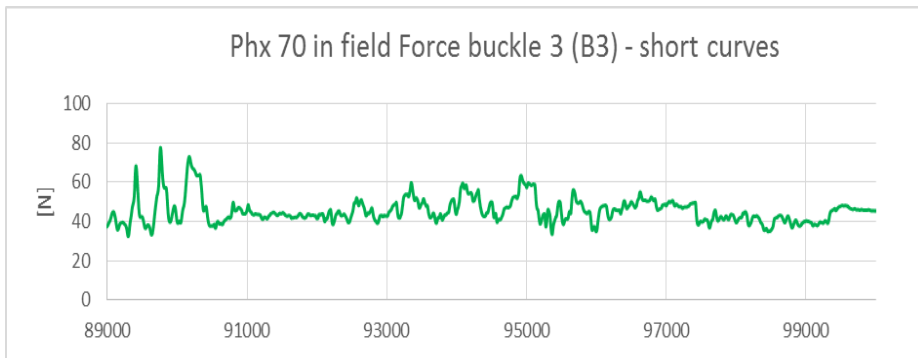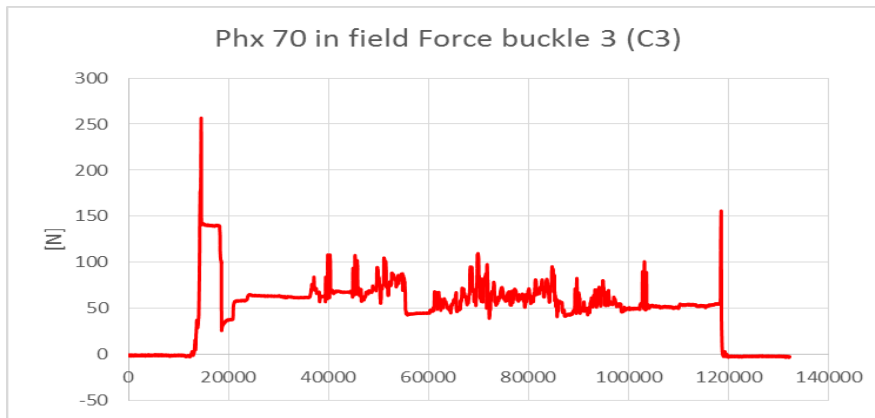The Average force acting on buckle 3 during the Free Slalom Session was:

$$_3 \quad = 4\ 7$$

Figure 4. 11 Short skidding curves

The Average force acting on buckle 3 during the Short Slalom Session was:

$$_3 \quad = 4\ 54$$

4.2.3 Signal for buckle 3 (C3)

Figure 4. 12 In field force for buckle 3 clip

From the graph of the full slope it is easy to find the 3 parts in which were divided by the slope:
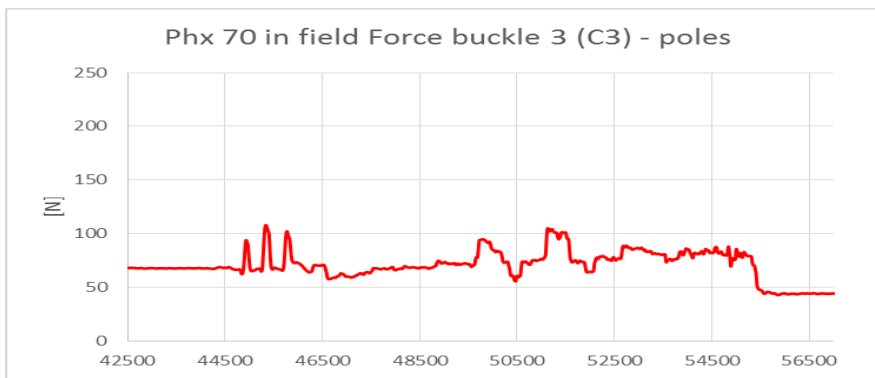

Figure 4. 13 Poles slalom

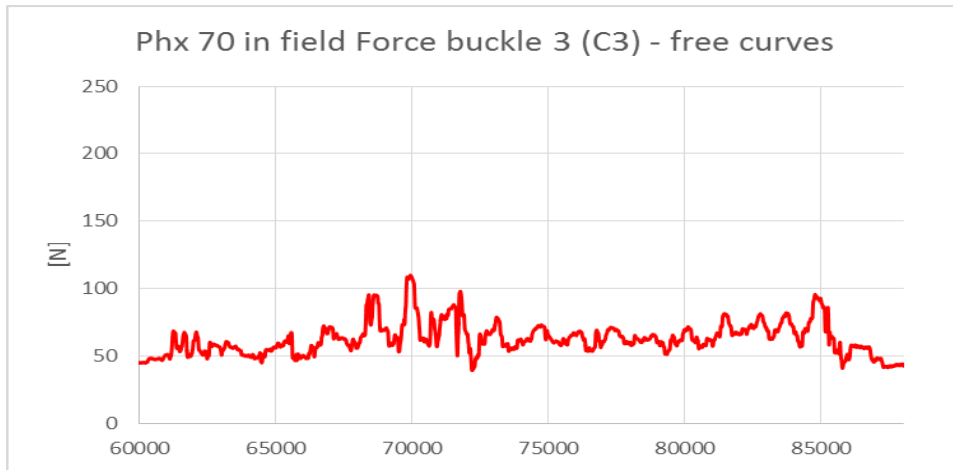The Average force acting on buckle 3 during the Poles Giant Slalom session was:

$$_3 \qquad = 7\ 1$$

Figure 4. 14 Free carving curves

The average force acting on buckle 3 during the Free Slalom Session was:

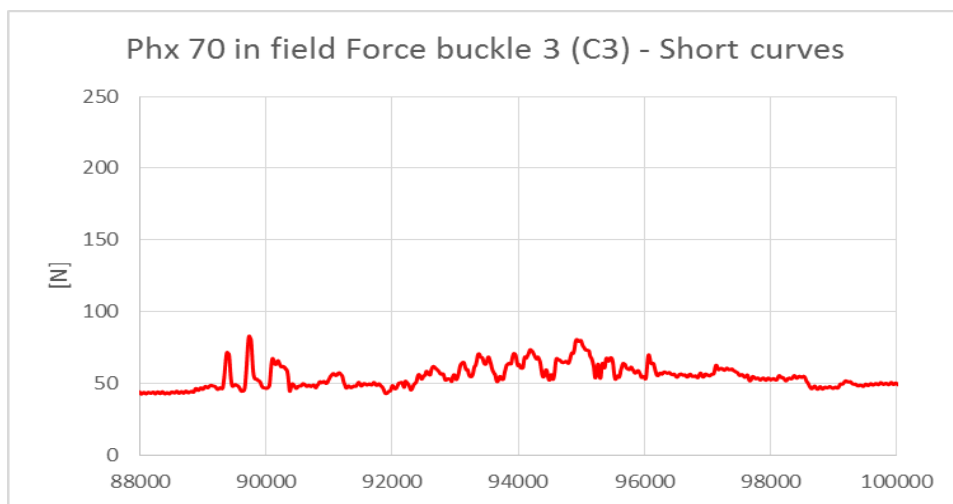$$_3 \quad = 6\ 5\ 6$$

Figure 4. 15 Short skidding curves

The average force acting on buckle 3 during the Short Slalom Session was:

$$_3 \quad = 5\ 7$$
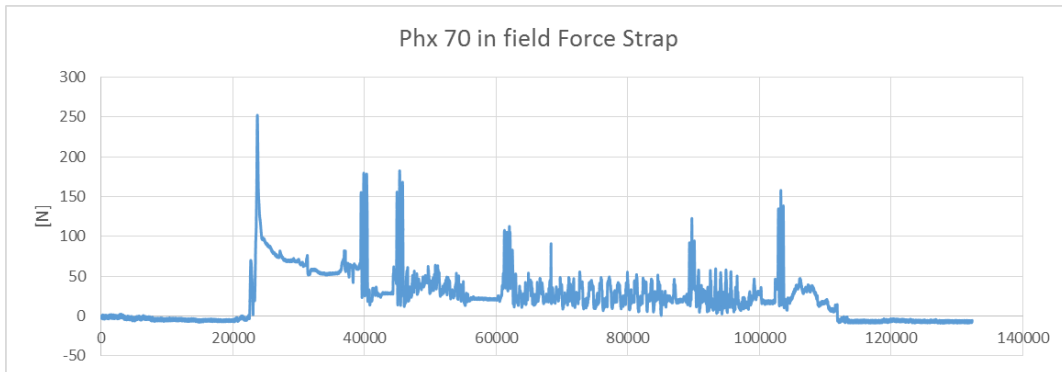
4.2.4 Signal for Strap

Figure 4. 16 In field force for strap

From the graph of the full slope it is easy to find the 3 parts in which were divided by the slope:
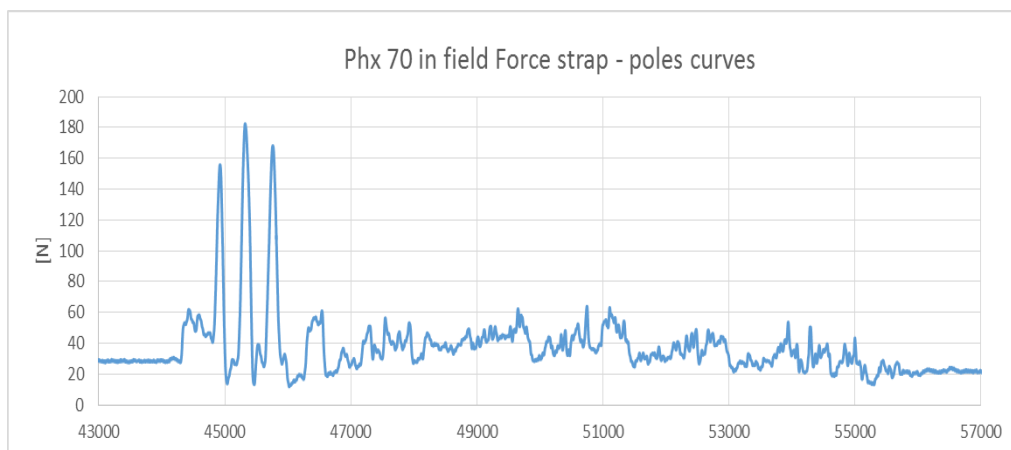

Figure 4. 17 Poles slalom

The average force acting on Strap during the Poles Giant Slalom session was:

$$= 3 \ 4$$
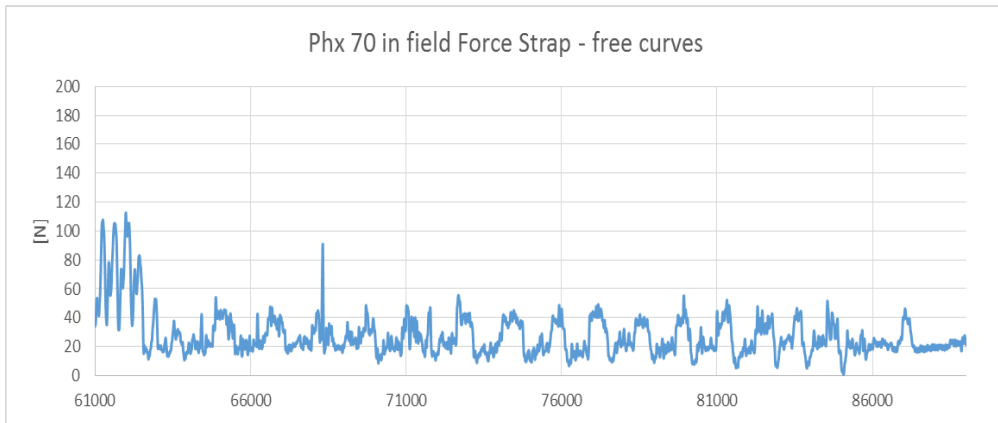
Figure 4. 18 Free carving curves

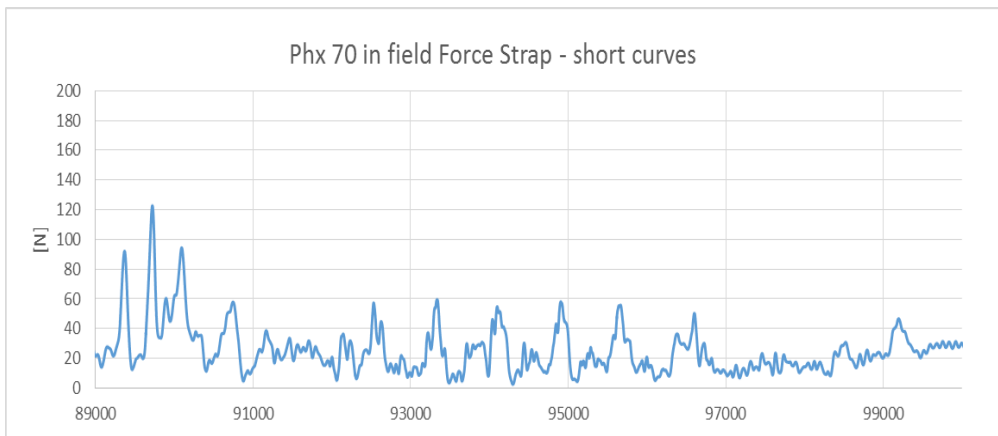The average force acting on Strap during the Free Slalom Session was:

$$= 2\ 5\ 6$$

Figure 4. 19 Short skidding curves

The average force acting on Strap during the Short Slalom Session was:

$$= 2\ 1$$

4.2.5 Results

The results are reported in the table below:

	F Buckle 2 (C2) [N]	F Buckle 3 (C3) [N]	F Buckle 3 (B3) [N]	F Strap [N]
Poles	102,5	71	45,8	34
Free	99,6	65,6	47	25,6
Short	102,4	57	45,4	21

It is possible to see that:

‹ The highest values of the force acting on the boot during all the skiing part are felt by the buckle 2 (C2)

‹ In field there is anymore the high correlation of the signal coming out by the strain gauged buckle and the clip on the same buckle ($^2 = 0.8$ 5). The reason of this probably is the different temperature o the slope.

‹ The strap is the one with the lowest value of the force but from its signal is simple to find the moment when the instrumented boot is inner one or the outer one.

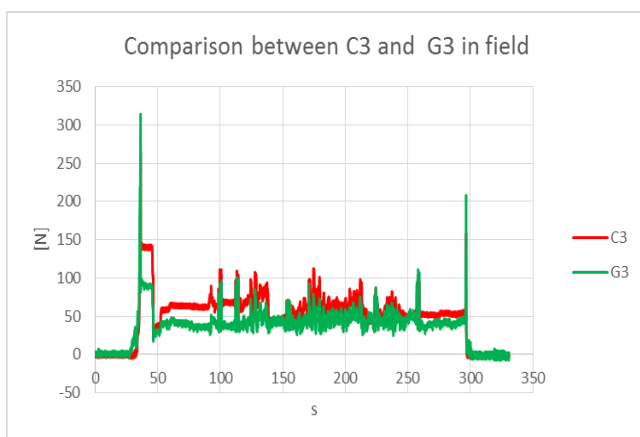‹ From the data above it could be say that the poles slalom session is the most stressing for the boot.

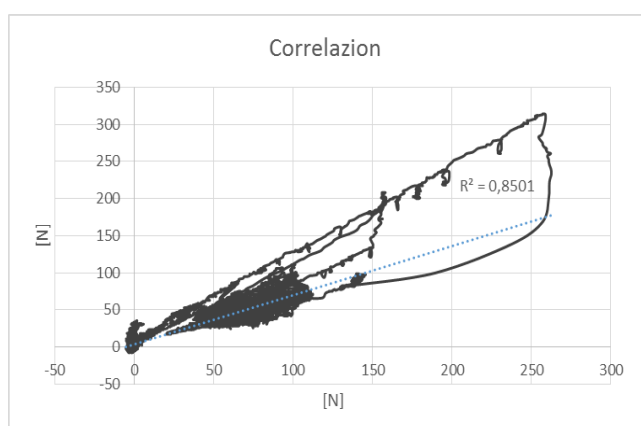Figure 3. 17 sifference of signals between C3 and G3 in field

Figure 3. 18 Correlation between C3 and G3

4.3 Comparison between Force B3 in subsequent runs

In order to understand the behavior of the boot it is relatively easy to analyze the force felt by the Buckle 3 (B3) during three subsequent runs with the same hard closure

These runs were all made at a distance of half an hour from the first to the last. In this period the buckle was opened at the end of every slope.

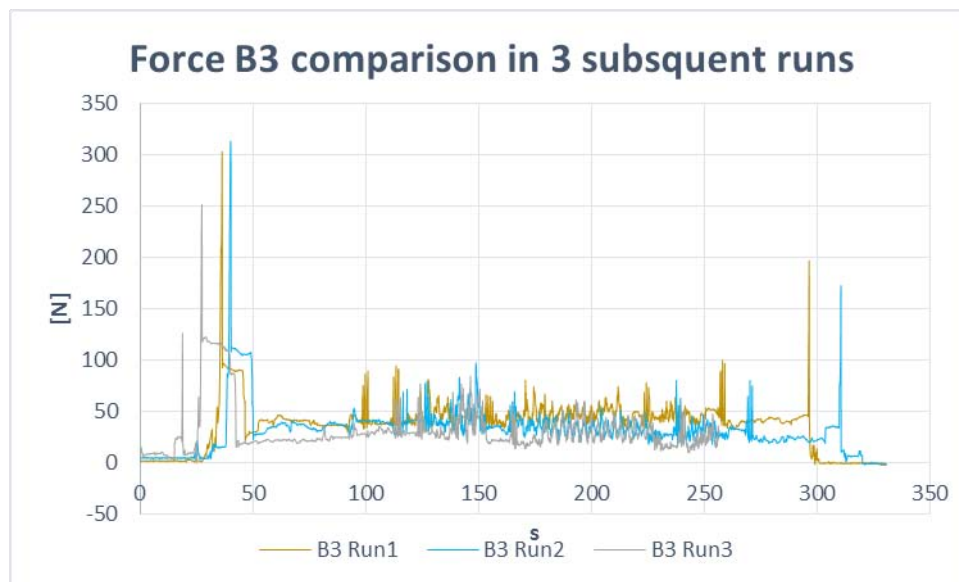 The thing that mostly changed was that the snow was becoming heavier over time.

Figure 4. 20 Force on B3 in different runs

Each run was divided in three parts; the first in which the tester was asked to perform a poles giant slalom. In the second run the tester performed free slalom curves at his own speed, and in the third part the tester performed a series of short skidding curves.

For each part of the run the average was calculated from the force acting on the strain gauged buckle 3 (B3). The results are reported below:

	Force B3 Run1 [N]	Force B3 Run 2 [N]	Force B3 Run3 [N]
Poles giant slalom	49,7	46,6	45,8
Free slalom curves	46,4	34,4	32,3
Short skidding curves	45,6	32,2	26,4

From the values reported above it is possible to see that for the analyzed buckle, the force decreases from the first to the last run.

It is as if all the structure of the boot relaxes after every run.

Chapter 5: The Modern Ski Boot DAHU

5.1 Project DAHU

The ski boot Dahu is a new product on the market because it can be used in multiple ways; in fact, it can be used as a normal ski boot while skiing but also as a comfortable shoe after the skiing session.

Figure 5. 2 Parts of Dahu

Figure 5. 1 Exoskeleton of Dahu

To reach this goal the ski boot Dahu is made by two different parts: a soft waterproof boot that can be inserted in a rigid exoskeleton which can be inserted in the ski bindings.

The inner boot can be extracted from the exoskeleton in order to use fore walking or even more, in order to drive the car.

The exoskeleton and the boot are completely independent but when they are together, they give the product the shape of a traditional ski boot.

Figure 5. 3 Name of the parts of Dahu

The upper part of the ski boot is that is usually called the "cuff." Here it is divided into two parts that could be named as "Front Cuff" and "Rear Cuff" in order to allow the insertion of the soft but inside the exoskeleton.

A rear beam in the posterior side of the boot connects the shell with the Rear Cuff. There also is a pin at the base and a button with an elastomer red part on the outer profile.

The exoskeleton is composed basically by plastic material except for the rear beam and he buckles which are composed in aluminum and the pins that are made in steel.

To fit the boot with the closed exoskeleton condition it is necessary to follow a simple procedure:

- ‹ Unhook the buckles (3) and (4)
- ‹ Apply a pressure on the button of the rear beam in order to unhook it
- ‹ Rotate the rear cuff as in figure
- ‹ Rotate the front cuff as in figure
- ‹ Insert the soft boot I the shell of the exoskeleton
- ‹ Close the rear cuff
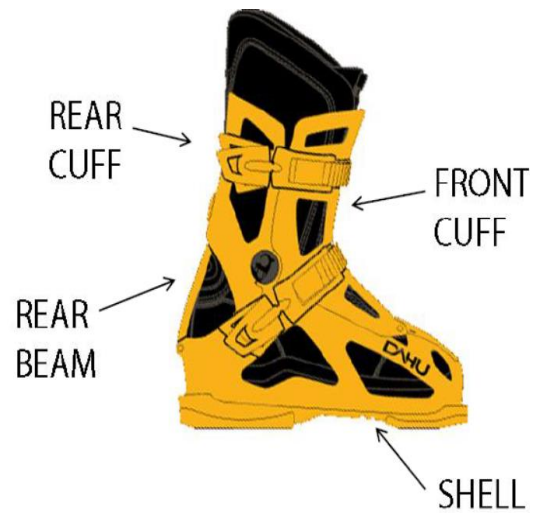- ‹ Close the front cuff
- ‹ Hook the buckles

Figure 5. 4 Opening Dahu

5.2 Sensors application to Dahu Boots

It has been decided to place 4 strain gages (2 longitudinal and 2 transversal) on the Front Cuff at the parting line of the mold. This determines the longitudinal centerline of the boot, in the positions in the figure. Other 4 (2 longitudinal and 2 transversal) on the Rear Beam, 2 (1 longitudinal and 1 transversal) in the outer surface and 2 (1 longitudinal and 1 transversal) in the inner surface at the same distance from the elastomer.

Every single strain gauge located on the Front Cuff will be linked to quarter-bridge in order to measure the single strain due to bending and traction.

The strain gauges located in the Rear Beam are connected in a full bridge and measure a tensile strain.

Overall, 5 channels of acquisition are obtained:

1 – FCLL - Front Cuff Lower Longitudinal (quarter-bridge connected);

2 – FCLT - Front Cuff Lower Transversal (quarter-bridge connected);

3 – FCML - Front Cuff Medium Longitudinal (quarter-bridge connected);

4 – FCMT - Front Cuff Medium Transversal (quarter-bridge connected);
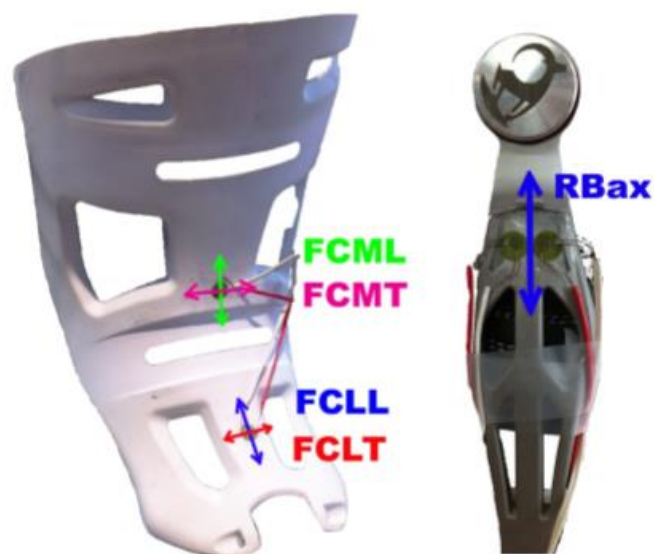
5 – RB - Real Beam (full bridge connected);

Figure 5. 6 Front cuff and rear beam sensitization

5.2.1 Rear Beam calibration

To determine the stress of the Rear Beam during flexion and extension, it is necessary to calibrate the system of acquisition. A possible way to calibrate it is to set the ski-boots and flip them upside down, fixed between two beams with the same height from the ground.

Figure 5. 7 Rear beam calibration

The value zero has been associated to deformation read by the system when a thin plate of a known weight is fixed in correspondence of the elastomer present on the upper part of the Rear Beam.

The next step of calibration is done by applying some known masses until a maximum value, after removing them with logic LIFO.

The last step is to calculate the coefficient of calibration.

The coefficient of calibration C, is calculated like the reciprocal of the slope of the trend line and it is defined like the value that allows one to calculate the value of the force that is acting on the load cell by multiplying it to the value read by the load cell in [mV].

$C = 1/S$

where S is the slope of the trend line of the calibration data.

$C \, \Delta V/V = F$

Where $\Delta V/V$ is the unbalance of the bridge.

The value of the calibration constant for the rear beam is C = 1005,6 [N/mV]

5.3 Dahu in field test

In order to see how the behavior was with the two closing buckles, tests were preformed on this new ski boot out in the fields.

The tests were performed in the afternoon on a typical sunny day in February. Therefore the work was forced to be used in a different type of slope.

The slope chosen was classified as a black part in the beginning with thick snow because of the lack of sun on it during the day because of the particular position of that part of the slope.

The second part of the slope presented a flat stretch with soft wet snow.

The test with this type of boot was performed only with the hard closure because for the tester it was the first time using this boot and to possibly have a better feeling with the ski during the skiing on the steep slope.

As all the tests done before also had a chosen protocol that provided the sequence below:

1. Starting acquisition of the channels with Somat
2. Hook the clips on the buckles
3. Performing a maximum forward flexion and a maximum backward extension
4. Up the instrumented leg in order to have the zeros of the systems
5. Three mild forward flexion in order to mark the position in the future signal's plot
6. Performing the steep part of the slope with a series a short slalom curves with controlled speed
7. At the end of the steep part mark the position with other three mild flexion
8. Performing the flat part of the slope with a normal conducted carve curves
9. Mark the end of the slope with other three mild flexion
10. Unhook the clips from the buckles
11. Stop the acquisition

The channel measured were the load cell clips in order to measure the force on the two dahu buckles and the full bridge strain gauges on the rear beam because. This was thought as the most important part of the structure because it gives most of all the rigidity to the boot.

The buckle nearest to the tip of the boot is called C1.

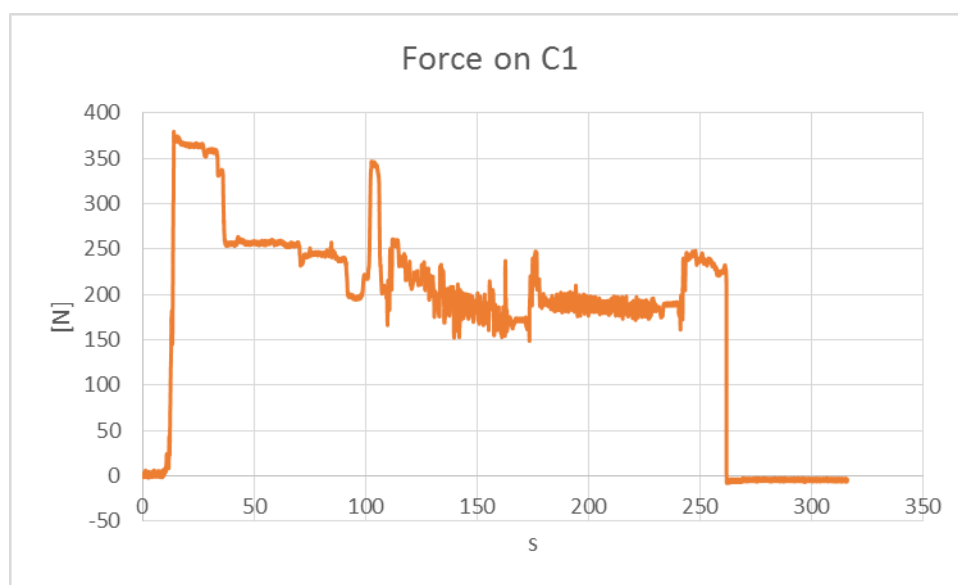The buckle on the cuff is called in the subsequent pages C2.

5.3.1 Signal for C1

Figure 5. 8 Force on C1

The first pick of the force is the closing moment.

The force when it is closed the C2 settles to an average value of 250 N.

This buckle has a similar behavior of the buckle 2 in a "normal" ski boot, In fact, during the maximum forward flexion the force acting decreases and in the maximum backward extension increase its value.

In the first steep part of the skiing the ski boot relaxes during performing the curves.
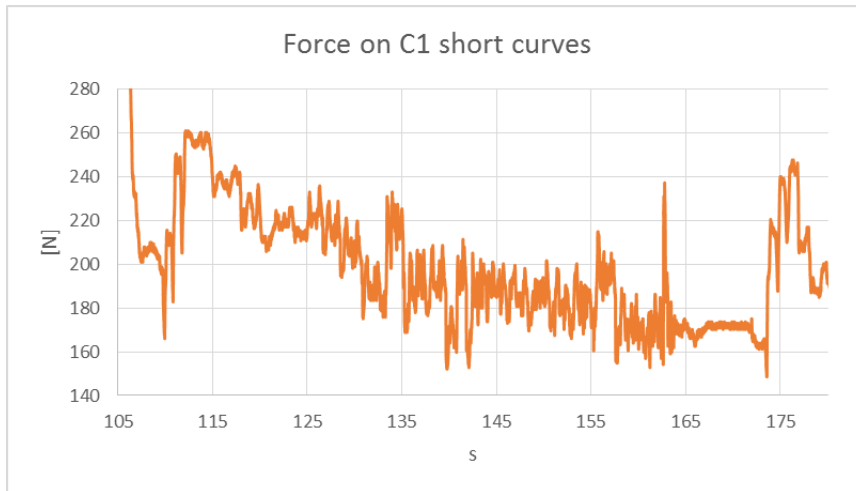
Figure 5. 9 Dahu short curves

The average force while performing the short curves on the steep part of the slope on C1 is:

$$= 1\ 9\ 9,6$$
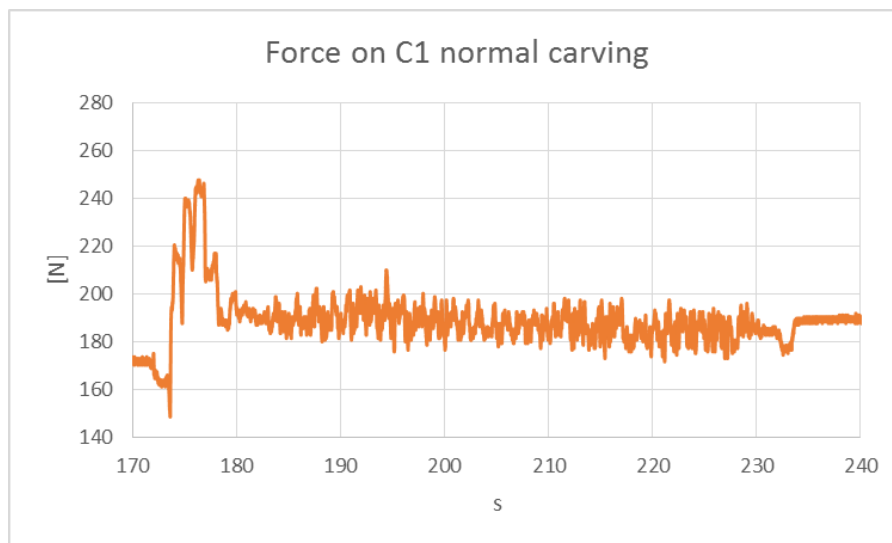
Zooming on the second part of the slope:

Figure 5. 10 Free normal curves

The average force acting on C1 during the normal curves in the flat part of the slope is:

$$= 1\ 8\ 8,4$$

It seems that if something strange was happening between the first and the second part of the slope.

In fact, it is clear on the graph at an average timing of 110s, that the three forward flexion's make the unloading of the force acting on C1.

If we see the moment at 175s in which the tester performed other three forward flexion's, it is clear that the C1 increases its force.
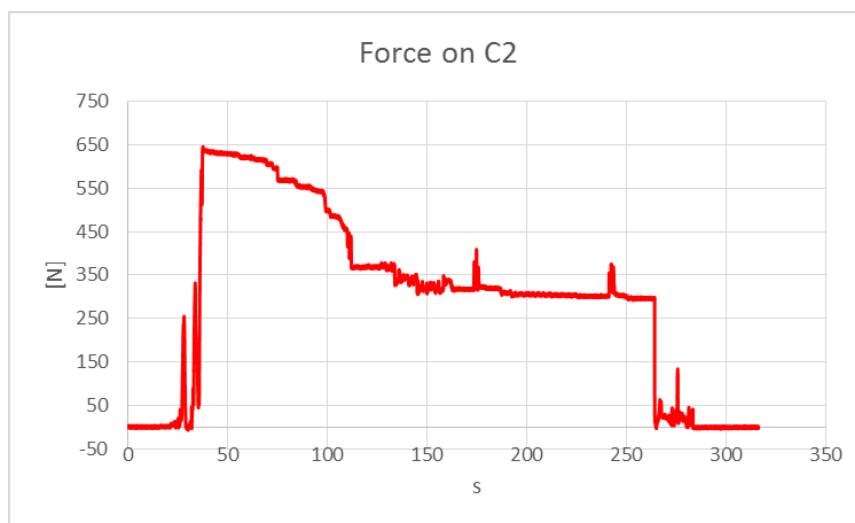
5.3.2 Signal for C2

Figure 5. 11 Force on C2

The first pick of the force is the closing moment.

The force when the buckle is closed goes straightly to settle to an average value of 370 N.

It seems that this buckle used the maximum forward flexion and the maximum backward extension to settle its force value.

It is slightly possible to notice the first series of the three mild flexion mark the position before skiing.

This mild forward flexion are instead visible after the steep slope and at the end of the acquisition.
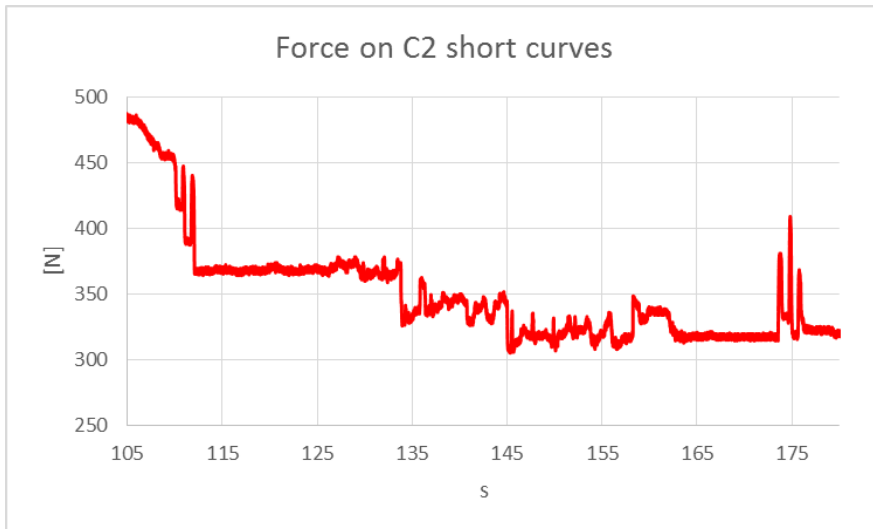
Figure 5. 12 Dahu short curves

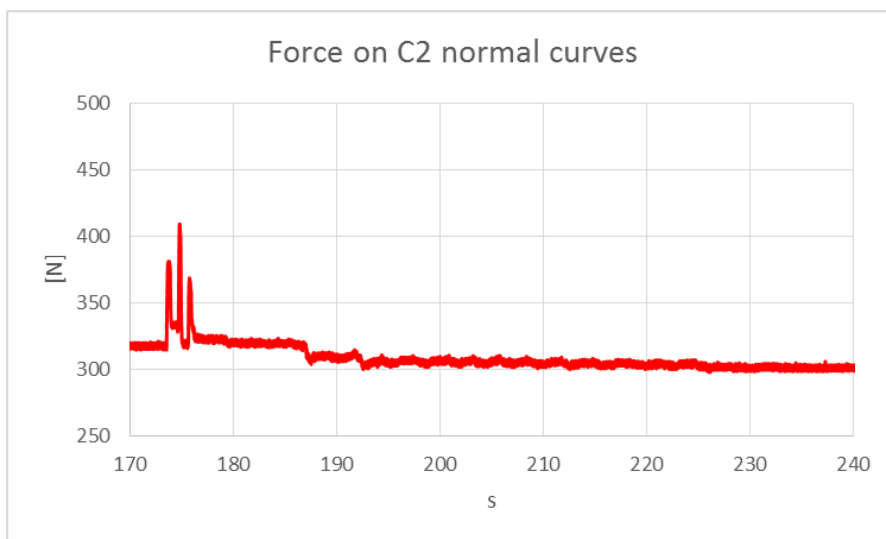The average force while performing the short curves on the steep part of the slope on C2 is:

$$= 3\ 4\ 0$$

Figure 5. 13 Dahu normal free curves

The average force acting on C2 during the normal curves in the flat part of the slope is:

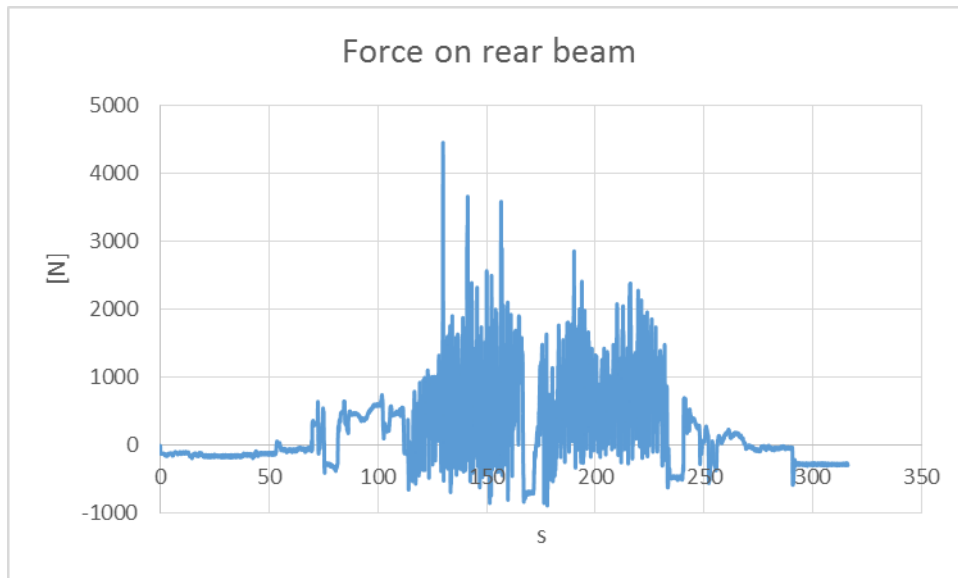$$= 3\ 0\ 5$$

5.3.3 Rear Beam

Figure 5. 14 Force on Rear beam

It is possible to see the force behavior during the test with the Dahu ski boot.

As it was expected during the test it is possible to see that the rear beam works mostly in traction and in the backward extension the value of the force decreases.
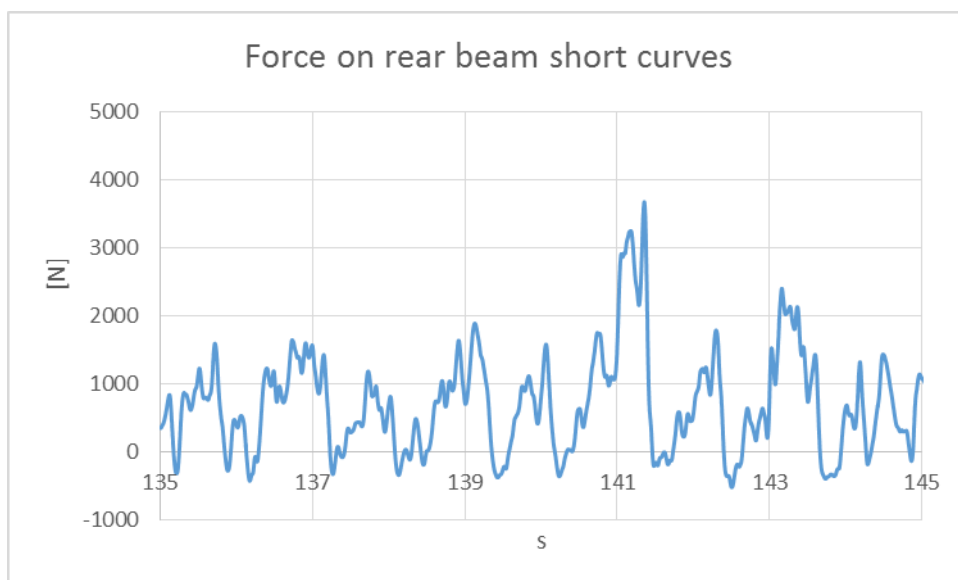

Figure 5. 15 Rear beam Dahu short curves

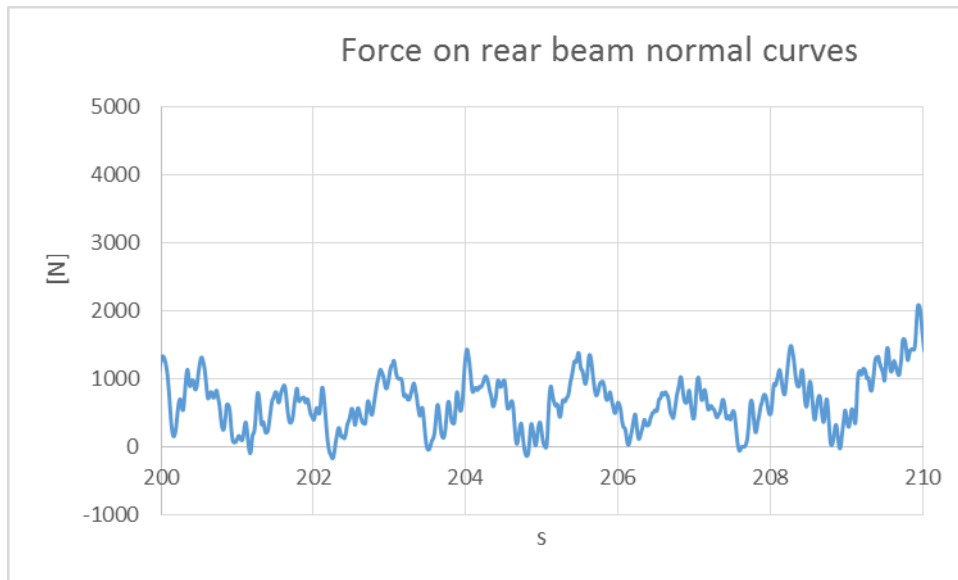The average force while performing the short curves on the steep part of the slope on rear beam is:

$$= 6\ 6\ 8$$

Figure 5. 16 Rear beam normal curves

The average force acting on C2 during the normal curves in the flat part of the slope is:

$$= 7\ 6\ 5$$

During the short curves, the force value on the rear beam is higher because this type of skiing is more impulsive.

Chapter 6: Bench Flex tests

6.1 Bench description

In University of Padua labs, a servohydraulic torsion bench has been adapted to be used for the execution of flexion test on ski boots like in Nordica.

In order to adapt this torsion bench to simulate a skiing session, some tools were designed.

A long plate with a section 100 x 20 mm x mm is fixed to the torsion bench with 4 screws at one extremity so that when the machine rotates around its center of rotation, even the plate rotates around the same axis of rotation. At the other extremity of the plate a "C" done by three shorter aluminum plates of the same section connected together is fixed, so to obtain a "P-arm". To connect the pole of the dummy foot to the "P-arm" could be use a set of two or four wheels.

The wheels drive the pole and allow small relative displacements during movement in the direction of the pole axis. The wheels are screwed to the "P-arm" into four holes; two of them have been bored to facilitate the coupling between pole and the four wheels.

6.1.1 Instrumentation

‹ DUMMY SILICON FOOT: In order to simulate the mechanical behavior of the human leg inside the ski boot a dummy silicon foot, realized by the Department of Mechanical Engineering of the University of Padua, was used. An aluminum pole 27mm diameter is connected to the dummy silicon foot so to allow the movement of

Figure 6. 1 Dummy silicon leg

the foot inside the ski boot. The pole could also represent the tibia of a man.

‹ SKI BINDING: A special ski binding, realized by the University of Padua has been used to anchor a ski boot to the bench ground in a rigid way. It is regulable for different size of boots and can be calibrated between 0 and 30Din. It has been regulated to the maximum value available (30 Din) so to block all nine degrees of freedom of the plant of the boot.
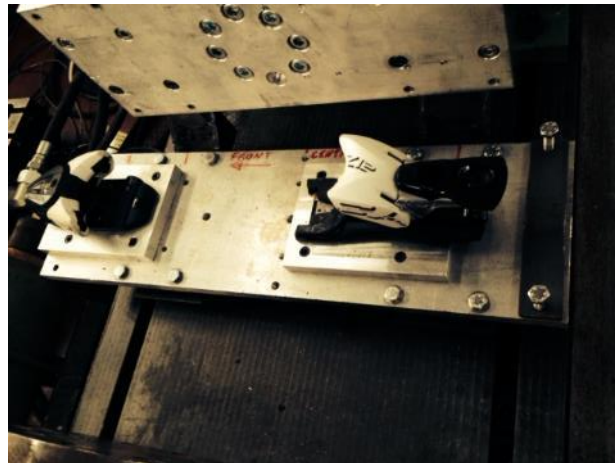

Figure 6. 2 Ski binding used for the bench

It Is possible to move together the "P-arm", the dummy silicon foot and the ski boot using the MTS software to a right angle of flexion.

For a proper use of the bench, it is necessary to assure the alignment between the ankle and the center of rotation of the torsion machine.

6.1.2 Test protocol

A test was performed in order to characterize the eFI of a particular type of boot (HEAD modified) and to find how the misalignment of the hinge of the boot affects the results of the machine.

The ski boot used is named Superflex. The Superflex is a particular ski boot that is custom made in Aalborg University (Denmark), obtained by properly cutting a normal ski boot in order to have a wider range of motion at the hinge.

It was thought to study three different conditions of alignment:

Figure 6. 3 Superflex boot

- ‹ Central alignment
- ‹ Misalignment 1: the hinge all forward (10 mm)
- ‹ Misalignment 2: the hinge all backward (10 mm)

For each alignment, 3 different kinds of angular velocity were tested:

- ‹ +15°/-5°, ω = 5°/s
- ‹ +15°/-5°, ω = 20°/s
- ‹ +15°/-5°, ω =50°/s

For each test 5 different parameters were measured, in order to see how the misalignment affects them:

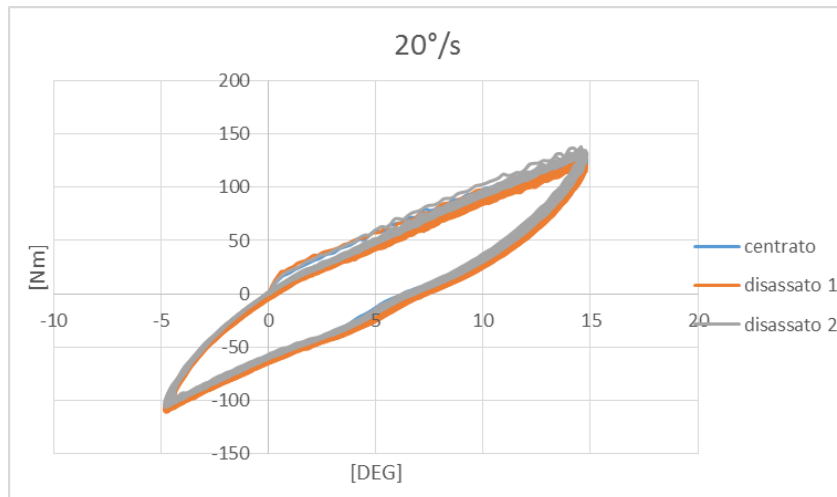- ‹ $_5$: slope of the curve around 5°
- ‹ $_{15}$ the inclination of the curve around 15°
- ‹ $= {}_{15}/{}_5$ progression ratio
- ‹ : the hysteresis area
- ‹ $_{10}$ the momentum necessary to obtain 10° of forward flexion eFI (FLEX INDEX)
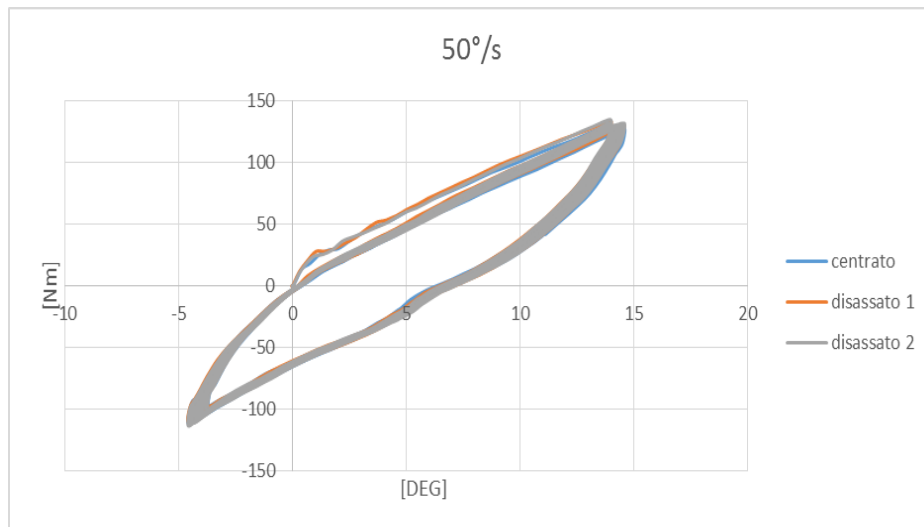
6.1.2.1 test 15°/
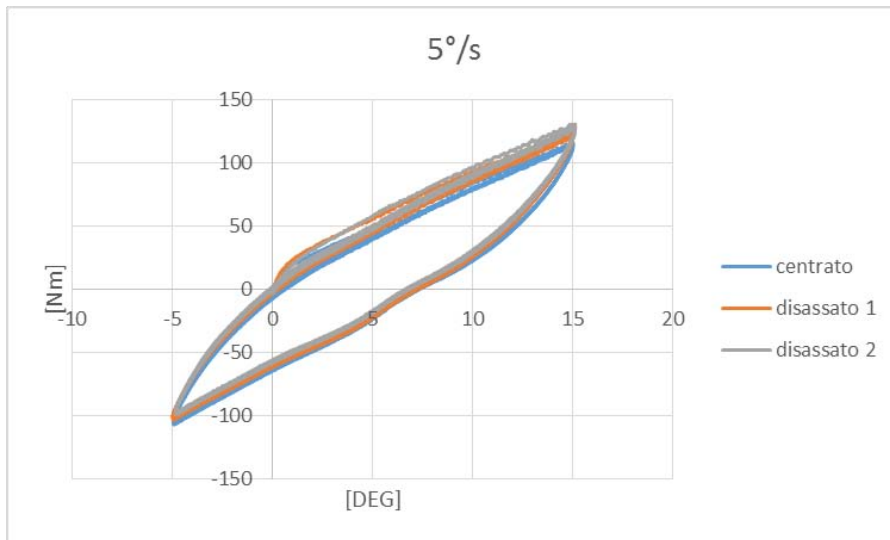
	M10 [Nm]	K5 [Nm/°]	K15 [Nm/°]	P	Ahyst [Nm°]
centrato	80,5	8,88	6,50	0,73	974,46
disassato1	85,6	8,19	6,04	0,74	991,64
disassato 2	89	9,01	6,99	0,78	985,30

6.2.1.2 test 15°/

	eFl [Nm]	K5 [Nm/°]	K15 [Nm/°]	P	Ahyst [Nm°]
centrato	90	9,68	7,54	0,78	780,09
disassato1	88	9,05	6,84	0,76	843,02
disassato2	95	9,02	7,64	0,85	765,92

6.2.1.3 test 15°/

	M10 [Nm]	K5 [Nm/°]	K15 [Nm/°]	P	Ahyst [Nm°]
centrato	91	10,14	8,52	0,84	544,10
disassato1	96	10,02	7,718	0,77	683,22
disassato2	97	10,22	8,74	0,85	646,79

From these tests it is possible to understand that the misalignment of the boot in respect to the machine rotational axes affects the eFI values but the difference between them never exceeds the 10%.

6.3 Different boots on the test bench

To complete the study of all the ski boots used it is important to know their behavior using the torsion test bench.

For each boot the tests were performed in angle control.

From the characteristic starting angle of the boot, it has been used the following procedures:

- ‹ +15°/-5°, ω=5°/s
- ‹ +15°/-5°, ω=20°/s
- ‹ +15°/-5°, ω=50°/s

For each test 5 different parameters were measured, in order to see how the misalignment affects them:

- ‹ $_5$: the inclination of the curve around 5°
- ‹ $_1$ $_5$ the inclination of the curve around 15°
- ‹ = $_5$/ $_1$ $_5$
- ‹ : the hysteresis area
- ‹ $_1$ $_0$ the momentum necessary to obtain 10° of forward flexion eFI (FLEX INDEX)

6.3.1 Superflex left/right comparison

As mentioned before, the Superflex is a particular ski boot that is custom made in Aalborg University (Denmark), obtained by properly cutting a normal ski boot in order to have a wider range of motion at the hinge.

It is interesting to understand the behavior of the boot in terms of flex index (eFI) by using the torsion test bench.

It has been decided also to test both the left and the right boot in order to understand if there were some differences between them.

Sflex left
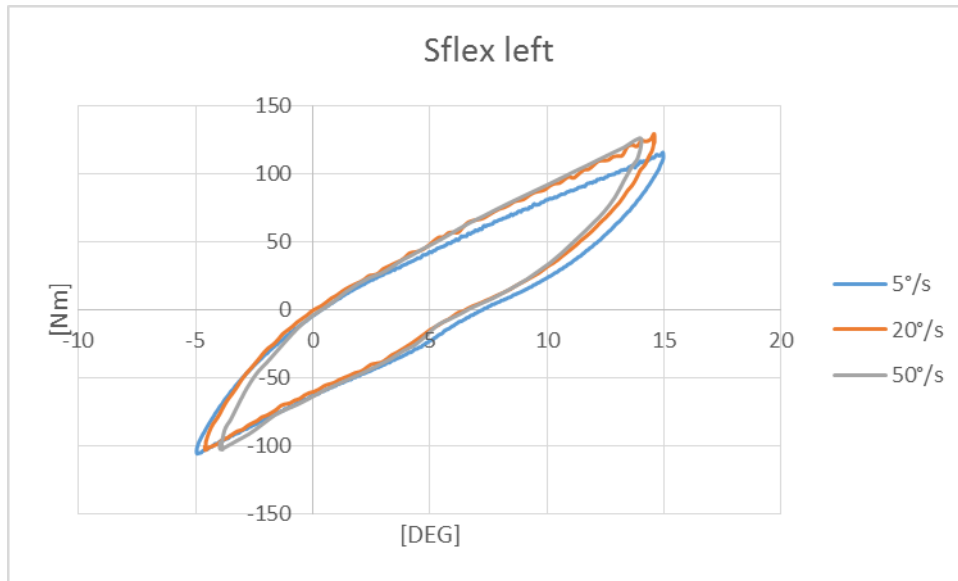
	M10 [Nm]	K5 [Nm/°]	K15 [Nm/°]	P	Ahyst [Nm°]
5°/s	80,5	8,88	6,5	0,73	974,46
20°/s	90	9,68	7,54	0,78	780,09
50°/s	91	10,14	8,52	0,84	544,09

Sflex right
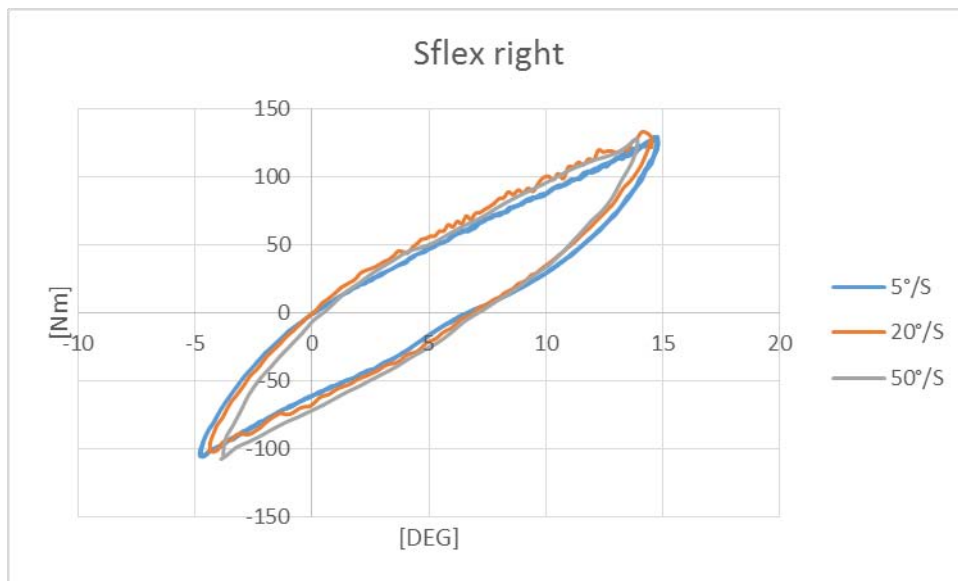
	M10 [Nm]	K5 [Nm/°]	K15[Nm/°]	P	Ahyst [Nm°]
5°/s	87	9,33	7,41	0,79	902
20°/s	95	10,57	7,38	0,70	862,8
50°/s	96	10,99	8,18	0,74	638,92

It is possible to see that:

- ‹ Left boot and right boot have different values of flex index for each ω value, maybe because left and right boot present some constructive differences between them.

- ‹ For both the boots the flex index increases with the angular velocity ω.

- ‹ When increasing the ω, it could be seen that the gradient of the curves K5 and K15 increases for both the left/right boot.

- ‹ The hysteresis area decreases with the increase of the angular velocity ω probably because, even if using the pick valley compensator, the machine cannot reach exactly the imposed angular values.

6.3.2 Tecnica Diablo 120
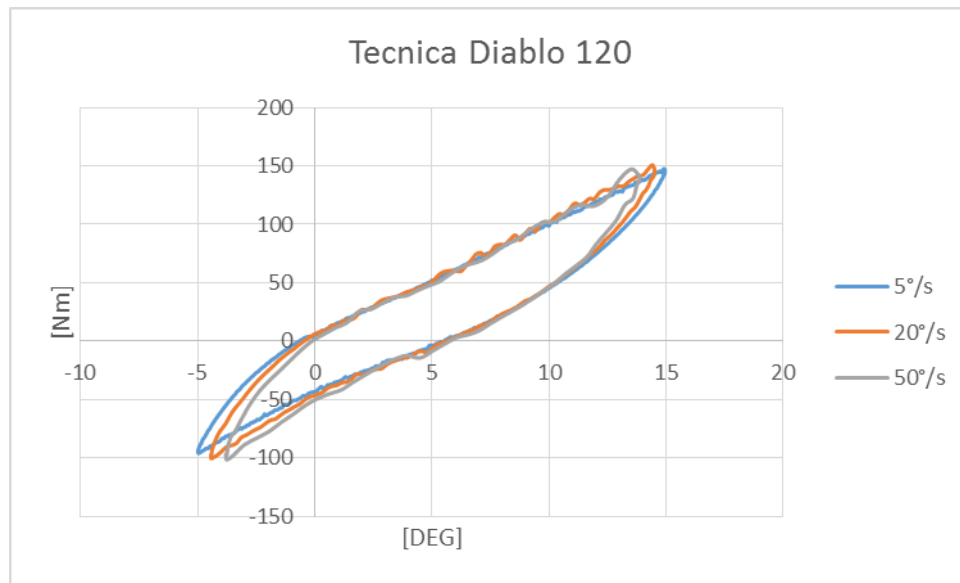
	M10 [Nm]	K5 [Nm/°]	K15 [Nm/°]	P	Ahyst [Nm°]
5°/s	98	8,9	8,69	0,976404	868,28
20°/s	102	9,03	9,45	1,046512	709,58
50°/s	102	9,27	9,88	1,065804	622,61

It is possible to see that:

‹ For the Tecnica diablo 120 the flex index increases lightly with the angular velocity ω.

‹ With the slowest ω it is possible to see that $_5$ is higher than $_{15}$

‹ When increasing the ω, it could be seen that the gradient of the curves K5 and K15 increases.

‹ The hysteresis area decreases with the increase of the angular velocity ω probably because, even if using the pick valley compensator, the machine cannot reach exactly the imposed angular values.

6.3.3 Tecnica Phx 70
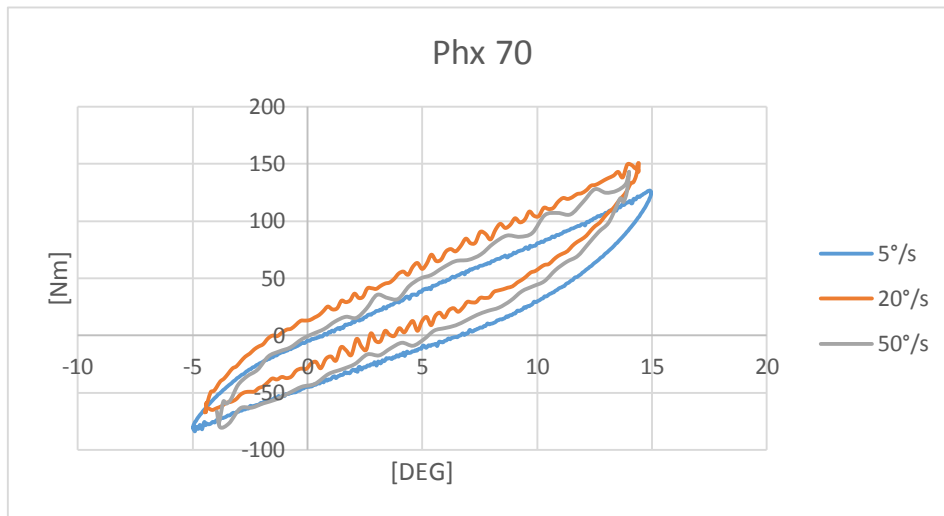
	M10 [Nm]	K5 [Nm/°]	K15 [Nm/°]	P	Ahyst [Nm°]
5°/s	80,5	8,82	8,98	1,02	783,77
20°/s	104	8	9,57	1,19	611,17
50°/s	100	10,35	11,62	1,12	481,14

It is possible to see that:

‹   For the Tecnica Phx 70 the flex index increases hardly with the angular velocity ω passing from 5°/s to 20°/s.

‹   The flex index lightly decrease from 20°/s to 50°/s

‹   For every ω it is possible to see that $_{15}$ is higher than $_5$

‹   The hysteresis area decreases with the increase of the angular velocity ω probably because, even if using the pick valley compensator, the machine cannot reach exactly the imposed angular values.

6.3.4 Dalbello Krypton
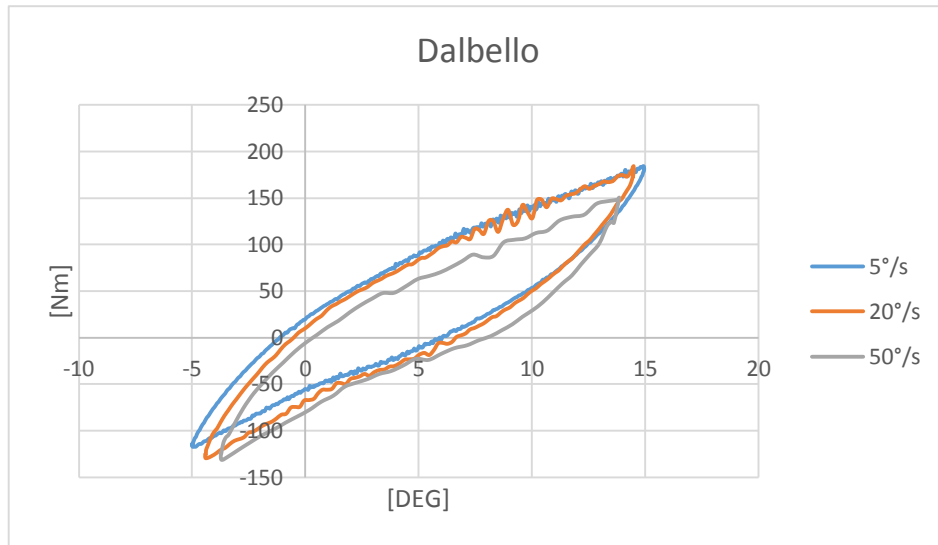
	M10 [Nm]	K5 [Nm/°]	K15 [Nm/°]	P	Ahyst [Nm°]
5°/s	139	12,57	8,11	0,65	1423,54
20°/s	135	13,4	9,69	0,72	1127,9
50°/s	110	12,79	10,26	0,80	971,26

It is possible to see that:

‹ For the Dalbello Yellow the flex index decreases with the angular velocity ω The flex index

‹ For every ω it is possible to see that ₅ is higher than ₁₅

‹ The hysteresis area decreases with the increase of the angular velocity ω probably because, even if using the pick valley compensator, the machine cannot reach exactly the imposed angular values.

6.3.5 Boots comparison

It is possible to compare the different boots studied graphing the results for the different values of ω.

It is choose to compare the three boots with the slowest ω and the fastest ω.

From the graphs is possible to appreciate the difference between the different boots and is possible to see that the Dalbello Krypton is the most stiffer boot for both the angular velocity studied.

The Tecnica Phx 70 is the softer boot as it was expected.
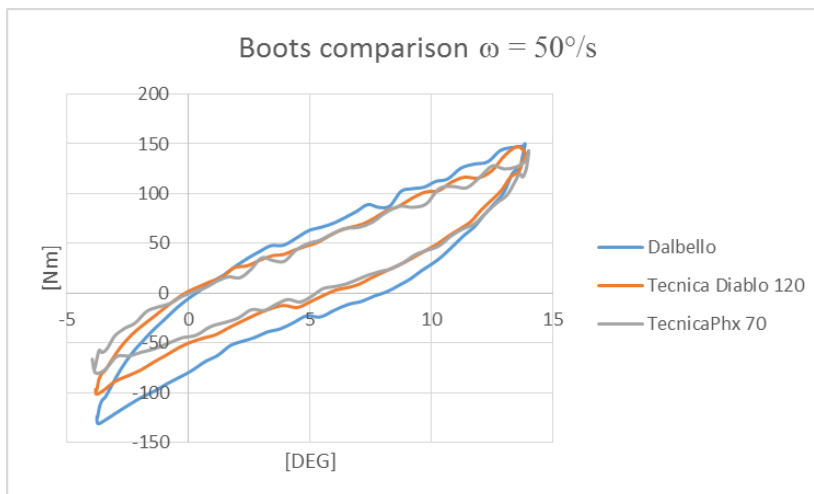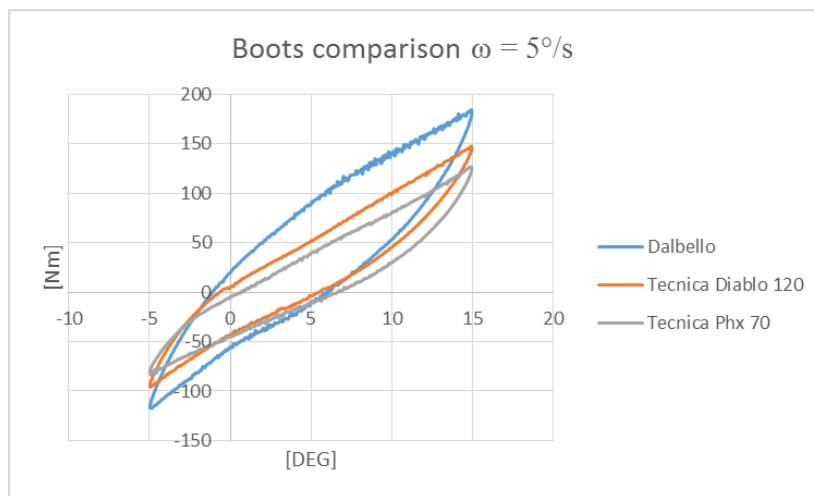
Chapter 7: Comparison between test methods

7.1 Aim of the chapter

In order to study the behavior of the boot the following test methods were investigated: the simulated skiing session using a real tester, the tests performed during a real skiing session and the bench tests.

These tests could be named as:

- ‹ IN VIVO TEST: simulated skiing in laboratory with the human tester
- ‹ IN FIELD TEST: real skiing session with the data collected on the slope
- ‹ IN VITRO TEST: the data are collected using the torque bench

Focusing on the moment ankle MA and on the Shell-Tibia angle, it could be useful to compare the difference of the values resulting from using the different types of test for every boot employed.

During the in field tests different types of skiing were performed.

In this chapter, it has been focused on the large free carving curves because, with this curves, it is easy to understand when the instrumented ski is the outer one or the inner one.

All test compared with the same strong flexion in the hard closure condition.
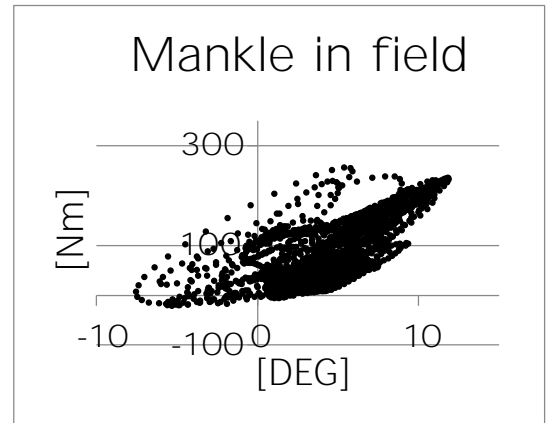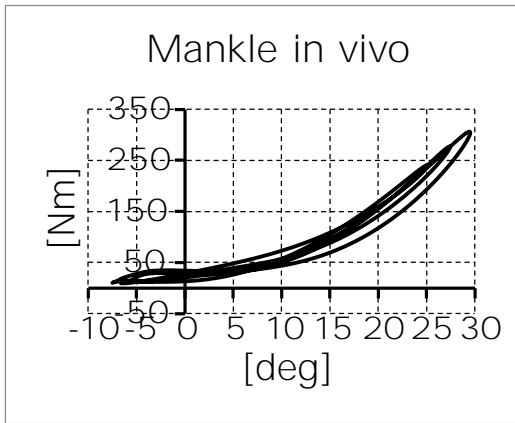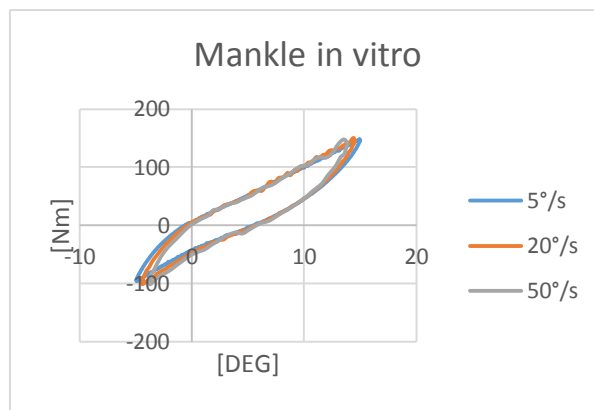
7.1.1 Tecnica Diablo 120

Mankle in vivo

Mankle in field

Figure 7. 1 Tecnica Diablo 120

Mankle in vitro

- 5°/s
- 20°/s
- 50°/s

7.1.2 Tecnica Phx 70

Mankle in vivo

Mankle in field

Figure 7. 2 Tecnica Phx 70

Mankle in vitro

- 5°/s
- 20°/s
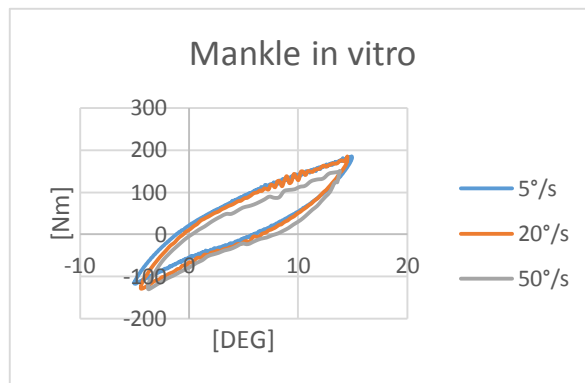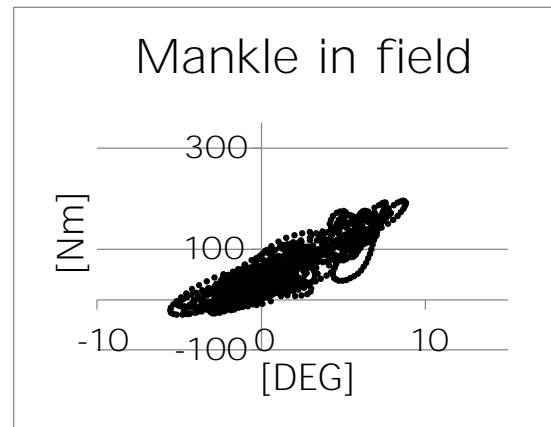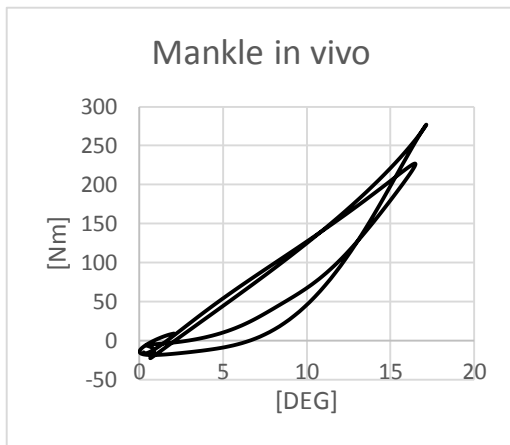- 50°/s
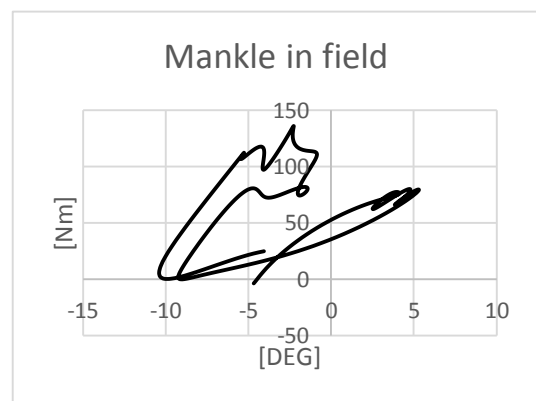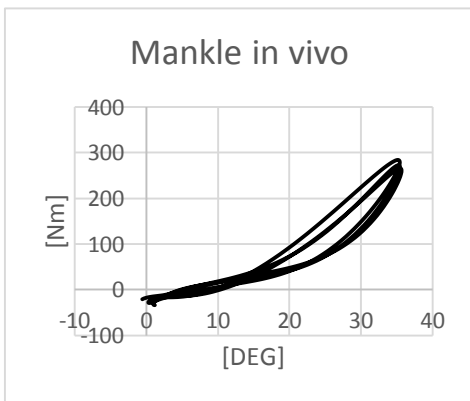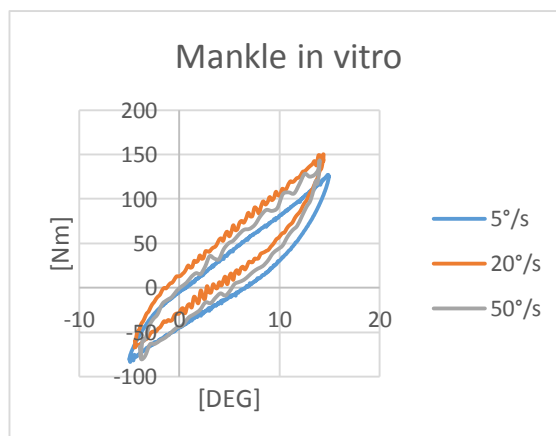
7.1.3 Dalbello Krypton

Figure 7. 3 Dalbello Krypton

7.2 Commenting results

It is possible to see that during the simulated skiing session the tester reaches high values of angle.

These angle values are higher than the ones reached with the procedure adopted when using the torque bench; in this case, the highest value of angle is +15°.

It is important to say that the in-field data were taken using three different pairs of ski boot and 3 different testers in three different days probably with three different type of snow.

Considering the previous limitations in the comparison of the field data, it is possible to understand that the real using of the ski boot when performing a ski session is different from both the laboratory tests.

According to this it is possible to say that in field the angle between shell-tibia almost always is included between -10°/+10°.

The simulated skiing session in laboratory and the tests on the torsion bench are over studying the boot behavior in an unused area.

Conclusions

As conclusion of this project, it is important to say that the force acting on the buckles is an interesting parameters to study, in order to analyze and optimize the structural behavior of the boot.

With the value of the force acting on the different buckles, it is possible to understand which could be the weak point during the skiing session.

The dynamometric clips are a good instrument to measure this kind of force.

With the clips in the present version, it is not possible to study the force acting on the first buckle, nor to study the maximum closure; for this reason it is suggest to design a load cell clip that can be used in compression in order to have the missing results.

Figure 8. 0.2 Existing clip in working in traction

Figure 8. 0.1 Possible design of a clip working in compression

It is also possible to see that the testing bench used in laboratory, is not so sensible to the misalignment.

In fact, the maximum misalignment affects less than 10% the results in respect to the aligned condition on the M10 (eFI) flex index measured.

As a developmet of the work could be possible to study other variables that could affects the results of the testing torque bench such as the use of two or four wheels as guide of the dummy tibia.

It could be possible to study a system to freeze the bench in order to control the temperature of testing and in order to reproduce in laboratory different conditions of temperature.

It is also possible to say that in field the angle between shell-tibia almost always is included between -10°/+10°.

The simulated skiing session in laboratory and the tests on the torsion bench are over studying the boot behavior in an unused area.

Bibliography

[1] *"Sviluppo di un Sistema per la determinazione delle forze di chiusura dei ganci degli scarponi da sci sulla gamma di modelli Nordica"* Petrone, Scapinelo, Cherubina, Progetto di corso Sport Engineering, 2011.

[2] *"The effect of boot stiffness on field and laboratory flexural behavior of alpine ski boots"*, Nicola Petrone, Giuseppe Marcolin & Fausto A. Panizzolo

[3] *"Development of experimental methods for the structural characterization of ski boots"*, Francesco Zambello; Master Thesis A.Y. 2012/2013

[4] "Ultimate skiing" Ron LeMaster